Intelligent Recognition of Texture and Material Properties of Fabrics

Xin Wang

Thesis submitted to the
Faculty of Graduate and Postdoctoral Studies
In partial fulfilment of the requirements
For the degree of Doctorate of Philosophy in Electrical and Computer Engineering

School of Electrical Engineering and Computer Science (EECS)
Faculty of Engineering
University of Ottawa

Abstract

Fabrics are unique materials which consist of various properties affecting their performance and end-uses. A computerized fabric property evaluation and analysis method plays a crucial role not only in textile industry but also in scientific research. An accurate analysis and measurement of fabric property provides a powerful tool for gauging product quality, assuring regulatory compliance and assessing the performance of textile materials.

This thesis investigated the solutions for applying computerized methods to evaluate and intelligently interpret the texture and material properties of fabric in an inexpensive and efficient way. Firstly, a method which allows automatic recognition of basic weave pattern and precisely measuring the yarn count is proposed. The yarn crossed-areas are segmented by a spatial domain integral projection approach. Combining fuzzy c-means (FCM) and principal component analysis (PCA) on grey level co-occurrence matrix (GLCM) feature vectors extracted from the segments enables to classify detected segments into two clusters. Based on the analysis on texture orientation features, the yarn crossed-area states are automatically determined. An autocorrelation method is used to find weave repeats and correct detection errors. The method was validated by using computer simulated woven samples and real woven fabric images. The test samples have various yarn counts, appearance, and weave types. All weave patterns of tested fabric samples are successfully recognized and computed yarn counts are consistent to the manual counts.

Secondly, we present a methodology for using the high resolution 3D surface data of fabric samples to measure surface roughness in a nondestructive and accurate way. A parameter FD_{FFT} , which is the fractal dimension estimation from 2DFFT of 3D surface scan, is proposed as the indicator of surface roughness. The robustness of FD_{FFT} , which consists of the rotation-invariance and scale-invariance, is validated on a number of computer simulated fractal Brownian images. Secondly, in order to evaluate the usefulness of FD_{FFT} , a novel method of calculating standard roughness parameters from 3D surface

scan is introduced. According to the test results, FD_{FFT} has been demonstrated as a fast and reliable parameter for measuring the fabric roughness from 3D surface data. We attempt a neural network model using back propagation algorithm and FD_{FFT} for predicting the standard roughness parameters. The proposed neural network model shows good performance experimentally.

Finally, an intelligent approach for the interpretation of fabric objective measurements is proposed using supported vector machine (SVM) techniques. The human expert assessments of fabric samples are used during the training phase in order to adjust the general system into an applicable model. Since the target output of the system is clear, the uncertainty which lies in current subjective fabric evaluation does not affect the performance of proposed model. The support vector machine is one of the best solutions for handling high dimensional data classification. The complexity problem of the fabric property has been optimally dealt with. The generalization ability shown in SVM allows the user to separately implement and design the components. Sufficient cross-validations are performed and demonstrate the performance test of the system.

Acknowledgements

First I am sincerely thankful to my supervisors Dr. Nicolas D. Georganas and Dr. Emil M. Petriu. They have managed to provide far more than just the required supervisory feedback, excellent guidance and encouragement throughout my Ph.D. study. I have been benefited greatly from their vision, technical insights and profound thinking. This dissertation would not be existed without them. They are the paragons of academic advisor and respectable human beings.

I also thank all other members in my doctoral committee, Professor Abdulmotaleb El Saddik and Professor Peter X. Liu for their thoughtful comments on my thesis.

I especially appreciate the help of Ms. Michèle G. Roy and the families of Dr. Emil M. Petriu for providing a rich collection of fabric samples and gratefully acknowledge XYZ RGB Inc. for providing help with the 3D laser scan of fabric samples.

I wish to thank the members of the Discover Lab for their suggestions and helps on my research. They have been the great colleagues during my doctoral life.

Last but not least, this dissertation is deeply indebted to my entire families. I would never have made it without their never-ending trust and support.

Contents

List of Tables

List of Figures

Chapter 1

Introduction

1.1 Background and Motivations

Textile is one of the human basic needs besides food, water and shelter. From ancient times to the present day, production methods of textile have unceasingly evolved. A rich selection of fabrics not only has great impact on how people carry their possessions, cloth themselves, and decorates their surroundings; but also can be utilized in multifarious applications. There are twelve main application areas for newly developing textiles [2]:

1. Agriculture, aquaculture, horticulture and forestry
2. Construction and building
3. Components of footwear and clothing
4. Geotextiles and civil engineering
5. Household textiles, components of furniture, floor coverings
6. Filtration, conveying, cleaning and other industrial textiles
7. Hygiene and medical
8. Automobiles, shipping, railways and aerospace

9. Environment protection
10. Packaging
11. Personal and property protection
12. Sport and leisure

The economic pressures are growing with the fast development of textile industry, for example, the growing demands of the consumers who are looking for more variety and personalization, the lack of flexibility in supply chain, and the lack of standards to satisfy the homogeneity need and so on. Under these pressures, there is a strong need to develop new methods in order to optimize the quality of textile products and textile management. Since the late of last century, information technologies have been involved into the study of textile greatly. The computational techniques have been already widely applied in textile industry for process and material structure modeling, simulation and control, marketing analysis, and production management. The related computational techniques include classic mathematical methods such as statistics, classic signal processing (frequency and temporal analysis) and statistical learning methods, and intelligent techniques such as soft computing and data mining. The classical methods have been proven an excellent performance for modeling and measuring mechanical features of textile. The soft computing techniques are capable of dealing with uncertainty and imprecision related to human knowledge on product process and expert systems. The selection of particular methods is largely depending on the nature of the problem of interest. In most of cases, an optimal solution to a complex textile problem can be found by combining several complementary techniques in a smart way. The representative application trends of computational techniques in textile and garment industry cover the following issues:

- Textile quality assessment by image analysis
- Modeling and simulation of textile structures

- Prediction of fabric performance in a computer aided design
- Textile property evaluations and computerized result interpretation
- Computerized textile production management and supply chain

Among these applications a computerized fabric property evaluation and analysis method plays a crucial role not only in textile industry but also in textile research. It relies on the following reasons. An accurate analysis and measurement of fabric property provides a powerful tool for gauging product quality, assuring regulatory compliance and assessing the performance of textile materials. It enables the prediction of the fabric performance. Knowledge of fabric property evaluation and its performance analysis can contribute to efficiency in solving consumer problems with textile products, and to the development of products that perform acceptably for consumers. During fabric production a number of separate processes are involved before the final fabric is manufactured. An efficient method for evaluating the quality of a fabric at every stage of its production is also desirable since it helps to detect defects of a fabric as early as possible. In addition, proper selection of fabric for particular end uses is also benefit from a good fabric evaluation system. Due to the above reasons researchers all over the world have been continually involved in developing new methods of fabric evaluation in order to meet the growing globalization and quality requirements.

This thesis is focus on computerized fabric surface property analysis and measurement, and intelligent interpretation of measured fabric properties. Matlab [3] is used to implement all of the proposed methods and evaluate the results as shown in section 3.3, 4.3 and 5.3.

The remainder of this chapter is organized as follows. In Section 1.2, we discuss the general sketch of this research work and the major challenges. Section 1.3 and Section 1.4 outline the contributions made in this thesis and the related publications respectively. Finally the organization of this thesis is laid out in Section 1.5.

1.2 Problem Statement

1.2.1 General sketch of the work

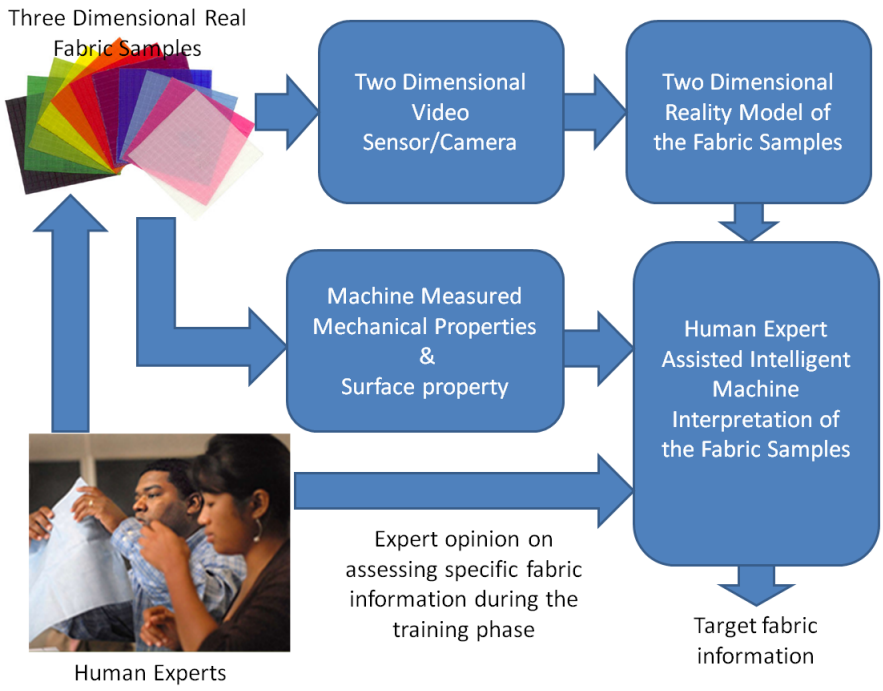

Figure 1.1: The general sketch of this research

The aim of this thesis is to exploit computerized solutions for fabric property analysis and interpretation. The general sketch of this thesis work is shown in Figure 1.1. Visual images of real fabric samples are captured by two dimensional video or camera. A vision based model is established for analyzing visual property of fabric such as the woven structure and yarn counts. Mechanical property can be measured instrumentally and the surface property can be gathered by three dimensional scans. The objectively measured information is intelligently interpreted by a computerized model which is set up with the assistance of human textile expert. The knowledge of human expert is used for off-line training only. The final output of the entire system is the target description that fulfills the requirement of the entire system.

1.2.2 Major challenges

Fabrics are unique materials which consist of various properties affecting their performance and end-uses. A key challenge in computerized fabric evaluation and analysis is to understand the complexity of the fabric properties, efficiently analyze the data obtained objectively and finally to interpret the property evaluation results in a systematic and scientific way. A deep research on modern information techniques are required simultaneously in order to select the proper techniques for solving the problem.

For vision based fabric image analysis, texture features are studied in order to recognize meaningful information such as the fabric woven types, and yarn counts. Numerous texture analysis techniques are available. None of the single method is sufficient to the problem and the optimal solution most likely is a combination of multiple techniques. A good understanding of fabric woven structures and a thorough knowledge of the texture analysis techniques are necessary.

For three dimensional data analysis, the major problem is how to extend a successful two dimensional data analysis method into a three dimensional case. The three dimensional surface data are usually irregularly distributed. The data analysis method only works on regular space. A feasible method, by which the original data map into a regular space without affecting the main characteristics of original data, has to be resolved.

Finally, a good intelligent integration method has to be decided from a various choices of artificial intelligence techniques. The method requires a good capability of tolerating uncertainty, complexity of the data to be analyzed. It should have a good generalization ability as well in order to fit into various interpretation requirements.

1.3 Contributions

This work contributes to several research domains, including, but not limited to: pattern recognition, image processing, 3D data processing, parameter estimation, machine vision, computation intelligence and fabric property evaluation. The following summa-

rizes the contributions of the thesis:

- Research on visual texture data analysis
  - Developed an image based woven fabric recognition algorithm.
  - Studied the robustness of the recognition algorithm by applying a number of tests.
  - Developed an image based automatic method for measuring yarn counts, consequently increased the accuracy of yarn count measurement and validated the robustness of the method with various real/simulated fabric sample images.
- Research on 3D surface data analysis
  - Developed an image based fractal GLCM method for roughness estimation.
  - Further extended the image-based roughness evaluation algorithm and applied FFT based fractal method to 3D surface data in order to estimate surface roughness.
  - Developed a novel method to compute standard roughness parameters from 3D surface data.
  - Developed an artificial neural network model for predicting the standard surface roughness parameters from the fractal estimate computed from the above method.
  - Studied the reliability of methods on high resolution 3D fabric surface scans through a number of experiments.
- Research on intelligent interpretation of fabric property
  - Proposed an intelligent model for interpreting physical/tactile features of fabric.
  - Studied the performance of the model on a number of validation experiments.

1.4 Publications Arising from the Thesis

The following refereed journal and conference publications have arisen from the work presented in this thesis.

Refereed Journals

1. X. Wang, N. D. Georganas, and E. M. Petriu, "Fabric Texture Analysis Using Computer Vision Techniques," *IEEE Transactions on Instrumentation and Measurement*, Vol. 60(1), pp. 44-56, 2011

Refereed Conference Proceedings

1. X. Wang, and N. D. Georganas, "Glcm Texture Based Fractal Method For Evaluating Fabric Surface Roughness , " *in Proc. IEEE CCECE'09 - Canadian Conference on Electrical and Computer Engineering*, pp. 104-107, May 2009

2. X. Wang, N.D. Georganas, and E.M. Petriu, "Fiber-Level Structure Recognition Of Woven Textile ," *in Proc. IEEE CCECE'09 - Canadian Conference on Electrical and Computer Engineering*, pp. 117-122, Lecco, Italy, Nov. 2009.

3. X. Wang, N.D. Georganas, and E.M. Petriu, "Automatic Woven Fabric Structure Identification By Using Principal Component Analysis And Fuzzy Clustering, " *in Proc. IEEE I2MTC'10-Instrumentation and Measurement Technology Conference,* 2010

4. X. Wang, and E.M. Petriu, "Neural Fractal Prediction Of Three Dimensional Surface Roughness, "accepted by *IEEE CIMSA 2011 - International Conference on Computational Intelligence for Measurement Systems and Applications,* 2011

1.5 Thesis Organization

The remainder of this dissertation proceeds as follows.

Chapter 2 seeks to introduce, discuss and synthesize issues on textile materials, the textile property measurement, and researches for fabric texture analysis, tactile sensing and haptic rendering. The information reviewed in this chapter is very important for understanding the scope of this thesis.

Chapter 3 introduces a novel textile geometric structure recognition techniques in order to develop an image analysis system particularly for analyzing textile geometric structure in an efficient way. The performance of the proposed recognition methods are studied in depth by a number of experiments.

Chapter 4 investigates the non-contact methods for measuring fabric surface roughness and presents a methodology for using the high resolution three dimensional surface data of fabric samples to acquire their surface roughness parameter measurement. An estimate of fractal dimension computed from three dimensional surface data by using 2DFFT is proposed as the indicator of surface roughness. The relationship between the proposed estimate and the standard roughness parameter is studied by using an artificial neural network model.

Chapter 5 an intelligent fabric property interpretation model is proposed and evaluated experimentally. The model uses the fabric human expert knowledge to guide a supported vector machine (SVM) based learning algorithm. The cross-validation technique is applied for performance tests.

Finally, Chapter 6 concludes the thesis by summarizing the contributions of this work as well as the possible improvements for future work.

Chapter 2

Review of Related Studies

This review seeks to introduce, discuss and synthesize issues on textile materials, the textile property measurement, and researches for fabric texture analysis, tactile sensing and haptic rendering. These topics are important for understanding the scope of this thesis. This chapter is organized as follow. It begins an introduction to textile material and the hierarchy of textile properties. This is followed by a section on the classic methods to evaluate textile properties. Later on, methods on computerized fabric analysis are discussed. Some new fabric rendering approaches which are inspired by the appearance of haptic devices are reviewed. In the last section a brief summary is given.

2.1 Introduction to Textile Material

Textile materials are manufactured for all kinds of applications from clothing, decoration in the household to numerous industrial uses. All textiles are made from fibers, which can be natural, manufactured(man-made) or mixed. Natural fibers used in textile today can be further divided into two major groups: plane fibers and animal fibers. Man-made fibers can be divided into two groups: regenerated fibers and synthetic fibers. For example, viscose rayon and cellulose acetate are regenerated fibers and Nylon, polyester, and acrylic are principal synthetic fibers. The variety of fiber composition offers a wide

range of properties.

Beside the raw material, the production methods and the treatments affect the textile products as well. The principal groups of textile production methods include weaving, knitting, and felting. The production methods develop different fabric structures. There are many treatments involved in textile production including spinning yarns, dying and printing fabrics, finishing treatments and so on. The textile production coupled with the complexities of the various treat processes gives a wide range of visual, physical properties of textile materials.

2.1.1 The hierarchy of fabric properties

The properties of a fabric can be divided into three classes: physical/structural properties, performance properties and aesthetic properties.

Physical properties include those that characterize the physical structure of the fabric, for example, fabric thickness, width, weight, and the number of yarns per unit fabric area.

Performance properties are those properties that typically represent the fabric's response to some type of force, exposure or treatment, for example, strength, abrasion resistance, pillingand color fastness.

Aesthetic properties are qualities that make a fabric attractive to look at, or pleasing to experience, for example, they describe the way a fabric feels or drapes in design and development processes.

As shown in Figure 2.1, the three types of properties are related with each other. Both aesthetic and performance properties actually depend very much on their physical properties. However, performance properties are often the primary characteristics in product development. Aesthetic properties are also equally important as performance properties in fabric selection for a textile product. A good textile product has to be

fit for its purpose. To choose the right fabric for a textile product means to match the performance and aesthetic properties of the fabric to the type of product to be made.

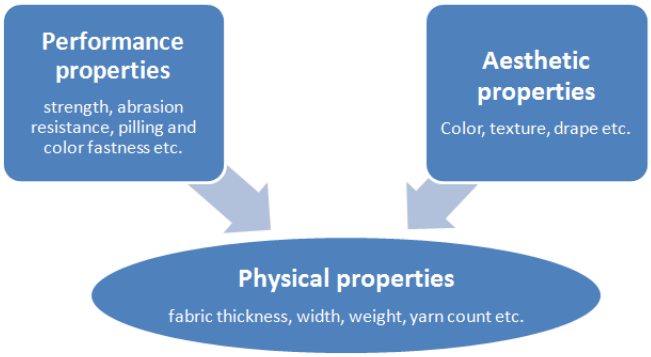

Figure 2.1: The hierarchy of fabric properties

2.1.2 Fabric hand

The term "fabric/textile hand" or " fabric handle" or simple "hand" has been defined as "the subjective assessment of a textile material obtained from the sense of touch " [4] or as "the tactile sensation or impressions which arise when fabrics are touched, squeezed, rubbed or otherwise handled" [5]. Fabric hand is a generic term to express the evaluation of the quality of a fabric [6] and generally the fundamental feature that determines the success or failure of a textile product. It is critical to textile manufacturers, garment designers, and customers in developing and choosing textile products [7].

There are numerous factors related to fabric hand. From this point of view, fabric hand is an elusive aspect and basically a reflection of overall quality, depending on a number of fabric properties, for example, flexibility, compressibility, elasticity, resilience, density, surface texture, roughness or smoothness, surface friction, and thermal character etc. Usually fabric hand is assessed by the reaction obtained from the sense of touch or the integration of the total sensations expressed. These sensations may imply the reaction to different handling actions such as touching, folding, cutting, transporting,

sewing, and pressing etc.

2.2 Methods to Evaluate Fabric Properties

Consumers and manufacturers consider quality the most important attribute in the purchase and production of a textile product. The quality of a textile product is determined by the characteristics of every component from fiber to fabric and to the very last finishing detail. The creation of new textiles, which have such a variety of new features, makes product quality difficult to define and evaluate [8]. The evaluation of fabric quality is still an open topic due to its complexity.

In the textile industry and research, fabric quality or fabric evaluation is performed in two ways: (1) subjective evaluation and (2) objective evaluation

2.2.1 Subjective fabric evaluation

The evaluation of fabrics, which is carried out by a panel of respondents(subjects), is called subjective evaluatiosn/assessment [9]. Subjective evaluation of fabric treats the fabric overall quality as a psychological reaction obtained from the senses of seeing, hearing, and touches. The subjective evaluation is also called sensory assessment [10]. The panel of respondents traditionally is a group of fabric experts and for research purpose may be mixed with a group of novices. During a process of evaluation, a fabric is looked carefully, touched, squeezed or otherwise handled. The felt sensations about the evaluated fabric are rated by a panel of subjects and described as components of the assessment result. The typical procedure of the experts' subjective fabric evaluation is illustrated in Figure 2.2.

In general, the subjective assessment is fast, convenient and apparently is a valuable method. However, the intrinsic problems of subjective assessment limit the reliability of subjective judgments. The variations are the most widely discussed aspects of fabric subjective evaluation. The sources of variations involve the following distinct areas:

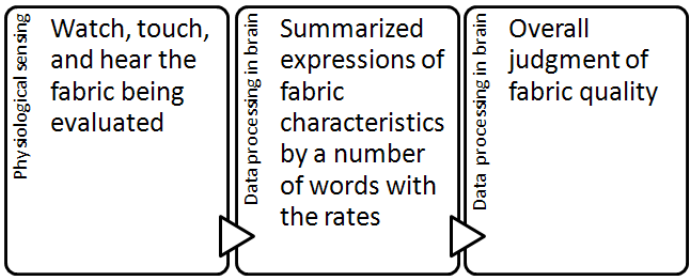

Figure 2.2: The procedure of the experts' subjective fabric evaluation

Individual difference This subjective evaluation technique is entirely based on a personal point of view. Thus, the evaluation results are affected by the individual temperament, age, gender, level of experience, cultural and racial differences.

Evaluation scales The sensitivity of the human assessment is not good as as the instrumental measurement [10]. The number of the rating scales and the number of the textile samples used in a single test affect the accuracy of the evaluation as well. For example, Grineviciute [11] found that a large number of the evaluated fabric specimens caused disagreement between subjective assessments.

Expression difference The vocabularies of human evaluators are varied because there is no commonly accepted and widespread terminologies for each fabric property. Although AATCC(American Association of Textile Chemist and Colorist) [5] has published guidelines for the standardization of the subjective fabric evaluations, there is no evidence that this standard is accepted and understood by the general public such as potential customers. Sülar [12] is one of several researchers who have commented that the difference between the expressions used for fabric evaluations are great enough to interfere with communication between textile producers and customers.

Due to the subjective nature the test properties cannot be evaluated accurately and the results are not consistent among different tests and different judges. Therefore,

subjective evaluations of fabric do not produce results that can be used to guide manufacturing and design of new fabric which require the consistent quality. The results of subjective evaluation are not sufficient to develop standards or to communicate preferences and desirable properties to industry professionals.

2.2.2 Objective fabric evaluation

The fabric evaluations made by using instruments (objects) are called objective measurements. These evaluations are also called instrumental evaluations [13]. The objective evaluations attempt to describe the quality of a fabric quantitatively by measuring its physical or mechanical properties objectively. Quantitative analysis of fabric quality or fabric hand is profitable for more accurate comparisons between all types of fabrics. Objective readings are not influenced by the individual difference of human evaluators, may be connected to some fabric performance properties or fabric aesthetic properties which cannot be measured instrumentally, and can be recorded into a database for the purpose of the future development of new fabric products, the quality control of fabric manufacturing, and the marketing control of fabric sales.

In 1930 Peirce [7] launched a set of instrumental measurements including bending rigidity, compression, friction and extensibility, for the purpose of relating fabric handle to fabric mechanical properties. His remarkable work represented the first key milestone for the development of fabric objective measurement.

In 1970s KES-F System (Kawabata's hand evaluation system for fabrics) [14] was developed in Japan by the Hand Evaluation and Standardization Committee (HESC). In this fabric objective measurement system the fabric mechanical properties, for example, the tensile force-strain curve, shear force-angle curve, bending torque-angle curve, pressure-thickness curve, surface friction coefficient variation curve and thickness variation curve, are recorded by specific testers. The characteristic values [15], as shown in Table 2.1, are calculated from these recorded data obtain from KES-F instruments. Kawabata and his colleagues also proposed a multi-stage method which links the objec-

tive measured properties to fabric hand [16]. In their method, fabric mechanical property parameters are converted into certain values (the hand value or HV) that express three primary hand values such as stiffness, etc. HVs are the primary factors characterizing fabric hand. Subsequently, HVs are converted into a single value (the total hand value or THV). Step-wise linear regression method was used for the prediction of HVs and THV.

Table 2.1: Characteristic values calculated in KES-F system

Group	**Variable**	**Symbol**	**Unit**
Tensile	Linearity of load-extension curve	LT	-
	Tensile energy	WT	$g \cdot cm/cm^2$
	Tensile resilience	RT	%
	Elongation at max. load (500 gf/cm)	EMT	%
Shearing	Shear rigidity	G	$g \cdot cm/^\circ$
	Hysteresis of shear force at 0.5° shear angle	2HG	g/cm
	Hysteresis of shear force at 5° shear angle	2HG5	g/cm
Bending	Bending rigidity	B	$g \cdot cm^2/cm$
	Hysteresis of bending moment	2HB	$g \cdot cm/cm$
Compression	Linearity of pressure-thickness curve	LC	-
	Compressional energy	WC	$g \cdot cm/cm^2$
	Compressional resilience	RC	%
Fabric thickness	Thickness at $0.5gf/cm^2$	T_0	mm
	Thickness at $50gf/cm^2$	T_m	mm
Surface	Coefficient of friction	MIU	-
	Mean deviation of MIU, frictional roughness	MMD	-
	Geometrical roughness	SMD	μm
Weight	Weight per unit area	W	g/m^2

The other wide-known objective measurement system is the FAST (Fabric Assurance

by Simple Testing) [17]. FAST measures the mechanical and dimensional properties of fabric that can be used to predict performance in garment manufacture and the appearance of garments in wear. It was established by the CSIRO Division of Wool Technology to meet industry's requirement for a simple, reliable method of predicting fabric performance. FAST system measures the similar properties as the KES-F system does. Four types of testers are involved in FAST system. FAST-1 gives a direct reading of fabric thickness over a range of loads. FAST-2 measures the fabric bending length and its bending rigidity. FAST-3 measures fabric extensibility at low loads as well as its shear rigidity. FAST-4 is a quick test for measuring fabric dimensional stability, including both the relaxation shrinkage and the hygric expansion.

The KES-F and FAST have reached a considerable acceptance mainly in textile research institutions. However, they are not widely accepted in the textile industries for the following reasons: (1) very high prices, (2) very complicated operation methods, and (3) lacking reliable methods to interpret the measuring results. Therefore, researches on alternative fabric measuring methods, which are simpler and faster, are still ongoing [12].

2.3 Computerized Fabric Analysis

Due to a strong need to develop new methods in order to optimize the quality of textile products and textile management, information theory as well as the computational techniques are widely applied in textile research and industry. The related computational techniques include traditional methods such as statistics, differential equations, signal processing, and especially the intelligent methods such as soft computing, data mining and pattern recognition. These techniques can be used in many applications, for example, simulation of textile structures, computer aided textile design, computerized textile management, textile quality assessment, and textile quality evaluation etc. This section is focus on the vision based texture analysis and fabric surface property measurement.

2.3.1 Vision based texture analysis

The texture of a fabric is one of the most important properties of a fabric. It varies with the fabric geometrical structures. It mainly can be perceived from the sensation of vision. Vision based texture analysis techniques undoubtedly helps to develop automatic methods for fabric texture pattern recognition. A brief review on vision based texture analysis is given and the automatic fabric pattern recognition is discussed as well in the following.

2.3.1.1 Brief review of texture analysis

Human beings can recognize texture when they see it, touch it or listen to the sound generated by scratching on the textured surface, but they can hardly give unique definition of texture. There are numerous ways to describe texture attempted by vision researchers. It has been defined by its mathematical extraction method, its particular application, or its perceptual properties. Texture analysis is an important and useful technique in the study of machine vision. A successful vision system should be able to deal with the textured environments. It has many application areas, such as quality control of textured images [18, 19], detection of defects in texture images [20, 21, 22], medical image analysis [23], document processing [24], remote sensing [25] and so on. In general, texture analysis deals with similar tasks as a typical computer vision algorithm does for example feature extraction and classification.

There are many different feature extraction methods that were involved in texture analysis. The texture features are measurements that describe the characteristics of a texture [26]. The most widely used methods for texture feature extraction in recent years are statistical and signal processing methods. The principal approaches for texture feature extraction are listed in the following.

GLCM Haralick [27] suggested the use of gray level co-occurrence matrices (GLCM) which have become one of the most popular and widely used texture features. It

is a second-order statistical method that computes the relationship between pixel pairs in the image. Haralick has proposed a number of useful texture features that can be computed from the co-occurrence matrix. In recent years, the GLCM is also combined with other methods depending on the application need [28, 29, 30].

Gabor filters and Wavelets The signal processing approaches include filtering and transform methods. Recently the most widely-used signal processing methods for texture extraction are Gabor [31] filter and Wavelet transform [32]. There is psychophysical evidence showing that the human brain does a frequency analysis of image [33]. This type of techniques is suitable for texture segmentation and classification due to the nature of texture.

Other methods (1) *Autocorrelation Features* are used for studying the repetitive nature of the placement of texture elements in the image which is a very important texture property. The autocorrelation function of an image can be used to assess the amount of regularity and the fineness/coarseness of the texture present in the image as well. (2) *Model based stochastic methods* for example fractals [34], Markov random field approaches [35], are most proposed recently not only to describe texture but also to synthesize it.

Once the texture features are measured, a typical classification method is applied for labeling the texture class to a set of measurements. Popular classifiers in most computer vision applications are also suitable for texture analysis. These classification methods can be grouped into two categories: supervised and unsupervised methods depending on whether training samples are used or not [36]. Supervised classifier requires sufficient reference data for training. The noted examples of this type classifier are artificial neural network (ANN) and its variations [37, 38], maximum likelihood classifier [39], support vector machine (SVM) [40] and so on. Unsupervised classifier does not need prior definitions of classes. Clustering based algorithms are used to separate samples into a number of classes based on the inherent information of the image. The famous examples of

unsupervised classifiers are K-means clustering [41], fuzzy c-means clustering [42].

This section has reviewed the basic concepts and listed some popular techniques for processing textured images. Texture is a prevalent property of fabrics in natural world. It is therefore crucial to select proper processing techniques for specific applications of fabric texture analysis.

2.3.1.2 Vision based fabric structure identification

Vision based automatic recognition of fabric structure is a very practical alternative objective fabric property measurement approach which takes advantage of the image texture analysis techniques. In recent years, the automatic recognition of woven structures has been reported by many researchers [43, 44, 45, 46, 47, 48, 49, 50, 51, 52, 53]. B. Xu [45] studied the periodicity of woven fabrics in frequency domain. He identified weave types by analyzing the distribution of peaks in the power spectra of woven fabric images. His approach was modified by M. Ralló [52, 53] et. al. They proposed a convolution model of woven fabric. They described the woven fabric as a convolution of an elementary unit by a pattern of repetition. Both Xu and Ralló et. al. found that the different weave patterns have different peak distributions in the their power spectra. They identified the weave patterns of real fabrics by visually identifying the most significant peaks of the power spectra of the fabrics. However, the power spectra of real fabric samples are too noisy and complicated to develop a reliable automatic algorithm to analyze.

The second approach is to extract global texture features either in spatial domain or frequency domain and then use a learning algorithm classifier to recognize weave pattern types [43, 46, 49, 51]. This approach is very sensitive to the selection of the set of training data used for the learning algorithm. Variations in the lighting condition and the image scale may lead to a failure of the classifier. Moreover, once a weave pattern is erroneously recognized by the classifier, it cannot be corrected.

The third approach consists of solving two problems: (1) How to detect the areas of

interlacing weft and warp yarns? The problems are termed as "crossed-area detection". In the crossed-areas it is important to notice that there are only two possible states: weft floats over warp or warp floats over weft. The second problem is then (2) how to detect the crossed-area states? Based on the assumption that width of yarn is fixed, the weave patterns are repeated uniformly periodically over the entire fabric surface. Under this assumption the crossed-area one can be detected by using either a two dimensional Fourier transform [47, 48] or a two dimensional auto-correlation in the spatial domain [50] to find the fixed widths of weft and warp. As the widths of the yarns are not constants for real fabric samples errors may occur when locating the crossed-area of uneven distributed yarns.

C. Kuo et. al. [44] developed an unsupervised automatic recognition method in the spatial domain by using of fuzzy c-means clustering (FCM). Their method can identify several woven fabrics which have different yarn densities and various geometric shapes for crossed-area of yarns. As there are only two possible crossed-area states in which the weft or the warp is interlaced over the other, they used FCM to classify the detected crossed-areas into two clusters. However, their method failed to decide whether the weft or the warp floats in a specific crossed-area.

2.3.2 Tactile texture analysis

In this section, a short review on textile sensor based texture analysis is discussed. Although there is no tactile sensor that was reported to meet the resolution requirement for very fine texture analysis such as fabric, the research on tactile texture analysis is still promising for future fabric texture analysis.

Information obtained from tactile sensors can be analyzed to extract meaningful properties such as roughness, shape, hardness and so on. Computer vision and pattern recognition technology now appear as standard approaches in sensor data analysis. Unfortunately, pattern recognition in tactile perception is more complicated than in visual task, especially for fine surface recognition. Due to lack of stable, high resolution

tactile sensors and many difficult-to-control factors, tactile sensing is mostly used as a supplementary to visual applications [54].

However, both vision and haptic information are required for a more complete characterization of object properties. In some circumstances the perception is clearly affected by the haptic information, although vision frequently dominates the perception of object's features. For example, in the case of object exploration in a dark environment the tactile sensing becomes important because of the lack of light, in the case of minimal access surgery [55] an artificial tactile sensing systems is also important for accessing the properties of tissues, and in the case of fine texture exploration, such as fabric surface property inspection, a high resolution tactile sensing is desired as well.

Among tactile sensing tactile texture recognition seems to be a very important research area with lots of interesting applications which include medical, geological and autonomous remote robotics. No much work is done in tactile texture data processing despite the great amount of works that all kinds of artificial tactile sensors are developed for numerous applications [56, 57, 58, 59, 60]. It may be the result due to the limited accuracy of existing sensing systems, sophisticated calibration procedures and a significant noise on the sensing data. Among existed tactile texture data analysis approaches, FFT based machine learning algorithms are the most popular for material/texture classifications. Mayol-Cuevas et al. [61] apply a learning vector quantization technique(LQV) to FFTs of the tactile data obtained by an electret piezoelectric microphone in order to classify 18 common materials. Jamali and Sammut [62] process the tactile texture data to detect the peaks in frequency domain and use naive Bayes learner to classify material. McDaniel and Phanchanathan [63] use support vector machines to classify surface roughness of 3D textures. Kim et al. [64] introduce a stochastic maximum likelihood estimation method to classify texture data by using a polymer-based MEMS tactile sensor.

2.4 From Physical Measurement to Fabric Simulation

An accurate measurement of fabric physical properties is not only very necessary for the quality control of fabric, but also very crucial to the fabric simulations. In traditional computer graphics, a fabric simulation refers to the visual cloth simulation. However, along with the evolution of Haptics multi-modal solutions start being shown in literature and significantly enhance the realism of fabric simulation. Texture as one of the most important tactile properties of a fabric is a key problem for haptic and visual rendering.

2.4.1 Brief introduction to Haptic texture rendering

2.4.1.1 Haptics and haptic rendering

Haptic, from the Greek $\alpha\varphi\acute{\eta}$(Haphe), means "relating to the sense of touch" [65], and is now commonly viewed as a perceptual system, mediated by two afferent subsystems, cutaneous and kinesthetic, that most typically involves active manual exploration [66]. The cutaneous system applies receptors embedded in the skin, on the other hand the kinesthetic system applies receptors located in muscles, tendons, and joints. The haptic sensory system requires both cutaneous and kinesthetic receptors, but it differs in some way that it is combined with an active motion. Touch is active when the sensory signal is associated with controlled body motion. For example, cutaneous sense turns to active when we explore a surface or grasp an object, and kinesthetic sense turns to active when we manipulate an object and/or touch other objects with it.

Haptics refers to the tactile/touch sensing and control for interaction with computer applications. These interactions can be between a robot end-effector and a real object; a human hand and a simulated object in a virtual environment; or a variety of combinations of human and device interactions with real, remote, or virtual objects. The introduction of a wide variety of force feedback devices, greatly increases the number

and variety of areas of computing which might benefit from interaction via the tactile sense. More and more applications have become feasible over the last twenty years. The different applications are related to many areas: tele-operation, medical training, games augmented with haptic feeling, robotics, and e-commerce. A haptic interface is a device that enables physical interaction with virtual environments or tele-operated remote systems. They are applied for tasks that are usually performed using hands in the real world [67]. Haptic devices generate computer-controlled forces to provide to the user a sense of natural feel of the virtual environment and objects within it.

In this aspect, haptic rendering is defined as the process of computing and generating forces in response to user interactions with virtual objects [68]. *Rendering* refers to the process which enables to create desired sensory stimuli to convey information about a virtual object to the user. This information is comprised of the representation of the object's physical properties, for example, shape, elasticity, texture, mass, and so on. The more detail is rendered; the realer is felt by user. It is obvious that a sphere haptically rendered with a simple penalty function is felt different from the same sphere rendered with physical textures and surface friction. Adding tactile texture data in virtual reality certainly enhances high-fidelity rendering in numerous virtual exploratory or manipulation tasks, especially, in applications required surface contact. These applications can include

- robotic navigation: judgments of surface properties could invoke different navigation plans and lead to better performance.
- e-commerce: for example, a tactile feeling aids in selling fabric remotely via internet.
- tele-surgery: simple judgments of smoothness or roughness of internal organs can improve the accuracy of medical decision.

In order to authentically represent the object's tactile properties, the data which are gathered from real object by tactile probes/sensors have to be analyzed and modeled. The

tactile sensors have been widely used in modern robotic systems which tend to emulate biological haptic perception recognition [69]. The state-of-art of tactile sensing has also been reviewed extensively [56, 57, 58, 59, 60]. However, the merge of haptic information which is obtained from real object with the virtual object which is represented in virtual environment has not yet been widely explored. In addition, numerous new possibilities are opened by taking advantage of the robotic haptic data analysis.

2.4.1.2 Haptic texture rendering

The haptic texture rendering is different from its visual counterpart. It is bidirectional since the haptic sense is not a passive perceptual sense like vision and audition, The haptic rendering update(1Hz) rate is higher than graphic update rate (20-30Hz). A low update rate causes an unstable haptic feedback. The type of haptic texture rendering algorithm is dependent on the type of tactile interface device and the representation used for modeling the virtual objects. In general, the haptic texture rendering algorithms can be classified into two categories: (1) image-based and (2) procedural.

Image-based haptic texture rendering: The haptic texture is constructed from a texture image data. It is quite similar to the texturing in computer graphics. A 3D object wrapped with a texture image looks more realistic. Like a graphical texture consists of texels, the fundamental units of texture surface used in computer graphics, with only color or gray level intensities, a haptic texture consists of texels with a height value. A two-stage haptic texture mapping techniques are proposed by using computer graphic techniques [70, 71]. In the first stage, the texture image is mapped to a simple intermediate surface. At second stage, the texels are mapped from the intermediate surface to the object surface. The gradient vector can be estimated using a finite difference technique and interpolation scheme [72]. Then, Ho et al. [73] introduced a technique similar to bump mapping [74] that perturbs the surface normal based on the gradient of the texture offset field. A combination of the original and refined normals is used for computing the direction of the feedback force.

Procedural haptic texturing: This technique is to use mathematical functions to generate haptic textures. The function usually takes the coordinate (x, y, z) as the input and computes the height value and its gradient. For instance, the stochastic haptic texture rendering is proposed by several researchers in 1990s [75, 76]. Fractals are also used for modeling textures [73]. Klatzky and Lederman [77] propose a textured surface as a surface with protuberant elements adding to a relatively flat substrate. Interaction with a textured surface results in perception of roughness. Otaduy et al. [78] introduce a method to estimate the penetration depth between two textured objects which are computed from low resolution geometric representations and haptic textures created from images that contain surface properties. Theoktisto et al. [79] employ local height field maps onto triangle mesh. The height fields are specified for every face. The algorithm is implemented in multi-stages.

2.4.2 Multi-modal fabric simulation

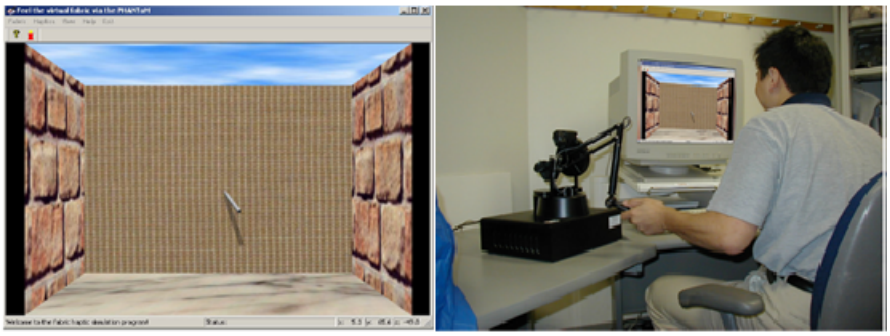

Figure 2.3: The audio-haptic fabric interface [1]

In 2000s, few researchers started to report the haptic rendering algorithms and new device designs for textile simulation. However, the haptic sensation of fabric is too complex to be rendered on current available haptic devices. Multi-modal fabric simulation is a good solution to overcome the limitation of haptic rendering and gives reasonable virtual experience of fabric.

Audio and Haptic simulation

Huang [1] developed a stylus based fabric characteristic sound simulation and related haptic-audio interface as shown in Figure 2.3. In his system, "PHANToM 1.5", a most widely-used force/torque feedback device from SensAble Technologies Inc., was chosen as haptic device. The KES-F system measured fabric surface properties such as roughness and friction were analyzed and represented for PHANToM. The fabric characteristic sound when a stylus rubs a fabric was generated and recorded. Spectral analysis was applied for sound simulation. Human user evaluation showed that difference between virtual fabric samples can be perceived from his audio-haptic fabric simulation.

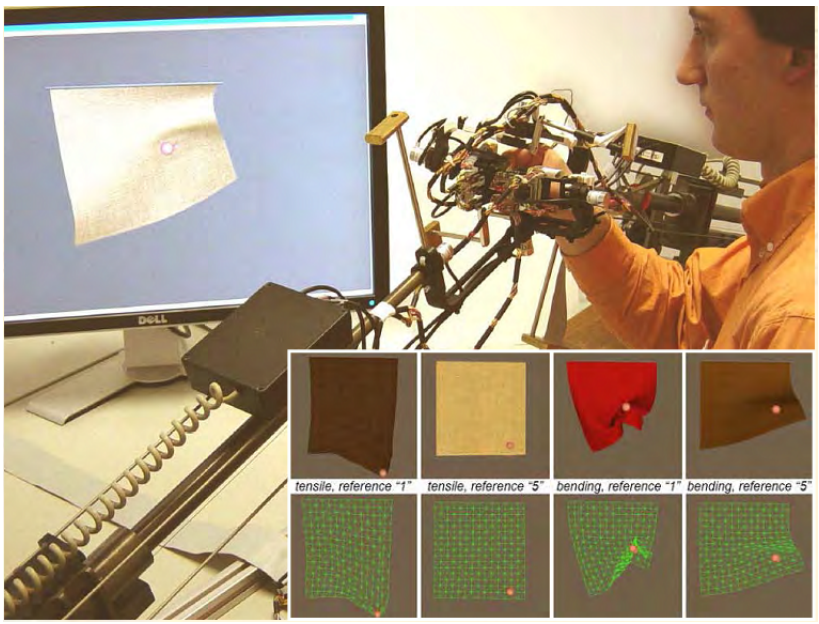

Figure 2.4: The demonstration of HAPTEX project

Visual and haptic simulation– HAPTEX

The most recent achievement on multi-modal fabric simulation is from HAPTEX (Haptic sensing of virtual textiles) [80]. HAPTEX was a visionary research project funded by the European Union. The goal of HAPTEX was to develop a complete virtual reality system for the visual and haptic rendering of textile. Multi-discipline researchers from five European universities were involved in the project.

Their pioneer works were focus on a two-finger interface design [81, 82], synchronization between graphic and haptic rendering, and textile mechanical model for visual rendering [80]. Figure 2.4 shows the demonstration system of HAPTEX. Due to the resolution limitation of the tactile devices and the complexity of the rendering algorithm, they did not propose any practical rendering method for haptic texture of textile by the end of the project. The simulation of haptic texture was only worked on computer simulated Brownian surfaces [83]. In addition, the problems on collision detection, accurate force response, and algorithm optimizations leave opening for the future researchers.

2.5 Summary

This chapter introduces the basic properties of textile material. Fabrics are unique materials, and have various kinds of applications from all areas of human life. Their quality is related to numerous properties and very hard to evaluate. Traditionally it is evaluated subjectively. The huge variation of the subjective evaluation results makes this method unreliable for new textile creations, textile simulation or being a standard of fabric measurement. The KES-F system, therefore, becomes the solution for providing reliable objective evaluation of fabric. However, because the KES-F system is very expensive and difficult to operate, alternative fabric property evaluation method is still opening for many researchers.

Vision based texture analysis techniques makes the vision based fabric texture analysis a potentially feasible research area. The computer intelligent algorithms provide the technical background for the automated recognition of fabric surface properties. The evolution of computer Haptics helps to enhance the realism of fabric simulation in virtual environment. However, the lack of high performance tactile sensor and tactile device still blocks the development of tactile fabric texture measurement and simulation. It leaves a beneficial area available for future researchers.

Chapter 3

Textile Geometric Structure Recognition

In this Chapter, a novel textile geometric structure recognition techniques is introduced to develop an image analysis system specifically for efficiently analyzing textile geometric structure. The focus of this work is on identifying basic weave patterns and measuring structural parameters, such as yarn count.

The chapter is organized as follows. Firstly in section 3.1 the basics of textile geometric structure is introduced. In section 3.2 the proposed automatic geometric structure recognition techniques are presented. In section 3.3 the experimental verifications are provided and a discussion of the results is presented as well.

3.1 Introduction

A textile is a cloth, which is either woven by hand or machine [84]. "Textile"has traditionally meant, "a woven fabric ". The term comes from the Latin word "texere", meaning to weave. Woven fabrics are highly structured materials, and they are formed by two sets of mutually perpendicular and interlaced yarns: "warp"and "weft". As shown in Figure 3.1, warp refers to the long, vertical yarns that are wrapped around the looms.

Weft refers to the horizontal yarns that are woven through the warp yarns.

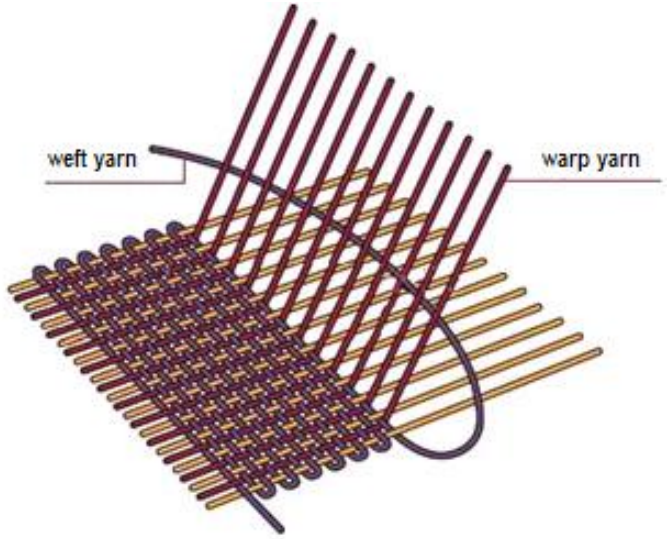

Figure 3.1: Weft and Warp

The type of woven fabric is determined by means of a weave pattern that consist of yarns forming a rectangular interlacing unit of n warp yarns and m weft yarns. Weave pattern refers to the basic unit of weave which is periodically repeated throughout the entire fabric area. There are three basic types of fabric weave: plain, twill and satin. Figure 3.2 illustrates the examples of three basic weave types respectively. The basic weave patterns or units of these examples are shown in Figure 3.3. The black blocks and white blocks represent warp float and weft float respectively.

The appearance, handling and physical properties of woven fabrics are influenced by their geometric structure. The weave types and the yarn count are two major geometric characteristics of woven fabrics. Both the weave types and the yarn count affect the physical properties and dynamic behavior of the fabric. For example, different weave types have different effects on the bending and shearing stiffness of fabric, the abrasion resistance of fabrics [85] and the impact strength of fabrics [86]. Obviously different weave types lead to different appearance of fabric. Satin weave fabrics are more lustrous with a smooth surface than plain and twill weave fabrics. Twill weave fabrics are more

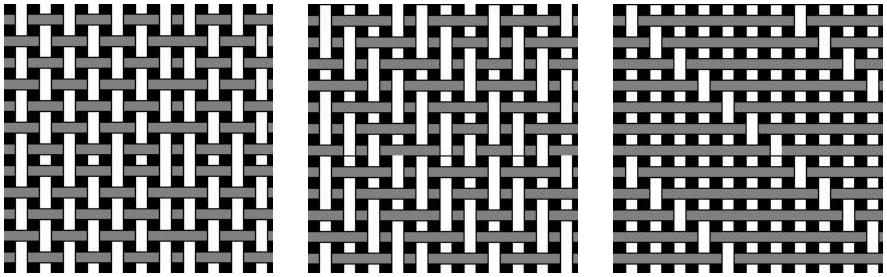

(a) Plain weave (b) Twill weave (c) Satin weave

Figure 3.2: Basic weave types

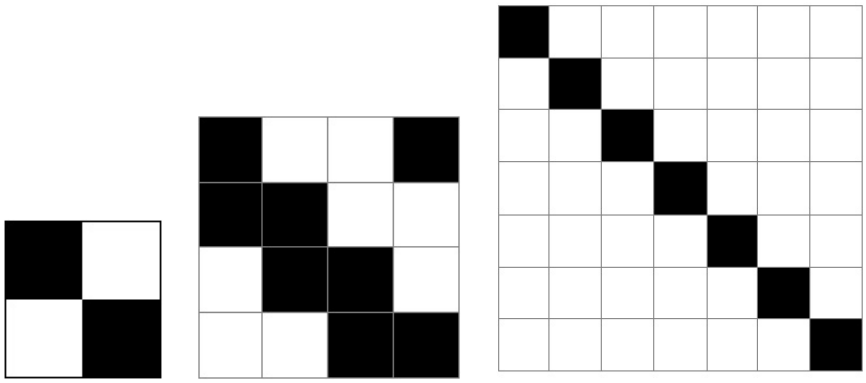

(a) Plain (b) Twill (c) Satin

Figure 3.3: Weave patterns

durable, heavier, wrinkle and soil resistant. Plain weave fabrics are the simplest type of construction which is inexpensive to produce. When yarn count is changed, the fabric handle, heat and water transfer property, wrinkle resistance and color brightness are all affected [87]. Yarn count, as a measure of the fineness or coarseness of woven fabric, is also used as a measure of the fabric quality.

Accurate identification of these geometric structural characteristics offers a tool for fabric appearance evaluation and quality control. In traditional textile industry, the work to analyze fabric structures still relies on manual operations with the help of microscopes, which are very tedious and time-consuming. Thus, an automatic analysis of

fabric structural characteristics is desirable in order to reduce labor cost and testing time.

3.2 Methodology

In order to recognize the accurate structure of woven fabrics and resolve the issues that stated in section 2.3.1.2 a novel method is presented in this section. The rest of the section is organized as follows. Section 3.2.1 depicts an automatic method for recognizing weave pattern. An method that can accurately measure yarn counts of different woven fabrics is presented in section 3.2.2.

3.2.1 Weave Pattern Recognition

The general steps for automatic weave structure recognition are shown in Figure 3.4.

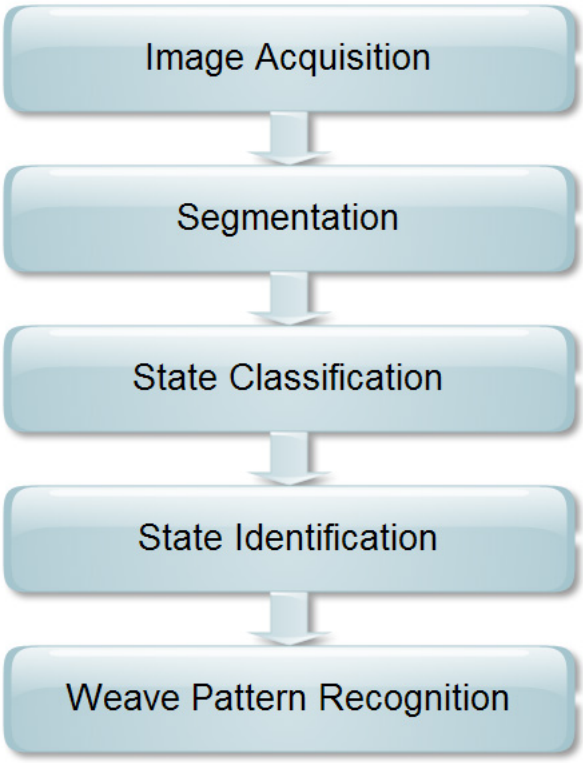

Figure 3.4: The general Steps of automatic weave pattern recognition

The detailed steps for each general step are listed as follows:

- Image acquisition
  - Scan fabric samples
  - Noise reduction filtering
  - Equalization
- Segmentation
  - Two dimensional spatial domain integral projection
  - Smoothing
  - Segmenting crossed-areas
- State Classification
  - Texture feature vector extraction
  - Principal component analysis
  - Fuzzy c-means clustering
- State Identification
  - Computing texture orientation features
  - Identifying crossed-area state
- State recognition
  - Autocorrelation
  - Finding the weave repeats
  - Correcting errors

By using two-dimensional integral projection to segment crossed-areas of yarns, the crossed-area of uneven distributed yarns can be detected. The FCM is applied to multi-scale texture features based on Grey level occurrence matrix in order to classify the different crossed-area states. The texture orientation features are calculated to determine the exact state of crossed-area. The further enhancement is made by using the principal component analysis (PCA) to improve the classifier performance. An error correction method is added as final step in order to correct the detection errors in some crossed-areas.

3.2.1.1 Image acquisition and pre-processing

The fabric sample images are obtained by using optical scanner. The images are resized in to 600×600 and then converted into gray scale in order to increase the processing speed.

It is inevitable there is image noise that is produced by the sensor and circuitry of the scanner.The image noise is the random variation of the brightness in images. It reduces the image quality. Especially it is significant when the interested object is the texture of fabric images. The recognition algorithm requires high contrast and detailed texture information. Therefore, noise reduction filter should be carefully chosen as the first step of the pre-processing. Spatial domain median filter, which is small and fast, is commonly used to reduce the noise caused by original image acquisition [43, 44, 50]. Instead of using median filter, the Butterworth filter in frequency domain is chosen in order to preserve the small details, such as hairiness, the orientation of fibers which are spreading over the crossed-area of yarns. It is because that the Median filter may blur the information as shown in the Figure 3.5. The loss of detailed information may cause recognition errors of the classifier.

The transfer function of the Butterworth lowpass filter of order n with cutoff frequency locus at a distance D_0 from the origin is defined by the following equation.

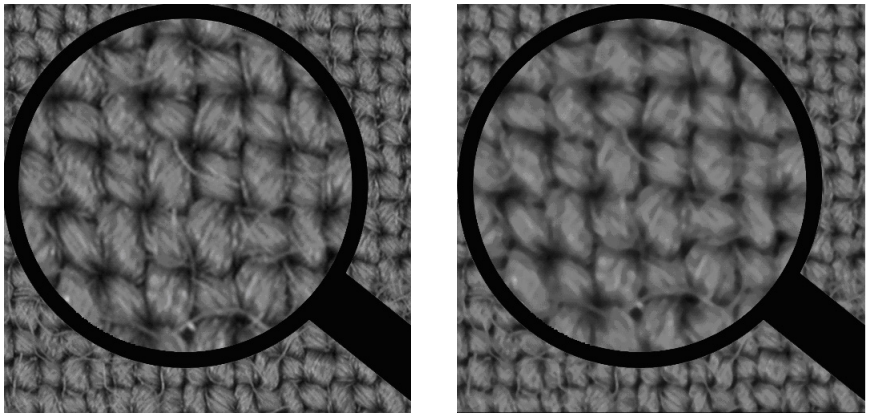

(a) 10^{th}-order Butterworth filter (b) 3×3 median filter

Figure 3.5: The performance of noise reduction filters

$$H(u,v) = \frac{1}{1 + (\frac{u^2+v^2}{D_0^2})^n} \tag{3.1}$$

where u and v are the frequency variables. A perspective plot of the Butterworth lowpass filter is shown in Figure 3.6a. The transfer function of the Butterworth highpass filter of order n and with cutoff frequency locus at a distance D_0 is defined by the Equation 3.2. Figure 3.6b shows a perspective plot of the Butterworth highpass filter. By combining a lowpass filter and a highpass filter, a bandpass Butterworth filter is constructed.

$$H(u,v) = \frac{1}{1 + (\frac{D_0^2}{u^2+v^2})^n} \tag{3.2}$$

For this study, a 10^{th}-order lowpass Butterworth filter with cutoff frequency 0.3 is chosen. Figure 3.7 illustrates the original fabric image and filtered fabric image and their power spectra.

The exponential transformation function is used for histogram equalization. The contrast of images is enhanced after equalization. Figure 3.8. shows the results of image enhancement.

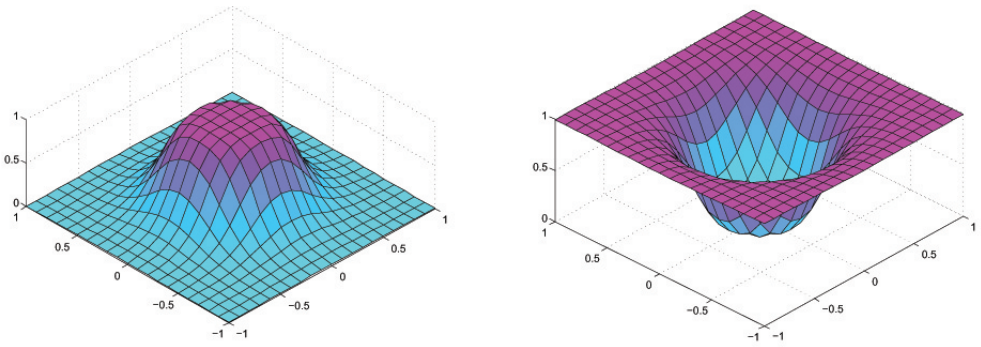

(a) 3^{rd}-order lowpass Butterworth (b) 3^{rd}-order highpass Butterworth

Figure 3.6: The perspective plots of lowpass and highpass Butterworth filters

3.2.1.2 Crossed-Area segmentation

In order to detect the interlacing area where weft yarn and warp yarn are crossed over each other, a spatial domain integral projection approach is applied. Interstices between yarns display darkness, therefore, the pixels around them have relative lower grey levels. By looking for the local minima of the horizontal and vertical integral projections, the positions of interstices among yarns can be located. Suppose $I(x, y)$ be an $M \times N$ gray scale image. The horizontal and vertical projection of the entire image is defined respectively as $H(y)$ and $V(x)$ shown in the Equations 3.3 and 3.4:

$$H(y) = \sum_{x=1}^{N} I(x, y) \tag{3.3}$$

$$V(x) = \sum_{y=1}^{M} I(x, y) \tag{3.4}$$

Due to image complexity and noise, there are some small weaves throughout the projection curve, which interfere with actual local minima location detections. Therefore, we use a moving average filter to smooth the curves. The enhancement of smoothing is shown in Figure 3.9. The left panel depicts an integral projection curve without smoothing. Undesired local minima, which are highlighted by a circle, are removed after

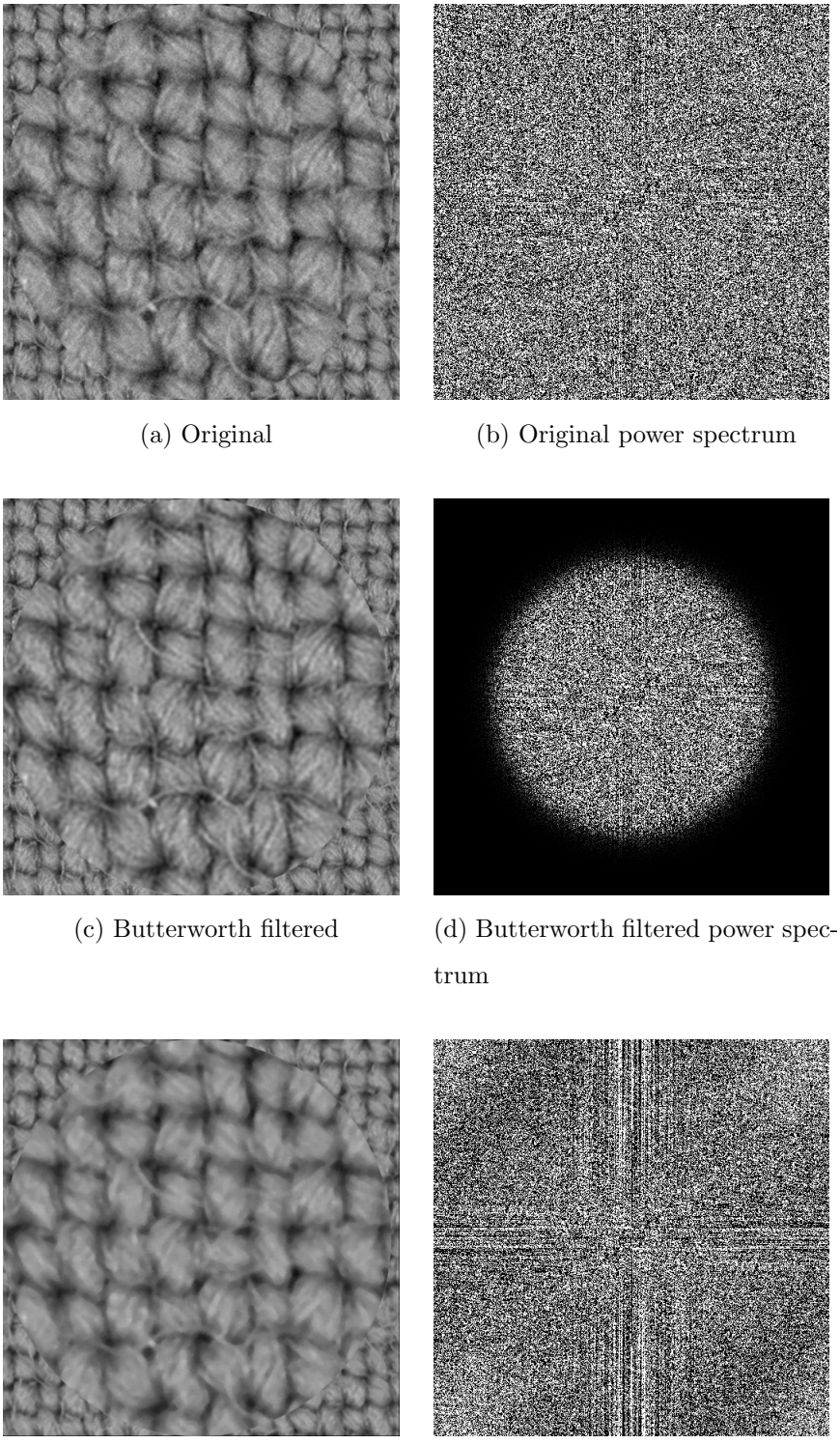

(a) Original

(b) Original power spectrum

(c) Butterworth filtered

(d) Butterworth filtered power spectrum

(e) Median filtered

(f) Median filtered power spectrum

Figure 3.7: The comparison between original fabric image and filtered images

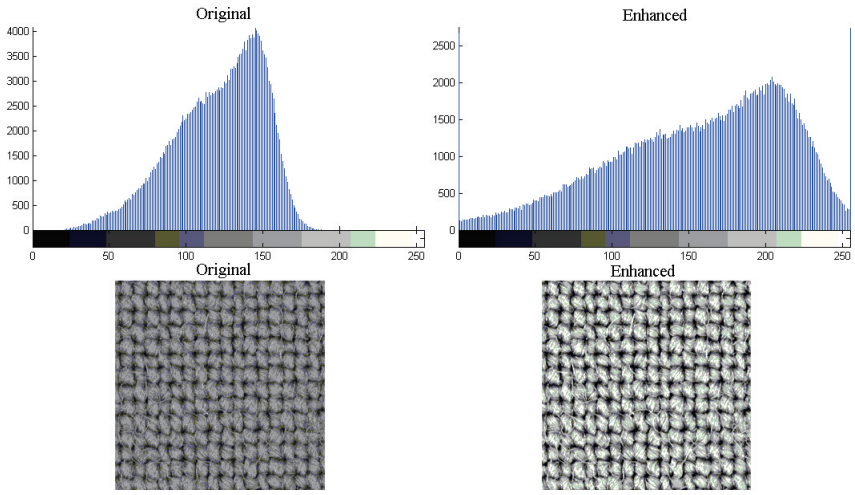

Figure 3.8: The comparison between original and enhanced fabric images

smoothing (shown in the right panel).

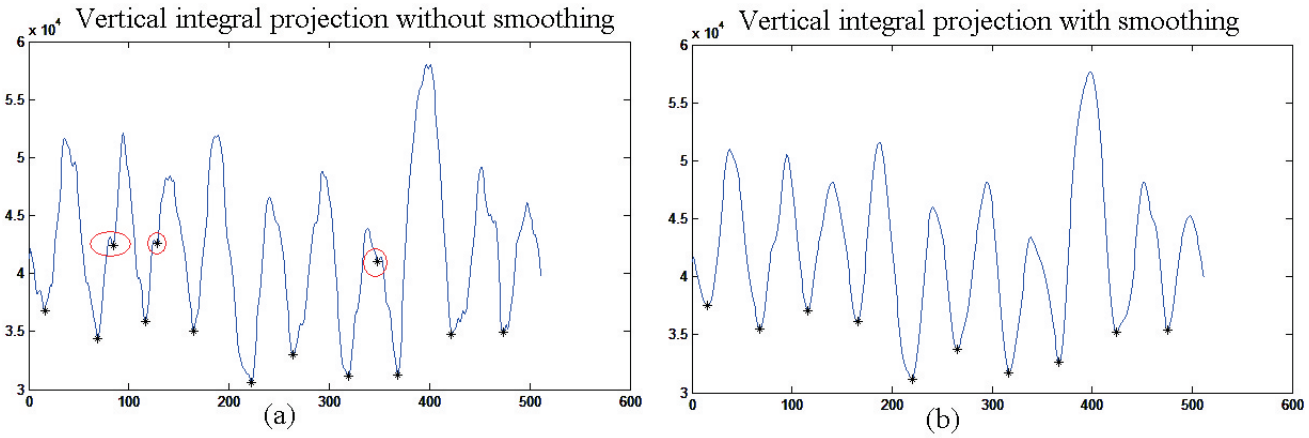

Figure 3.9: Integral projections (a) original projection curve (b) projection curve after smoothing

Figure 3.10 illustrates the relation between a woven fabric sample and its integral projections. The interstices between yarns exhibit the local lowest values. By finding the local minima of horizontal and vertical integral projections, the warp separation lines and weft separation lines are found respectively. The crossed-areas are identified by intersecting the warp separation lines with weft separation lines.

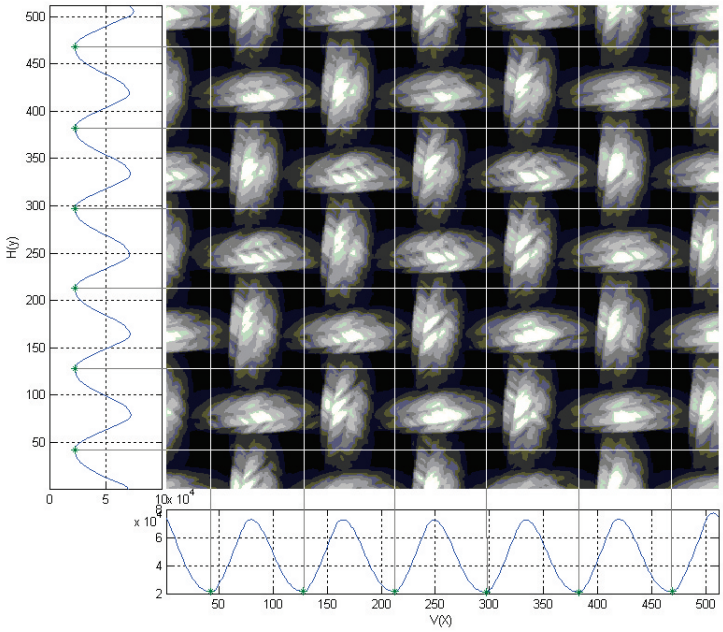

Figure 3.10: Crossed-area detection

3.2.1.3 Crossed-Area State Recognition

Once the crossed-areas of weft and warp yarns are detected, the fabric image is segmented into small image cells which express the detected crossed-areas. In order to determine the state of a crossed-area its texture features have to be analyzed.

Multi-scale and Direction Invariant Texture Feature Extraction based on Grey Level Co-occurrence Matrix (GLCM)

Image textures, defined in this work, are measurements, which characterize an object's surface. An image usually contains more than one texture descriptions. The texture measurements are used as vehicles being collected together to recognize different objects. Among approaches, which derive the texture features (i.e. measurements) are the gray level occurrence matrix (GLCM) based measurements-the most famous statistical method. Haralick [27] first proposed GLCM for texture descriptions in the 1970s. It is still popular until today, because of its good performance. The texture of an im-

age is represented by the change of image gray levels. The gray level occurrence matrix (GLCM) of an image shows the statistic characteristics of gray level or gray level gradient under the condition of a certain spatial position. The features extracted from GLCM are related to the density of fiber and the orientation of yarn on a crossed-area. The GLCM based texture features are used to discriminate the different crossed-area states.

The GLCM is computed based on two parameters, which are the distance d between the pixel pair and their angular relation θ. θ is quantized in four directions (0°, 45°, 90° and 135°). For rectangular $M \times N$ image segment $I(x, y)$, gray levels i and j, the non-normalized GLCM P_{ij} are defined by:

$$P_{ij}(\theta, d) = \sum_{x=1}^{N} \sum_{y=1}^{M} C\left\{(I(x, y) = i) \wedge (I(x \pm d\theta_0, y \mp d\theta_1) = j)\right\} \tag{3.5}$$

where $C\{\cdot\} = 1$ if the argument is true and $C\{\cdot\} = 0$ otherwise. The $\pm$ and $\mp$signs in 3.5 mean that each pixel pair is counted twice: once forward and once backward in order to make the GLCM diagonal symmetric. For each direction, θ_0 and θ_1 are shown in Table 3.1.

Table 3.1: Detection Value

θ	0°	45°	90°	135°
θ_0	0	1	1	1
θ_1	1	1	0	-1

Before texture calculation, the non-normalized GLCM is normalized, thus, it represents probabilities instead of occurrence counts. Normalization involves dividing by the total number of counted pixel pairs.

Eight GLCM texture features are calculated. They are studied by Haralick [27]: contrast(CON), dissimilarity (DIS), homogeneity (HOM or inverse difference moment), angular second moment (ASM), entropy (ENT), GLCM mean (μ_i, μ_j), variance (VAR:

σ_i^2, σ_j^2), and correlation (COR). For normalized GLCM $P_{i,j}$ and L gray levels, the eight features are defined as follow.

$$CON = \sum_{i,j=0}^{L-1} P_{i,j}(i-j)^2 \tag{3.6}$$

$$DIS = \sum_{i,j=0}^{L-1} P_{i,j}|i-j| \tag{3.7}$$

$$HOM = \sum_{i,j=0}^{L-1} \frac{P_{i,j}}{1+(i-j)^2} \tag{3.8}$$

$$ASM = \sum_{i,j=0}^{L-1} P_{i,j}^2 \tag{3.9}$$

$$ENT = \sum_{i,j=0}^{L-1} P_{i,j}(-\ln(P_{i,j})) \tag{3.10}$$

$$\mu_i = \sum_{i,j=0}^{L-1} i(P_{i,j}) \; and \; \mu_j = \sum_{i,j=0}^{L-1} j(P_{i,j}) \tag{3.11}$$

$$\sigma_i^2 = \sum_{i,j=0}^{L-1} P_{i,j}(i-\mu_i)^2 \; and \; \sigma_j^2 = \sum_{i,j=0}^{L-1} P_{i,j}(j-\mu_j)^2 \tag{3.12}$$

$$COR = \sum_{i,j=0}^{L-1} P_{i,j} \left[\frac{(i-\mu_i)(j-\mu_j)}{\sqrt[2]{(\sigma_i^2)(\sigma_j^2)}} \right] \tag{3.13}$$

The eight texture features are correlated with one another [88]. According to the structure of calculation, the eight features can be divided into three groups: the contrast group, the orderliness group, and the descriptive statistic group. DIS and HOM are measures related to CON by using weights related to the distance from the GLCM diagonal. All three features highlight the similarity or dissimilarity of grey tones in the test window. They can be grouped together consequently. ASM and ENP, as a group, both describe how regular the pixel grey levels are within the test window. The last three features are statistics derived from GLCM.

The width of yarns varies from sample to sample. The orientations of fibers which form the yarn also change over the detected crossed-areas. To reduce the recognition errors caused by the above issues, the features, which are defined by equation 3.6-3.13 are computed by using multiple distance $d = 1, 2, 4, 6, 8, 10$ pixels and four angular directions respectively. Thus, for each detected crossed-area we have $8 \times 6 \times 4 = 192$ texture features. A feature vector of detected crossed-area is formed by these 192 values.

Principal Component Analysis

A feature vector has 192 elements. By definition [27], GLCM features are interrelated. Moreover, the diversity of the fabric samples also makes the measured feature vectors become confusing. The measured feature vector sets appear clouded, and may be redundant. This obstructs the accuracy of the next classification. As a standard tool in modern data analysis, PCA applies to large areas from image processing to bioscience. The goal of PCA is to extract relevant information from data sets consisting of a large number of interrelated variables [89]. Therefore, PCA is the optimal method to solve our above problems. The goals for using PCA are (i) to minimize redundancy in our feature vector sets and (ii) maximize the signal which expressed by our feature vectors.

The basic idea of PCA is to identify the most meaningful basis to re-express the data set. In this work, we assume that each fabric image has m detected crossed-areas and each crossed-area is expressed by a feature vector with 192 elements. The feature data set for a fabric image is a $192 \times m$ matrix X. By using PCA, we aim at finding a new basis B which will reveal an optimal representation Y of the original data set X. The row vectors of B will become the principal components of X. Geometrically, B is a linear transform which rotates and stretches X into Y:

$$BX = Y \tag{3.14}$$

The basic steps for determining B in our studies are:

Step 1: Calculate the mean of each dimension:

$$\bar{x}_i = \sum_{j=1}^{m} x_{ij} \tag{3.15}$$

Step 2: Subtract off the mean for each dimension in order to produce a zero mean data set $\tilde{X}$

Step 3: Construct the matrix Y where $Y = \tilde{X}^T/\sqrt{m-1}$.

Step 4: Compute singular value decomposition (SVD) [90] of matrix of matrix Y. SVD produces a diagonal matrix S with nonnegative diagonal elements in decreasing order, and unitary matrices U and V so that $Y = USV^T$. The column vectors ν_i of V are the principal components.

Step 5: Choose first k principal components ν_i by using the following criterion:

$$\frac{\sum_{i=1}^{k} \lambda_i}{\sum_{i=1}^{n} \lambda_i} > Threshold \tag{3.16}$$

where λ_i represents the main diagonal elements of S. m is the number of dimension in our case 192. We choose the threshold as 0.95. Thus a new linear transform B is formed by $B = [v_1 v_2 \dots v_k]^T$.

Step 6: Project the data set to an optimized feature vector set Y by applying equation 3.14.

The first benefit of the PCA method is dimension reduction. The dimension of our new feature data set Y is no longer 192 but $k << 192$. According to our experimental results, k varies over the range from 1 to 17 for different fabric samples. k tends to be larger when the hairiness and orientation of fibers in crossed-areas are messier. The average size of k is around 6. The other primary motivation behind this method is to de-correlate the original data in order to remove second-order dependencies for accurate classification in next step.

Fuzzy C-means Clustering

We use FCM [91] to classify the two possible different crossed-area states. FCM is based on minimizing the following objective function for the partition of data set, $X = \{x_1, x_2, \ldots, x_n\}$, given by:

$$J_m = \sum_{i=1}^{c} \sum_{k=1}^{n} u_{i,k}^{m} \left\| x_k - v_i \right\|^2 \tag{3.17}$$

In equation 3.17, n is the number of data vectors, c is the number of clusters with $1 < c \leq n$, $u_{i,k}$ is the degree of membership of x_k in the i^{th} cluster, $m(1 < m < \infty)$ is a weighting exponent that influences the fuzziness of the membership function , and v_i is the center of the i^{th} cluster. The norm $\|x_k - v_i\|$ is the distance between the sample x_k and the centers of classes v_i.

In our studies, we want to classify a set of texture feature vectors with k dimensions into two clusters. The algorithm can be summarized by the following steps:

Step 1: Initialization (iteration 0)

Scan the yarn crossed-areas through the whole sample image to construct the data set X containing the feature vectors of each crossed-area segments.

Set $c = 2$, $m = 1.5$.

Randomly choose the centers of clusters v_i.

From the iteration $t = 1$ to the end of the algorithm.

Step 2: Compute the membership function $u_{i,k}$ using:

If $\|x_k - v_i\| = 0$ then set $u_{i,k} = 1$ and $u_{i,k} = 0$ (for $i \neq k$)

If $\|x_k - v_i\| \neq 0$ then

$$u_{i,k} = \left(\sum_{j=1}^{c} \left(\frac{\|x_k - v_i\|}{\|x_k - v_j\|} \right)^{2/m-1} \right)^{-1} \tag{3.18}$$

Step 3: Update the positions of the centers v_i using:

$$v_i = \frac{\sum_{k=1}^{n} u_{i,k}^m x_k}{\sum_{k=1}^{n} u_{i,k}^m} \tag{3.19}$$

Step 4: Termination test: If $\|U^{(t+1)} - U^{(t)}\| > \varepsilon$, then increment the iteration t, and back to the **Step 2**, otherwise, stop the algorithm. ε is the termination criterion.

Since the feature data set has more than three dimensions, the results of classification cannot be shown in a single diagram. Figure 3.11 illustrates the clustering of FCM by the two texture features (ENT and VAR) for a fabric sample.

Once we find two clusters of crossed-area segments, we have to determine their exact states in which the warp is interlaced over the weft or vice versa. Since the woven fabric is made only by interlacing the warp yarns in the vertical direction and the weft yarns in the horizontal direction, the orientations of the texture in detected segments are different depending on the type of the float yarn as shown in Figure 3.12. By analyzing the texture orientation features of the clusters, we can recognize their actual states.

We compute average 'covariablilities' [92] as the texture orientation features in order to determine the state of the crossed area. These features show gray level average difference between two pixels according to their distance d and orientation. Horizontal and vertical covariablilities in a detected segment $I(x, y)$ with size $M \times N$ are calculated as following:

$$COV\_H(d) = \frac{1}{M \times (N-d)} \sum_{y=1}^{M} \sum_{x=1}^{N-d} |I(x, y) - I(x+d, y)| \tag{3.20}$$

$$COV\_V(d) = \frac{1}{N \times (M-d)} \sum_{x=1}^{N} \sum_{y=1}^{M-d} |I(x, y) - I(x, y+d)| \tag{3.21}$$

We compute the average horizontal and vertical covariablilities of each classified cluster. A fuzzy rule based decision is made for each cluster. The cluster with higher

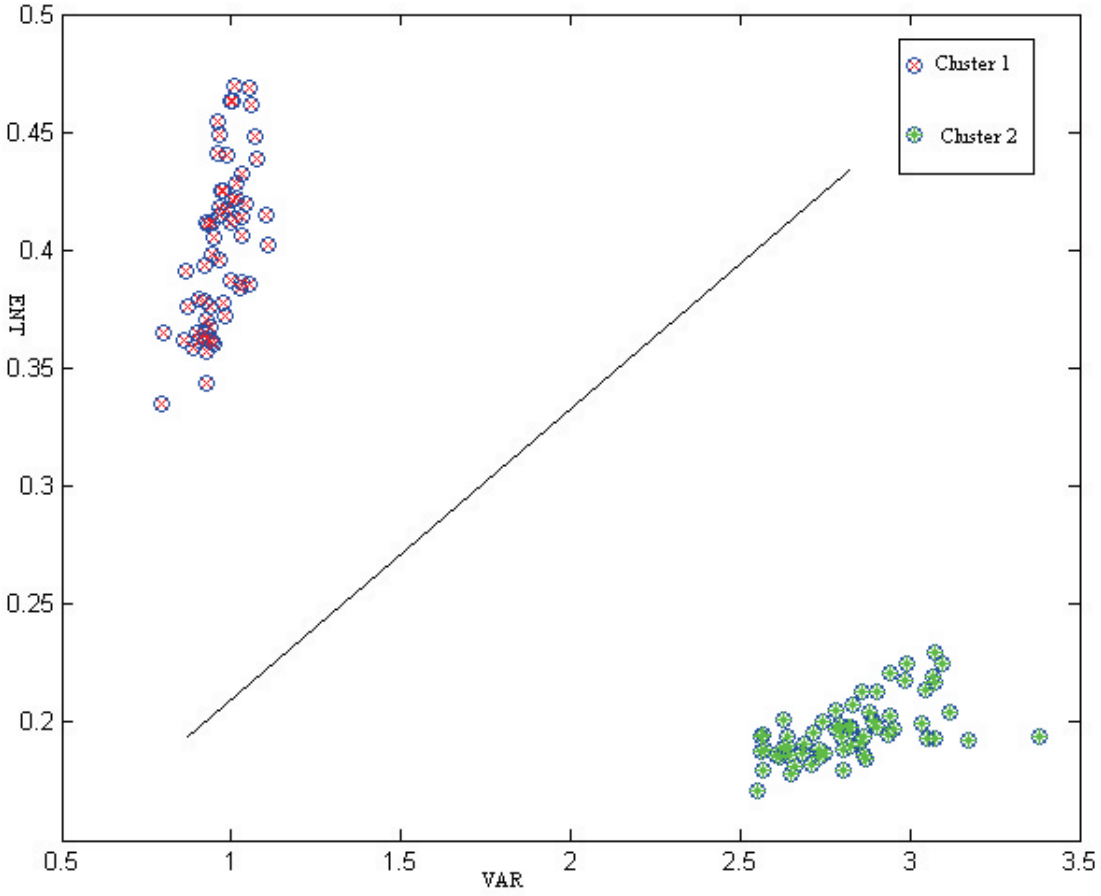

Figure 3.11: An example of FCM clustering

horizontal covariablilities and lower vertical covariablilities is determined as weft float, namely the weft yarn is crossed over the warp yarn, and the other cluster is warp float.

3.2.1.4 Weave Pattern Detection and Error Correction

We use $0s$ and $1s$ to denote two different crossed-area states i.e. the weft float and the warp float respectively. For a fabric sample, a matrix C, which represents the detected crossed-area states, is formed with $0s$ and $1s$. We assume that the fabric sample has M warp yarns and N weft yarns. Thus, there are $M \times N$ crossed-areas detected in the fabric sample and the size of C is $M \times N$. Let matrix W denote the basic unit of weave, i.e.

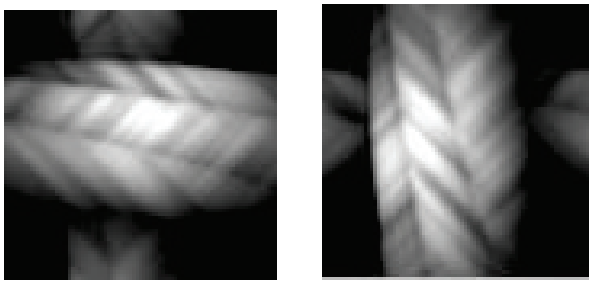

(a) Weft float (b) Warp float

Figure 3.12: Detected crossed-areas

weave pattern. Thus, C can be formed by tiling the basic unit matrix W periodically. The size of W can be found from the two-dimensional autocorrelation of C by finding the fundamental periods in weft and warp directions. The autocorrelation matrix R is computed as follow:

$$\begin{aligned} R(i,j) &= \sum_{m=1}^{M}\sum_{n=1}^{N} C(m,n)C(m+i,n+j) \\ i &= 1,\ldots,2M-1; j = 1,\ldots,2N-1 \end{aligned} \tag{3.22}$$

The fundamental period in warp direction (n_0) is determined by the integer distance from the center element $R(M,N)$ to the nearest peak in the $N-th$ column. Similarly the fundamental period in weft direction (m_0) is the integer distance from $R(M,N)$ to the nearest peak in $M-th$ row. The size of W is $m_0 \times n_0$. In order to determine W, we cut an $m_0 \times n_0$ tile W' from C randomly. A matrix C' is formed by repetitively titling W'. In most cases, there are detection errors in C, the selected W' may have error as well. C', as an estimate of C, may have a number of different elements from C. The detection error of the fabric sample is computed by counting these different elements. We assume that the majority of the crossed-area states are detected correctly. Therefore, the tile W' with the lowest value of detection error is chosen as the basic weave pattern. The corresponding C' represents the correct detected crossed-area states.

Figure 3.13 illustrates an example of weave pattern detection and error correction.

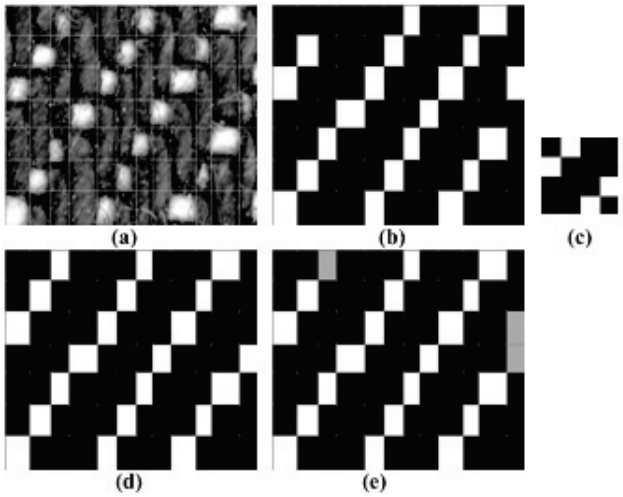

Figure 3.13: An example of weave patterm detection and error correction. (a) a fabric sample (b) the detected crossed-area states (c) the basic weave pattern (d) the estimation of crossed-area states (e) the detected error

A fabric sample is shown in (a). The black blocks and the white blocks represent the warp float and weft float respectively. The detected crossed-area states without error correction are shown in (b). The basic weave pattern is identified in (c). After the error correction process, three errors, which are denoted by grey blocks, are detected as shown in (e). The detection errors occur in the classification step. Figure (d) illustrates the correct crossed-area states.

3.2.2 Automatic Measurement of Yarn Count

Yarn count is defined as the number of yarns per centimeter. Vision-based image analysis has been used to monitor yarn density and yarn counts in many papers. For example, H. Sari-Sarraf and J. S. Goddard [93] determined the yarn density by analyzing the power spectrum of fabric images. However, the power spectrum of the original fabric image is too noisy to analyze in most cases. Instead of applying FFT to entire original fabric image, we take advantage of horizontal and vertical projections i.e. $H(y)$ and $V(x)$

which are computed in section A. We consider $H(y)$ and $V(x)$ as weft profile and warp profile respectively. Yarn counts are determined from the one dimensional FFT of the profiles. In power spectrum, an overwhelming spike next to the zero depicts that the individual share of the width of a yarn. The reciprocal of the distance from the spike to origin is the estimate of the yarn count. Figure 3.14 illustrates a weft profile, a warp profile of a plain weave sample and their power spectra.

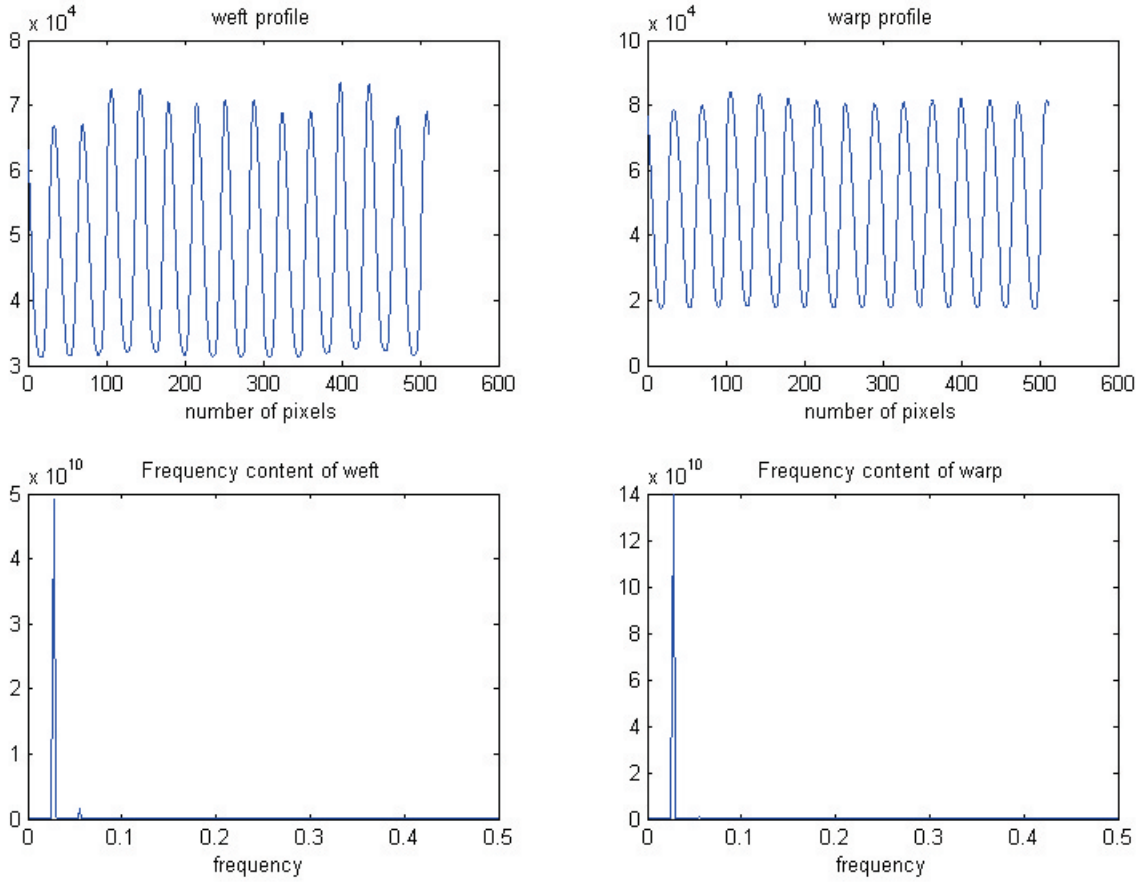

Figure 3.14: An example of weft, warp profiles and their power spectra

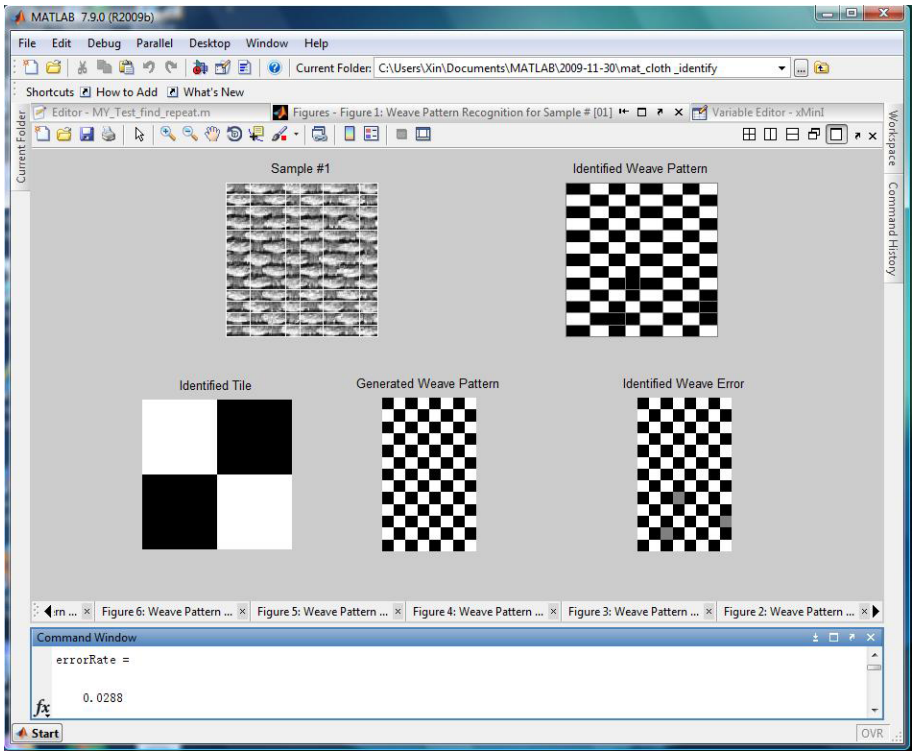

Figure 3.15: The interface of weave pattern recognition

3.3 Experiment and Results

The proposed method is implemented in Matlab. A screen shot of the interface is shown in Figure 3.15. A number of computer simulated woven material images, and a number of fabric images extracted from different real woven fabrics are used for evaluation. These images have different weave types, fiber appearances, and yarn counts. Simulated woven samples are generated in Filter Forge by applying programmable image processing filters. The real fabric images are scanned by using an HP scanner (Scanjet 4570c) with a resolution of 2400dpi. For real fabric scan, it is very important to arrange the warp and the weft yarns properly along x and y directions in order to achieve best performance for the crossed-area detection. Then the images are resized into 600 $\times$ 600 pixels and then converted into gray scale for increasing the processing speed.

To evaluate the proposed method, both computer simulated samples and real woven

Table 3.2: The Detection Error Rate for Real Fabric Samples

Sample	**P1**	**P2**	**P3**	**P4**	**P5**	**P6**	**T1**	**T2**	**Average**
Error Rate	0.029	0	0.044	0.035	0.028	0.029	0.036	0.018	0.027

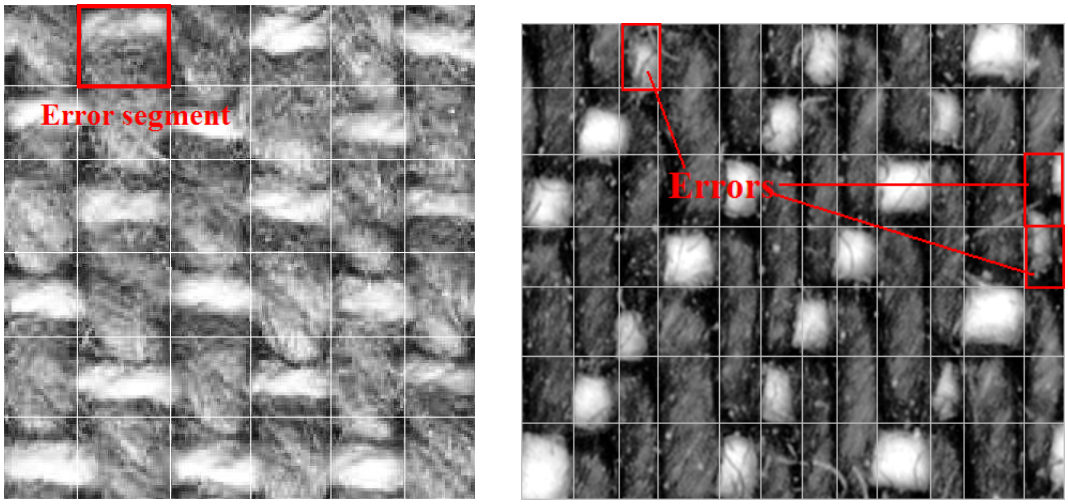

(a) sample 5 (b) sample 7

Figure 3.16: The examples of detection errors

fabric images were used. These images have different weave types, fiber appearances, and yarn counts. Figure 3.18 shows part of computer simulated woven material images and Figure 3.19 shows the real fabric samples that we used. The recognition rate for computer simulated images is 100% before the error correction module. The error rate for real fabric samples is shown in Table 3.2. The error may be caused by a local defect of the fabric surface, low quality of the fabric image, or a bad segmentation. Figure 3.16 illustrates some examples of error. Since more than 95% crossed-area states are correctly detected, the result conforms to the assumption we made for our error correction algorithm. The recognition rates increased to 100% after error correction.

From the obtained results, we can conclude that with the proposed method for au-

tomatic weave structure recognition, all actual weave structures are well detected in different samples which have different weave types, yarn appearances and yarn counts. The yarn counts were repetitively computed five times with different segments of the same fabric sample. The results are shown in Figure 3.17. The high consistency with the manual measurements shows the validity of our method. The low average variance demonstrates the reliability of our method. The test variance tends to be higher when the variance of the yarn width or the variance of yarn distribution is larger. The manual counts are slightly higher than the computer determined yarn count because we round up the decimal numbers of yarn to integers during the manually count.

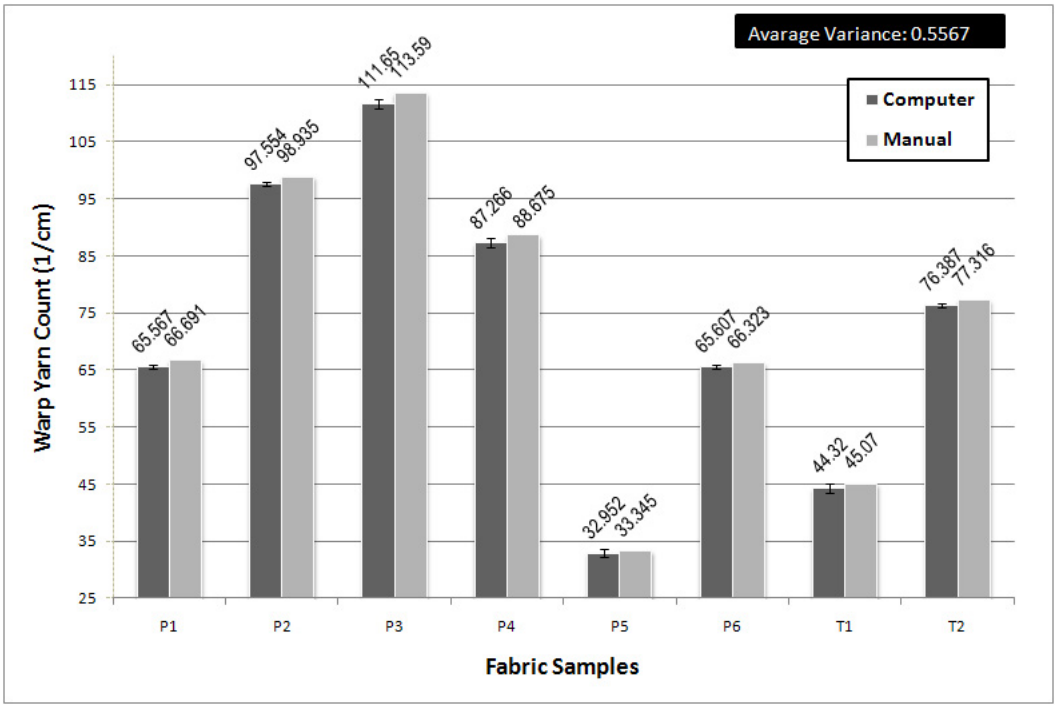

(a) Warp count

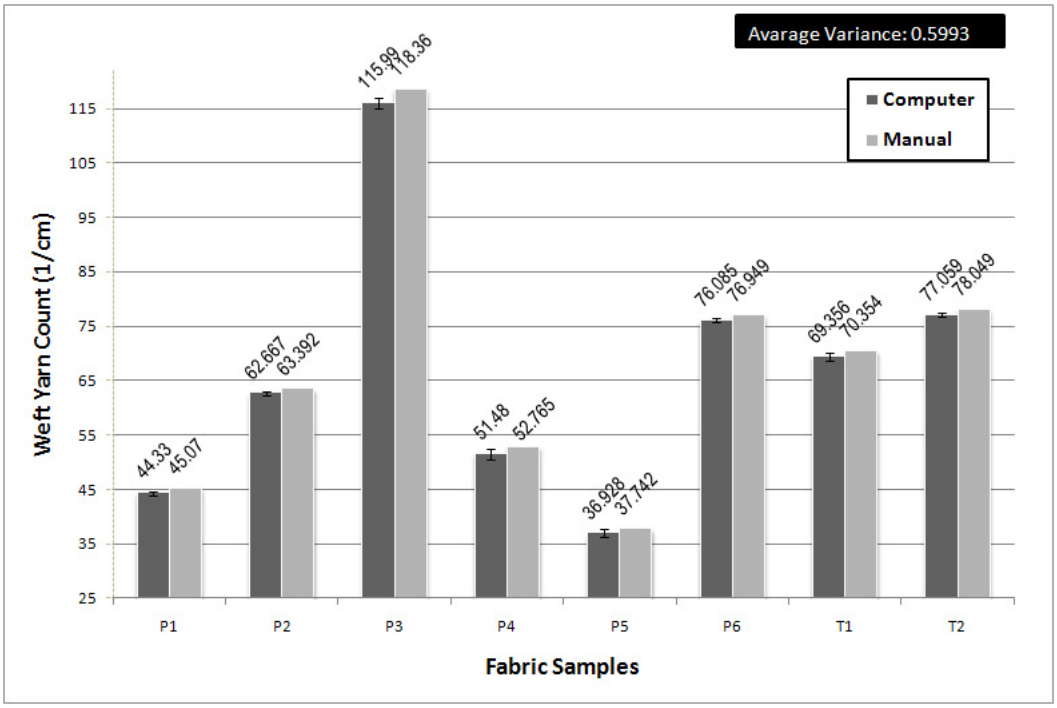

(b) Weft count

Figure 3.17: Yarn counts for real fabric samples. p1-p5: plain weave samples. t1-t3: twill weave samples

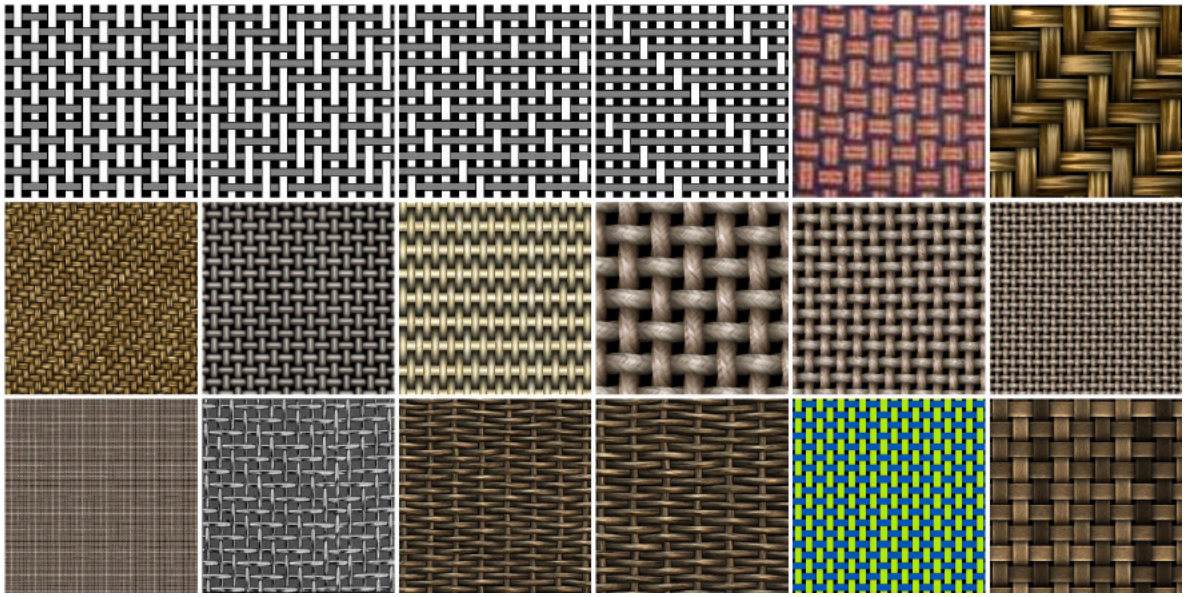

Figure 3.18: Part of computer simulated samples used in weave structure recognition

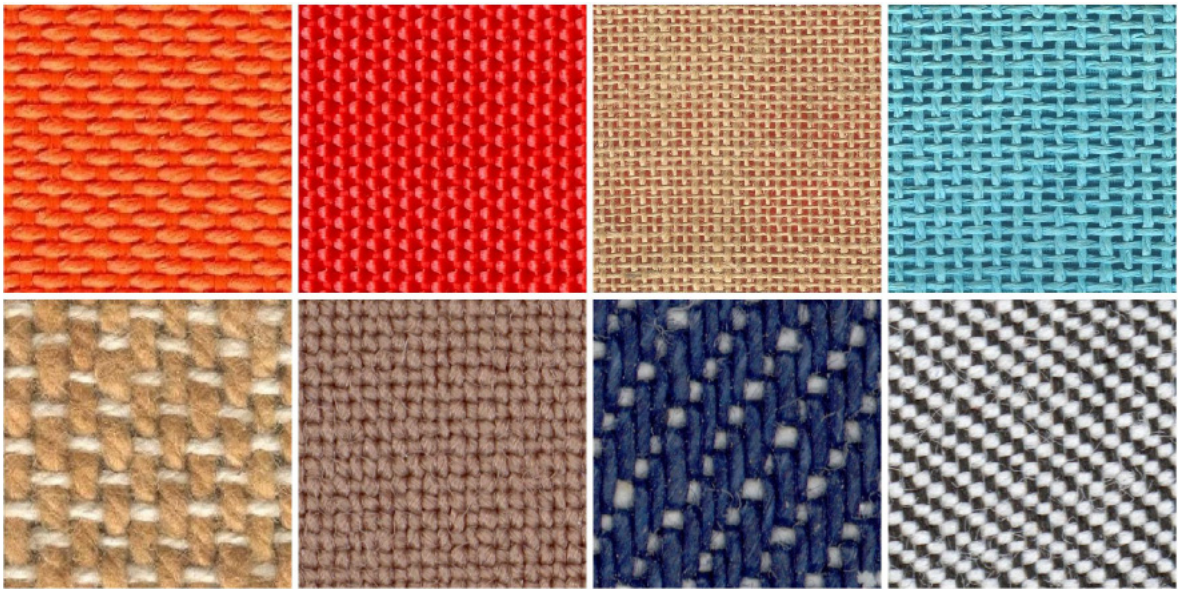

Figure 3.19: Real woven fabric samples used in weave structure recognition

Chapter 4

Surface Roughness Measurement

This chapter presents a methodology for using the high resolution three dimensional (3D) surface data of fabric samples to acquire their surface roughness parameter measurement. Firstly, a parameter FD_{FFT} , which is the fractal dimension estimated from the two-dimensional fast Fourier transform (2DFFT) of 3D surface scan, is proposed. The rotation-invariance and scale-invariance of FD_{FFT} is validated by using fractal Brownian images. Secondly, in order to evaluate the correctness of FD_{FFT} , a method of calculating standard roughness parameters from 3D fabric surface is presented. The test results demonstrate that FD_{FFT} is a fast and reliable parameter for fabric roughness measurement based on 3D surface data. Finally, we attempt a neural network model using back propagation algorithm and FD_{FFT} for predicting the standard roughness parameters. The performance of the prediction model is shown experimentally.

The chapter is organized as follows. In section 4.1 the basics and related works of surface roughness measurement are introduced. In section 4.2 the proposed parameter of surface roughness and the modified traditional roughness parameter computation are presented. A neural network model is stated for prediction of the traditional roughness parameter. In section 4.3 the experimental validations are provided and a discussion of the results is presented as well.

4.1 Introduction and Related Work

Surface roughness is a very important property of fabric in terms of both physical quality and aesthetic aspect. For instance, to a certain extents it affects the human being's appreciation of the fabric. The feeling of comfort can be influenced greatly by the sensation perceived from the contact of clothing with the skin. There are two types of fabric surface roughness assessment: subjective methods and objective method. Primarily fabrics are evaluated subjectively in a few minutes by textile professionals. The organization AATCC (American Association of Textile Chemist and Colorists) has published guidelines for the standardization of the subjective fabric assessment, which propose possible evaluation conditions [8]. The human evaluator should fully concentrate and be in contact with no other materials than the fabrics. To assess the roughness property, the evaluator's fingers stroke over the fabric. Both sides in warp and weft direction are assessed separately. Roughness is evaluated by his/her thumb as shown in Figure 4.1a. Standard references are presented to the evaluator during the assessment(Figure 4.1b). This is a fast and convenient method to determine the sensory properties of fabric samples. However, the subjective nature may cause serious variation when determining the evaluation levels. For example, if a panel of people is assessing the fabrics, individual evaluator maybe perform the test under different physical and psychologic conditions and a consistent test results can not be guaranteed.

An objective measurement of fabric roughness is relatively more stable in the evaluation of different fabric samples. The most widely used objective measurements system is Kawabata Evaluation System for Fabrics (KES-F) [15].

The KES-F system has an instrument specifically designed for evaluating fabric surface roughness (Figure 4.2). It measures a one dimensional height/thickness profile along a segment of the fabric. The fabric is moved under the sensor as shown in Figure 4.3. The tension of the fabric is kept at certain level along the measurement direction. The contactor of the sensor is a steel piano wire as depicted in Figure 4.4.

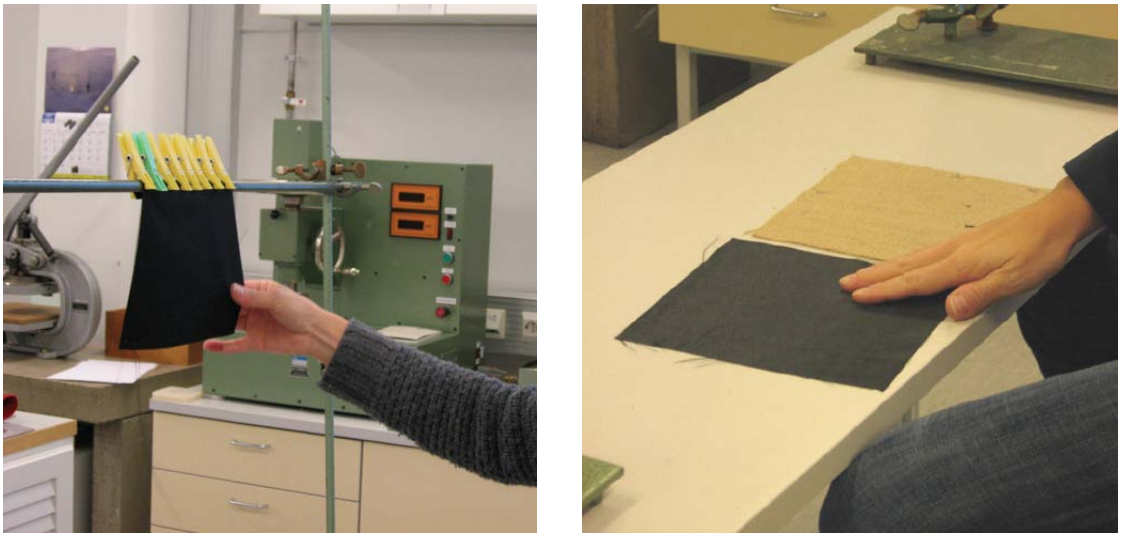

(a) Evaluation on face side (b) Standard references

Figure 4.1: An example of subjective evaluation of fabric roughness

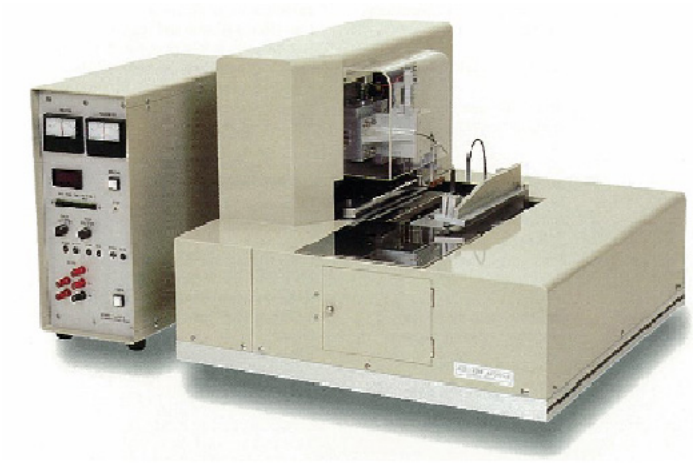

Figure 4.2: The KES-F surface tester

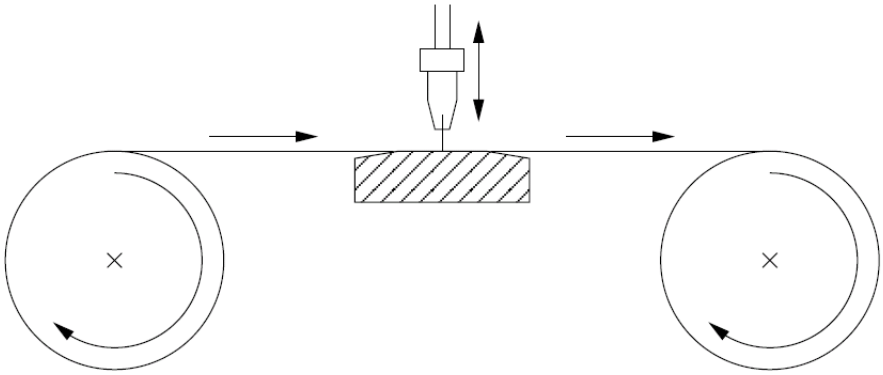

Figure 4.3: Schematic diagram of the KES-F surface tester

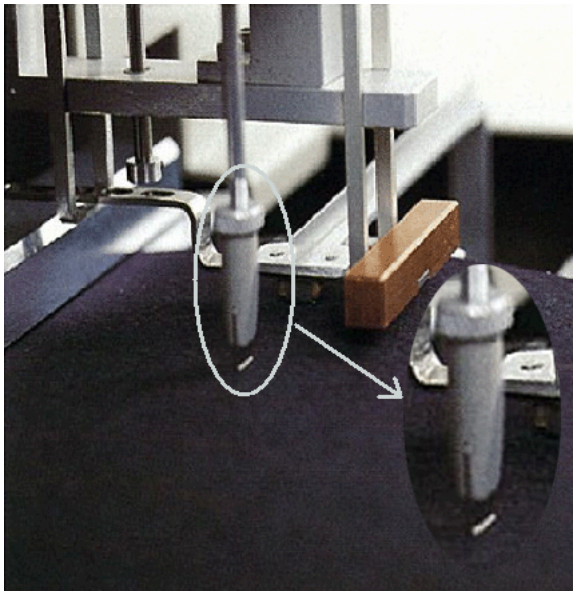

Figure 4.4: The contactor of the KES-F surface tester

Figure 4.5: Fabric stretching and accumulation and yarn twisting during KES-F roughness measurement

However, the force, which is imposed when measuring, actually affects the accuracy of the roughness measurement. The deformation of textile fabric, which is caused by the direct physical contact of the KES-F instrument, disturbs the measured surface profile. For example, as shown in Figure 4.5, when sensor travels on the surface some sample tend to stretch during the measuring and accumulate a fabric ridge in front of the sensor which may cause peak values when the sensor jumps over the ridge. Moreover, the roughness profile obtained from the KES-F tester is just one dimensional. 3D surface roughness data can only be acquired by doing multiple scans of fabric surface. It is slow and needs a complicated operation of the instrument. Therefore, the trend to use the non-contact method of surface roughness assessment on 3D surface data is inevitable and beneficial.

In recent years, along with the revolution of computer vision and image processing technology, numerous methods for non-contact surface roughness assessment were proposed by scientists. For example, G. Gunarathne [94] introduced the specular reflection coefficient as a surface roughness measure by using ultrasonic spectroscopy technique.

Optical fiber sensors had been employed to accurately measure surface roughness in [95, 96]. S. Moslehpour et. al. [97] developed a portable surface roughness inspection probe to optically evaluate surface finish quantitatively. From their work, it can be concluded that a non-contact surface roughness measurement is faster than the traditional stylus based method with high accuracy, and especially nondestructive.

Fractal dimension (FD) is a parameter frequently used to analyze surface roughness. There are several alternative definitions of the fractal dimension and consequently many algorithms have been proposed to determine its value. For example, Kang et al. [98] uses wavelet based fractal dimension measurement to evaluate the surface roughness of wrinkle replicas and seam pucker samples. The estimation of fractal dimension is computed by applying linear regression on the averages of absolute wavelet coefficients in horizontal and vertical directions with respect to the decomposition levels. Although their measurement is claimed to be scale-invariant, it actually is not robust to image rotations because only two direction data are studied.

In our studies [99, 100], we found that the fractal dimension measurement based on 2DFFT analysis of fabric images is a scale-invariant and rotation-invariant parameter to evaluate surface roughness of fabrics. A two dimensional Fourier Transform(2DFFT) based fractal method is applied to three dimensional(3D) surface data which are obtained from high resolution 3D laser scanning. A parameter called FD_{FFT} is obtained from this method. The reliability of FD_{FFT} is studied as well. A neural network model for predicting the standard surface roughness characteristic value is proposed. The calculation of standard roughness characteristic values using these 3D scans is also introduced as a supplementary reference in order to train and evaluate our neural network model. The performance of our proposed neural network model has been tested in the experiment as well.

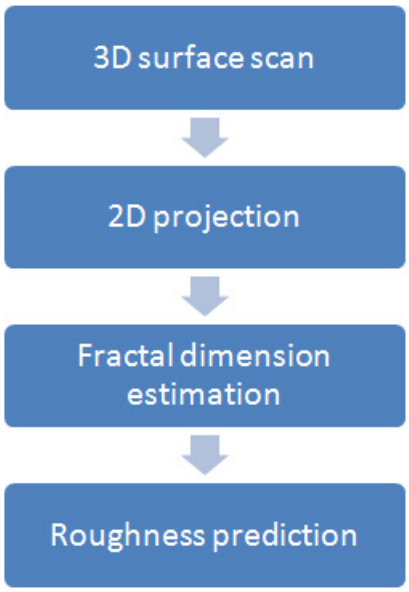

Figure 4.6: General steps

4.2 Methodology

The general steps of the algorithm is shown in Fig. 4.6 The fabric samples are scanned into three dimensional(3D) surface data. Fig. 4.7 shows two examples of 3D fabric sample surfaces. Later on, we use triangular linear interpolation to estimate fabric surface profiles on a two dimensional(2D) grid. In third step, we estimate the fractal dimension of the surface 2D profile. A neural network model is set up in the last step in order to predict the traditional roughness indicator.

4.2.1 The Estimation of Fractal Dimension

Bergmann et. al [101] proved that the tactile surface property, especially the surface roughness, can be evaluated by the fractal dimension of the surface. As shown in [102], the power spectrum $P(\omega)$ is proportional to the certain power β of the radial frequency ω.

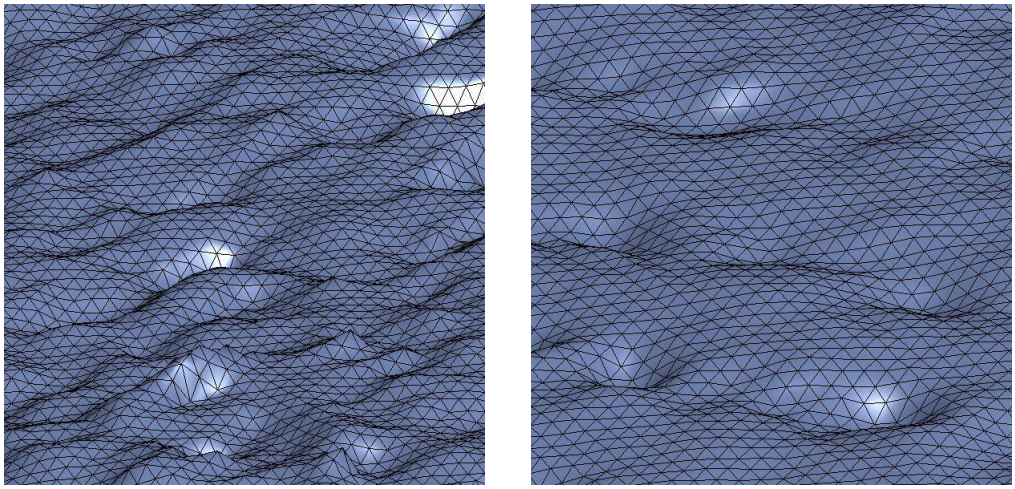

(a) Fabric sample 1 (b) Fabric sample 2

Figure 4.7: The example of high resolution 3D surface scans

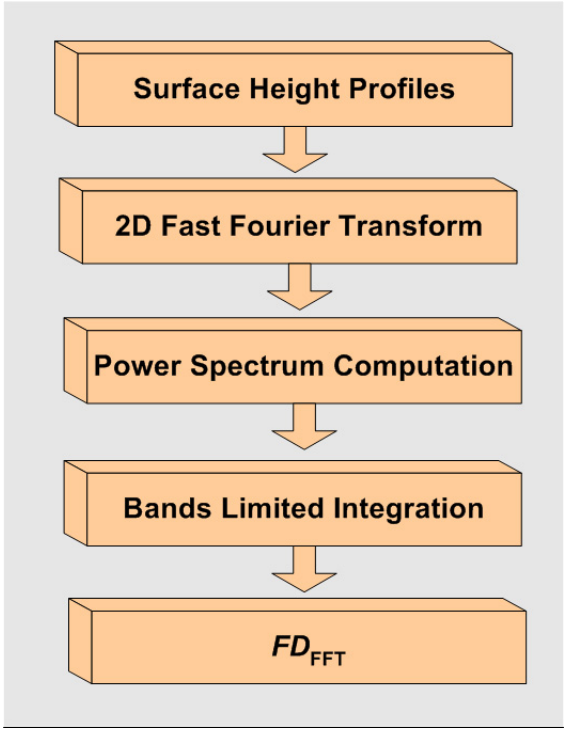

Figure 4.8: General steps of the computation of FD_{FFT}

$$P(\omega) \propto \omega^{-\beta} \tag{4.1}$$

where $\beta \geq 0$. The fractal dimension (FD) of an image is related to the exponent β in Equation 4.1.

$$FD_{FFT} = \frac{8-\beta}{2} \tag{4.2}$$

where FD_{FFT} denotes our fractal dimension estimate based on 2DFFT.

The general algorithm of our fractal dimension estimation is shown in Figure 4.8. Fabric samples are cut into pieces of size $5cm \times 5cm$. 3D points of the fabric surface are gathered from 3D laser scanning with very high resolution up to 1 micron. The raw 3D data consist of a large number of 3D coordinates with range from 281,880 to 523,308 points per fabric sample. Thus, there are around 11,230 to 20,930 points per square centimeter. Originally these points are not uniformly distributed over the 3D space; therefore, it is too difficult to apply a data processing algorithm. In order to simplify the problem, we use triangular linear interpolation to estimate fabric surface profiles on a uniformly spaced rectangular 2D grid. The reconstructed surface profiles are denoted by $h(x, y)$, where x and y represent the horizontal and vertical indices. By applying the 2DFFT to $h(x, y)$, the information is transformed to the spatial frequency domain. The power spectrum is calculated in order to remove the imaginary part of 2DFFT result. We want to make a rotation-invariant measurement. For this purpose, the power spectrum is cut into 24 radial slices and integrated respectively. The final step consists of determining the exponent β by using linear regression to find the slopes of the fourth step results on a log-log scale, and applying Equation 4.2 to compute FD_{FFT} . According to the properties of Fourier transform, theoretically this measurement is robust to linear translations and scaling as well. The results of our robust test shown in section 4.3 also prove its reliability.

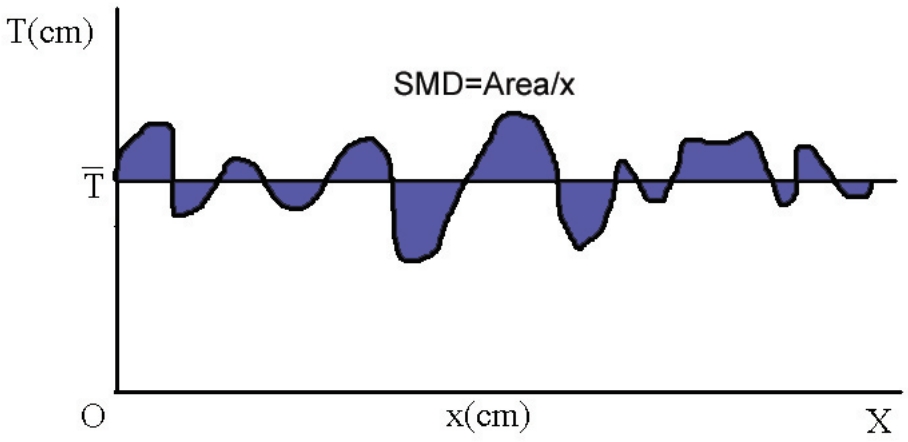

Figure 4.9: The definition of geometrical roughness (SMD)

4.2.2 The Estimation of Standard Surface Roughness Parameters

The geometrical roughness in the KES-F system is described in Equation (4.3) and shown in Figure 4.9, where T represents the thickness of the fabric sample and $\overline{T}$ denotes the average of T.

$$SMD = \frac{1}{X}\int_0^X \left|T - \overline{T}\right| dx \tag{4.3}$$

In practical terms, another standard roughness parameter is the root mean square (RMS) given by:

$$RMS = \sqrt{\frac{1}{X}\int_0^X \left|T - \overline{T}\right|^2 dx} \tag{4.4}$$

In order to extend the measurements of SMD and RMS to 3D surface, we replace the average line $\overline{T}$ by a reference surface. The reference surface $z = f(x, y)$, which has minimum-distance values at all points of the fabric surface scan, is taken as global surface from which SMD and RMS can be calculated. The surface profile $h(x, y)$ is obtained from the 3D fabric surface scan on an $N \times N$ mesh grid. We assume that the surface profile

is a noisy observation of the reference surface, and then we have

$$h(x, y) = f(x, y) + \varepsilon \tag{4.5}$$

where ε represents the error. A least square polynomial regression method is applied to minimize ε. Thus, the reference surface $z = f(x, y)$ can be determined.

We modify Equation (4.3) and Equation (4.4) in order to fit our 3D cases as follow:

$$SMD_i = \frac{1}{N^2} \sum_{m=1}^{N} \sum_{n=1}^{N} d_{m,n}^i \tag{4.6}$$

$$RMS_i = \sqrt{\frac{1}{N^2} \sum_{m=1}^{N} \sum_{n=1}^{N} (d_{m,n}^i)^2} \tag{4.7}$$

where N is the number of mesh point along each direction, $d_{m,n}^i$ is the minimum distance from the point of the 3D surface profile at m-th row and n-th column to the reference surface.

The simplest reference surface is the flat plane $z = a_0 + a_1 x + a_2 y$ and the $d_{m,n}^i$ can be computed by:

$$d_{m,n}^i = \frac{|a_0 + a_1 x_n + a_2 y_m - h_i(x_n, y_m)|}{\sqrt{a_1^2 + a_2^2 + 1}} \tag{4.8}$$

We also consider the second order polynomial surface

$$z = a_0 + a_1 x + a_2 y + a_3 x^2 + a_4 xy + a_5 y^2 \tag{4.9}$$

as an alternative reference surface. The minimum distance $d_{m,n}^i$ is determined by looking for distances from the interested 3D surface points to the close points of the reference surface. Searching minimum distance from the 3D surface points to the reference surface points limits the whole algorithm speed considerably. Figure 4.10 illustrates an example of the relation between the reference surfaces and the actual fabric surface points. It shows that the second order polynomial surface may fit the points better than the flat plane in some cases. However, a tradeoff has to be made between computation time and accuracy.

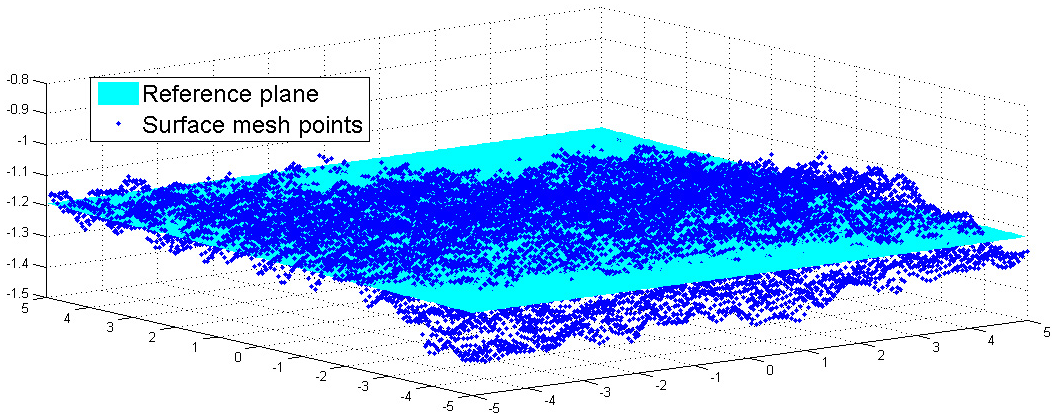

(a) 1st Order

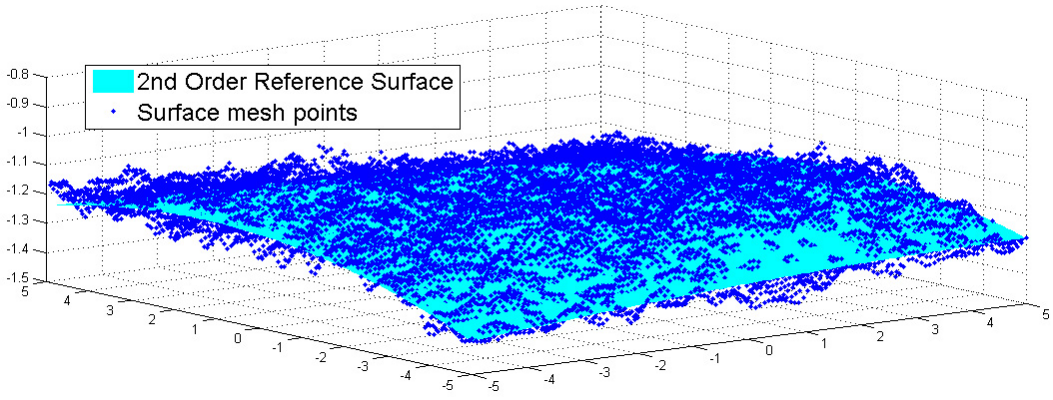

(b) 2nd Order

Figure 4.10: An example of the reference surfaces w.r.t. surface points

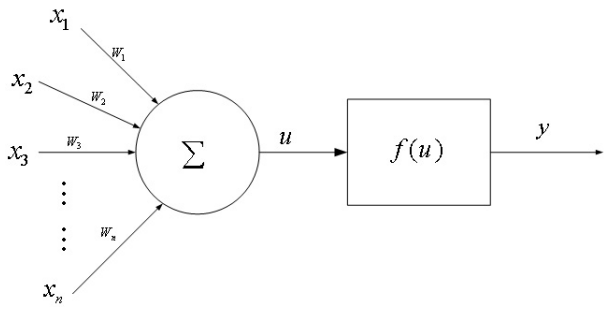

Figure 4.11: The elementary neuron

4.2.3 The Neural Network Prediction Model

A neural network computing technique was proposed to predict the standard roughness parameters from the FD_{FFT} estimated in previous steps.

Artificial neural networks are widely used in many applications, for example, prediction or forecasting, function approximation, clustering and pattern classification [103, 104, 105]. The basic unit in an artificial neural network is the neuron, which has nonlinear input/output characteristics similar to biological neurons. The elementary neuron with n inputs is shown in Fig. 4.11.

In this work, we chose a feed-forward artificial neural network [106]. The structure of this network consists of an input layer, two hidden layers, and an output layer. The estimated FD_{FFT} are fed into the input layer. From there, they propagate forward through hidden layers and then gives two roughness characteristic values at the output layer. During this propagation the mapping from the fractal dimension estimate to roughness characteristic values occurs. The proposed neural network use the Levenberg-Marquardt algorithm [107] to speed up the training process. Hyperbolic tangent sigmoid transfer function and linear transfer function are used for hidden layer and output layer respectively as the activation function. We use two hidden layers because it has been proved that the neural network with two hidden layers are enough to accurately approximate any multidimensional function [108].

4.3 Experiment and Results

4.3.1 Robustness test for FD_{FFT} estimation

In order to demonstrate the robustness of our fractal dimension measurement FD_{FFT} , we used computer simulated fractal Brownian surfaces as shown in Figure 4.12 Two simulation algorithms were used: one is the interpolated method (FBMs) and the other is the random midpoint displacement (RMDs). The original size of test images is 256×256 pixels. For testing the effects of scaling we magnified the simulated fractal images into 512×512 pixels. The computed FD_{FFT} s comparing with the theoretical fractal dimension are shown in Table 4.1. Pearson's correlation coefficients were computed between theoretical values and each group of FD_{FFT} s as well. The computed correlation coefficients are all greater than 0.978. It shows that FD_{FFT} s are highly correlated with the theoretical ones. For testing the effects of rotations, we rotated the images in counterclockwise direction by an angle every 15 degrees from -90° to 90°. The nearest neighbor interpolation was used for image rotation. Table 4.2 lists the average values of FD_{FFT} s measured from image rotations and the corresponding measurement variance. Due to the smoothing effect of interpolation, the FD_{FFT} measurement after angular rotation is slightly lower than that of the previous test. The variance of the measurements for multiple angular rotations is of the order of 10^{-3} and it proves that our measurement is robust to rotation.

4.3.2 The experiment for evaluating the influence of interpolation

Ten real fabric samples (as shown in Figure 4.13) with different surface appearance are used for the remaining experiments. To validate the goodness of FD_{FFT} as a parameter for evaluating fabric surface roughness, ten 3D fabric surface scans were cut into square pieces of size $1cm^2$ and converted into surface profiles based on 256×256, 128×128,

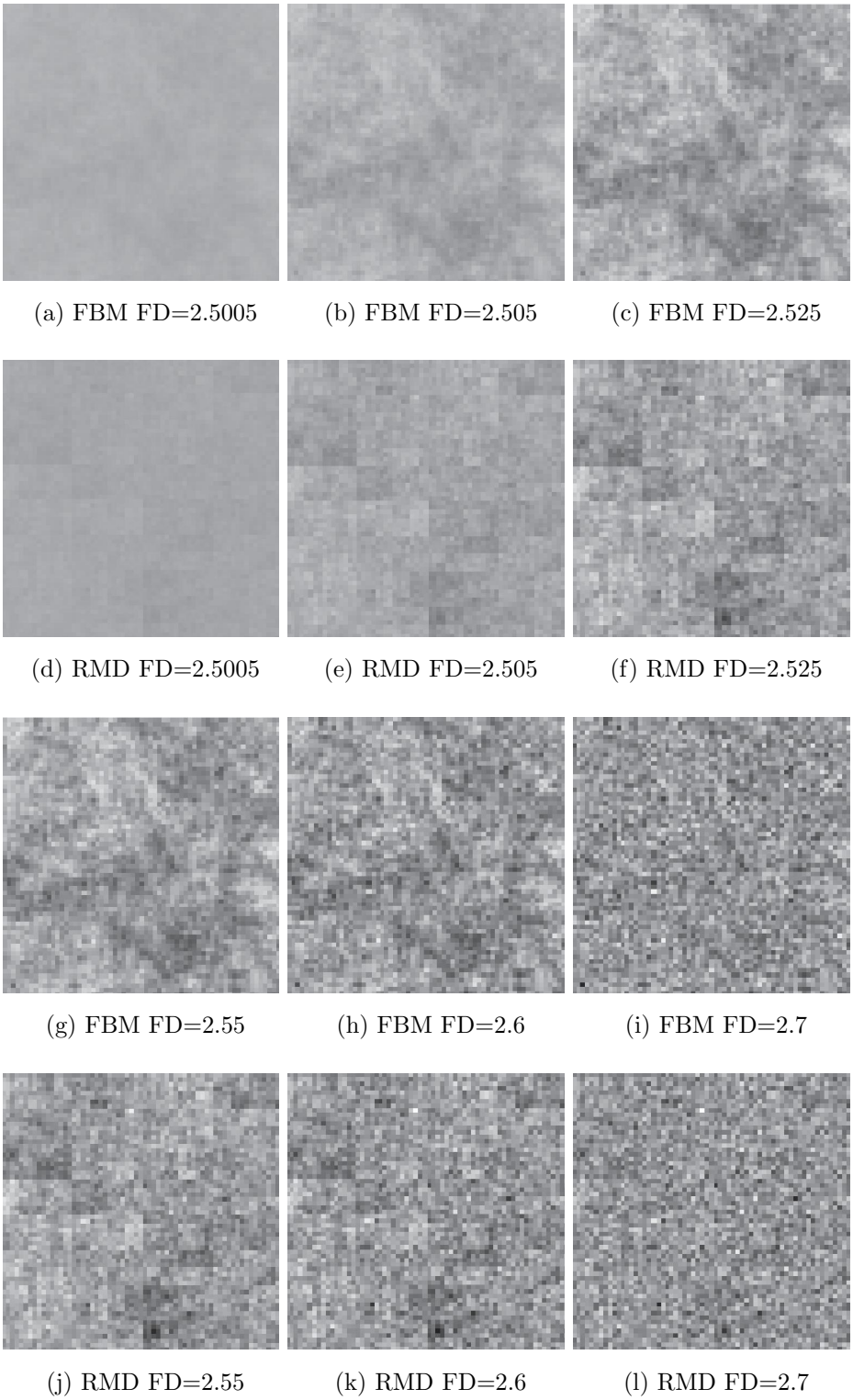

(a) FBM FD=2.5005 (b) FBM FD=2.505 (c) FBM FD=2.525

(d) RMD FD=2.5005 (e) RMD FD=2.505 (f) RMD FD=2.525

(g) FBM FD=2.55 (h) FBM FD=2.6 (i) FBM FD=2.7

(j) RMD FD=2.55 (k) RMD FD=2.6 (l) RMD FD=2.7

Figure 4.12: Computer simulated 2D Fractal Brownian motion images with different theoretical fractal dimension.

Table 4.1: Fractal Dimension Measurements on Computer Simulated Fractal Brownian Surfaces

Theoretical FD	**FBMs**	**FBMs (×2)**	**RMDs**	**RMDs (×2)**
2.5005	2.4512	2.5964	2.4546	2.5858
2.5050	2.4515	2.5988	2.4524	2.5909
2.5250	2.4906	2.6338	2.4887	2.6247
2.5500	2.5383	2.6733	2.5348	2.6636
2.6000	2.6407	2.7735	2.6358	2.7639
2.7000	2.8554	2.9288	2.8476	2.9170
Correlation Coefficient	0.9993	0.9789	0.9903	0.9784

Table 4.2: Fractal Dimension Measurements on Fractal Brownian Surfaces with Multiple Angular Rotations

Theoretical FD	**FBMs (Average μ)**	**FBMs (Variance σ^2)**	**RMDs (Average μ)**	**RMDs (Variance σ^2)**
2.5005	2.3818	0.0023136	2.3971	0.0021236
2.5050	2.4204	0.0018512	2.4630	0.0010234
2.5250	2.5052	0.0013555	2.5488	0.0007033
2.5500	2.5511	0.0010023	2.5962	0.0006849
2.6000	2.6058	0.0005921	2.6543	0.0007527
2.7000	2.6994	0.0013178	2.7147	0.0013980

Figure 4.13: The fabric samples for evaluation

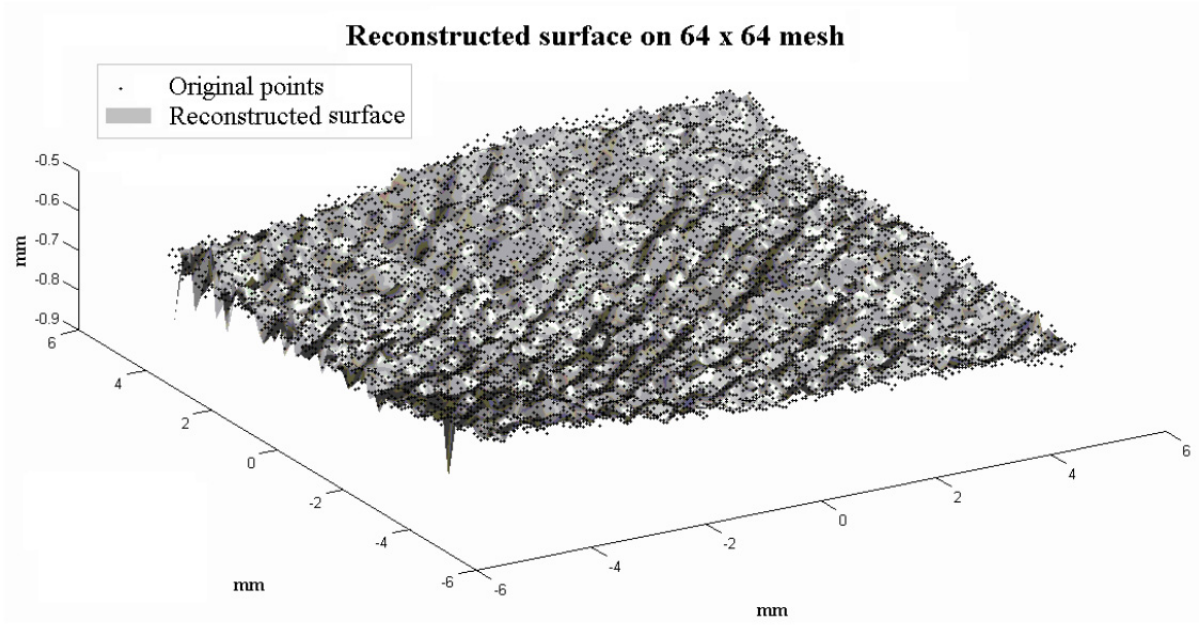

Figure 4.14: An example of the original 3D surface points vs. the reconstructed surface based on rectangular 64 $\times$ 64 mesh grid

64×64 mesh grids respectively. In order to investigate the effects of the conversion from the uneven distributed 3D points to the uniformly distributed mesh points, we compared the mean and variance of original points to those of the corresponding mesh points. The results are shown in Figure 4.15. The values of mean and variance are quite close to each other. It shows that the original surface points and the corresponding mesh surface points represent the same surface under high probabilities. Figure 4.14 illustrates a comparison between the original surface points and the reconstructed surface on a 64×64 mesh grid. Even the number of surface points has been reduced to 64^2, most of the original surface points still sit on the reconstructed surface. Therefore, the noise introduced by the triangular interpolation can be neglected.

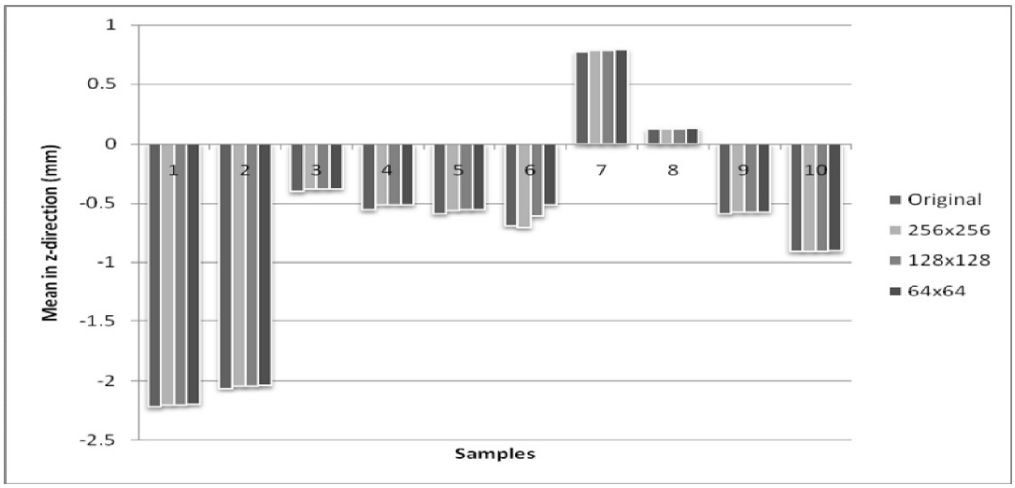

(a) Mean

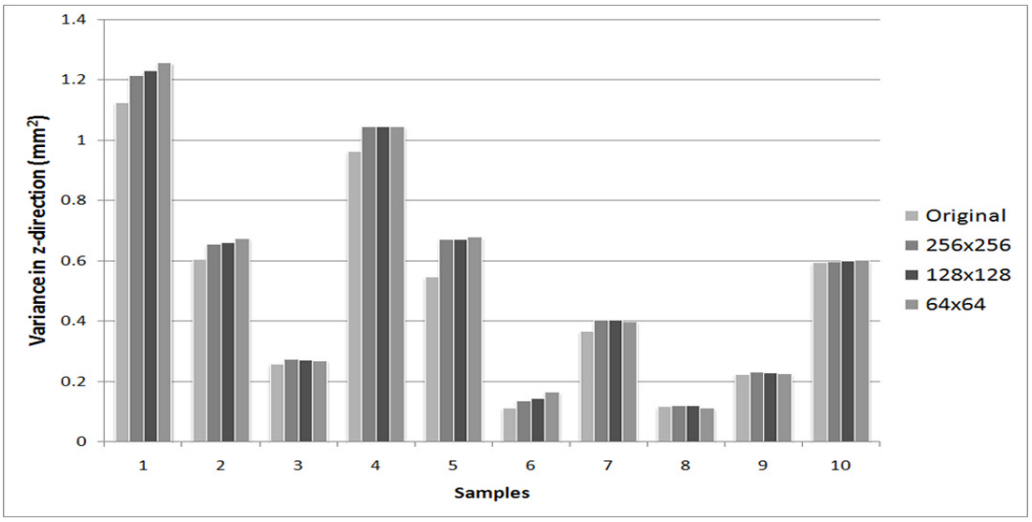

(b) Variance

Figure 4.15: Comparison of the original 3D data points and the reconstructed surface points after interpolation

4.3.3 The correlation between FD_{FFT} and the roughness parameters

Both standard roughness parameters and the FD_{FFT} s were computed in order to examine the relationship between FD_{FFT} and the standard roughness parameters. The FD_{FFT} measurements are plotted with respect to the standard roughness parameters as shown in Figure 4.16. The computation times of FD_{FFT} , SMD and RMS are shown in Figure 4.17. The FD_{FFT} calculated from mesh data consistently decrease as the SMD and RMS increase. The Pearson's correlation coefficients between the FD_{FFT} s of 256×256, 128×128 mesh grids and the corresponding SMDs and RMSs are greater than 0.93. For 64×64 mesh data, the Pearson's correlation coefficients are around 0.82. The results demonstrated that the FD_{FFT} was highly related to SMD and RMS. Moreover, the computation of FD_{FFT} is much faster than the computation of the standard roughness parameters. We can conclude that FD_{FFT} is a fast reliable parameter for evaluating fabric surface roughness.

4.3.4 The performance of the neural network prediction

The FD_{FFT} is used as the input of the neural network model and the computed SMDs and RMSs are used as desired outputs. The training target error is set to 1e-6, which is very tight for good generalization. Once the training is finished, the trained network has memorized the training target. The early stopping methodology is used to reduce the generalization error caused by over-fitting. The results of the prediction model is shown in Fig. 4.18. The prediction values are almost overlapped the target values. It proves that the fractal dimension estimates of 3D fabric surface scans can be modeled to predict the standard roughness characteristic values without using complicated destructive measurement devices.

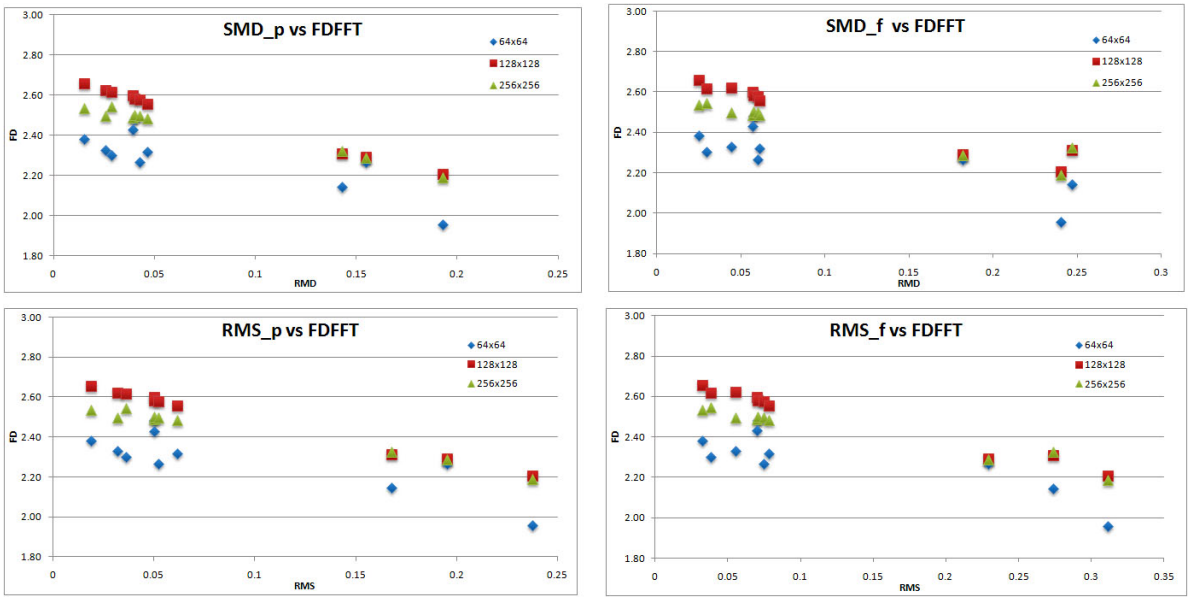

Figure 4.16: Comparison of FD_{FFT} '_p' refers to the 2nd order polynomial surface, '_f' refers to the flat plane

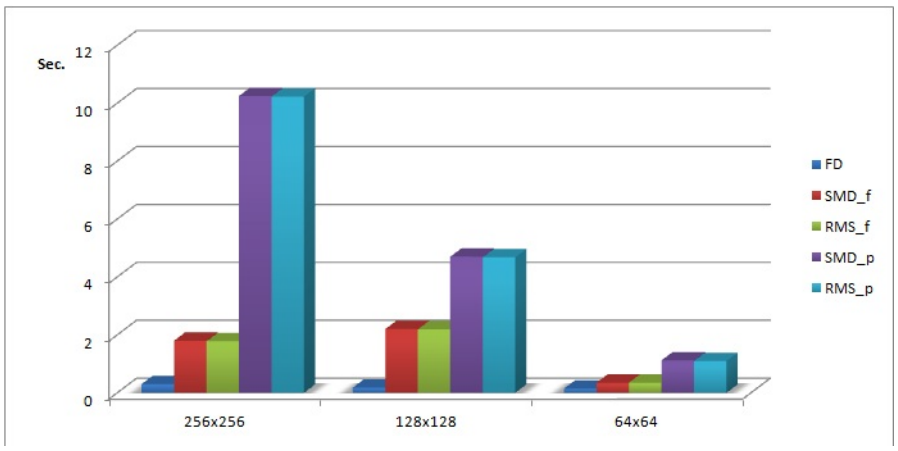

Figure 4.17: Comparison of the computation time

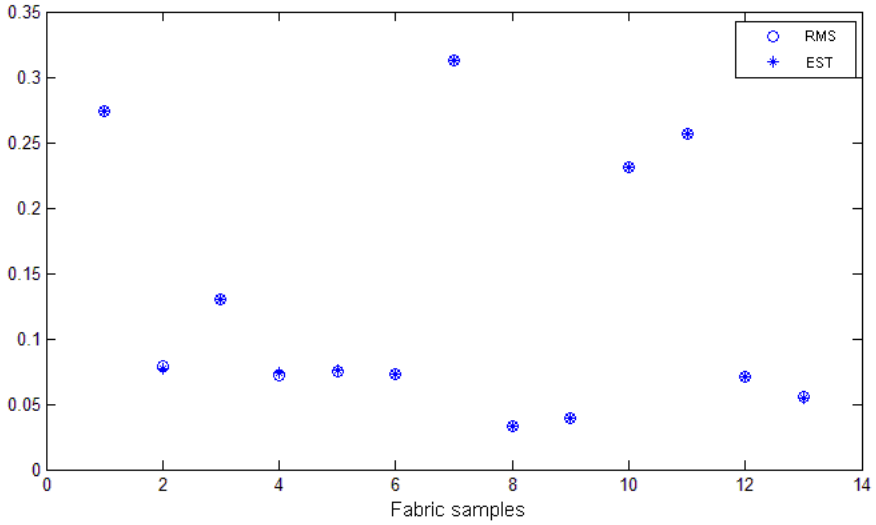

(a) RMS vs ANN prediction

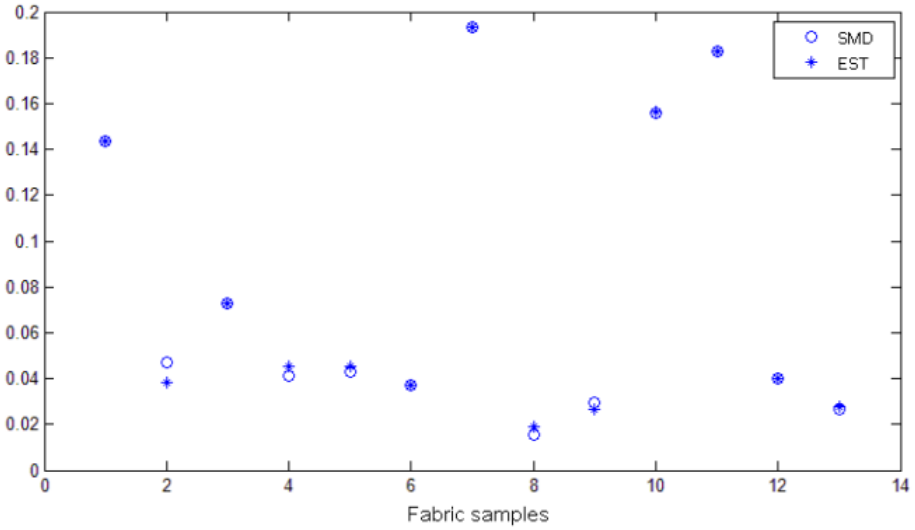

(b) SMD vs ANN prediction

Figure 4.18: The comparison of the outputs of ANN prediction model to the desired target values

4.3.5 Summary

A 2DFFT based fractal dimension parameter FD_{FFT} , which is for characterizing the surface roughness of fabrics from 3D fabric images, is presented. Its robustness to image rotations and scaling has been validated with fractal Brownian images. The standard roughness parameters SMD, RMS are used to test the validity of FD_{FFT} as a reliable parameter for fabric roughness characterization. Tests have shown that FD_{FFT} values are highly correlated to the standard roughness characteristic values.

In the design of prediction model, we consider the good generalization capability. In this work a feed-forward artificial neural network with Levenberg-Marquardt training algorithm is used. This method is to speed up the training process and can be used to overcome the problem of determining optimum number of neurons in hidden layer. The results obtained after simulations proved the accuracy of this methodology.

Chapter 5

Intelligent Interpretation of Fabric Properties

In this chapter, an intelligent fabric property interpretation model is proposed and evaluated experimentally. The model uses the fabric human expert knowledge to guide a SVM based learning algorithm. The cross-validation is applied for performance test.

The chapter is organized as follows. Firstly in section 5.1 a brief introduction to the background and related works is given. In section 5.2 the proposed method is discussed. Finally, in section 5.3 the validation experiments and results are shown and analyzed.

5.1 Introduction and Related Works

As stated in Chapter 2, textile is a very special material and has wide application related to every aspect of human life. Its complicated manufacture process leads to various properties which are very difficult to evaluate. In traditional textile industry, fabric evaluation is performed subjectively. This evaluation is relied on human sensitivity and experience, thus, it varies with time, personal preference, and cultures. The results of subjective evaluation are difficult to quantize and restricts the scientific understanding of fabric performance for those who wish to design or analyze high quality fabric in

engineering ways.

With the help of instruments, the physical/mechanical features can be accurately measured. The objective property measurement can generate a set of precise quantitative data which indirectly describe the performance, appearance and quality of the fabric. The measured feature data can be used to build a database. This database is useful to many applications such as the textile production development, fabric simulation, production control, customer management, and end product prediction. The interpretation of measured data with respect to the goal of different application is a still under-exploited area. Lack proper interpretation method obstacles the development of objective evaluation of fabric.

To fill this gap, researchers made effort on modeling the relationship between objective and subjective measurements. Dreby [109] used rank correlation in linking sensory data with objective measurements. He was a pioneering in linking fabric objective measurements to finishing processes. Many techniques rather than ranking correlation were reported to study the relationships between subjective measurements and objective measurements as well. For example, the multiple factor analysis was utilized to study the relationships between subjective rates of smoothness, softness, coarseness, thickness, weight, warmth and stiffness and objective measurements [110]. Factors of multiple dimensions were estimated from this method in order to describe the above relationships. Linear regression or multi-step regressions analysis were used to generate equations between subjective ratings and objective measurements [16, 111, 112]. Psychophysical laws such as Weber-fechner law and Stevens's power law were also used to translate a wide range of fabric mechanical properties into corresponding human sensational parameters [113, 114, 115]. Some advanced techniques such as fuzzy logic [116] and neural networks [117] were also used to model the relationship between subjective evaluation parameters and objective physical measurements of fabric.

These researches provide strong evidence that there are high correlations between subjective measurements and objective measurements and the objective measurements

are sufficient to predict some high level performance, aesthetic properties of fabric. However, the practicability of their methods is rather limited due to the following difficulties: (1) there are uncertainties and imprecision in subjective evaluation, for example, different rating scores often give to the same fabric sample from different evaluators or different tests; (2) it is very difficult to find a feasible analytical model due to the complexity of the fabric properties; (3) it is hard to generalize their model to new applications because the models were build based on a particular subjective test the results of which cannot be reproduced from different tester in different test and are not widely accepted by public.

In this chapter, an intelligent approach for the interpretation of fabric objective measurements is proposed using supported vector machine techniques. The human expert assessments of fabric are used during the training phase. The outputs of the system are not the subjective evaluation parameters but meaningful classes of fabric, for example, the end-uses of textile and the finishing treatments. Since the human knowledge on judging these meaningful classes of fabric is stable and consistent in most cases, the uncertainty which lies in current subjective evaluations does not affect the performance of proposed model. The support vector machine is one of the best solutions for handling high dimensional data classification. Thus, it effectively eases the difficulties caused by the complexity of the fabric properties. The inputs of the model are objective measurements which can be repeated consistently. The general model itself is not complicated, and after a new training process without changing the structure of the mathematical model and the organization of inputs it can be adjusted to generate new outputs for matching new requirements.

5.2 Methodology

5.2.1 The overlook of the procedures

The main task of this work is the development of a system with the highest possible ability to interpret target information of a fabric sample from a set of quantitative phys-

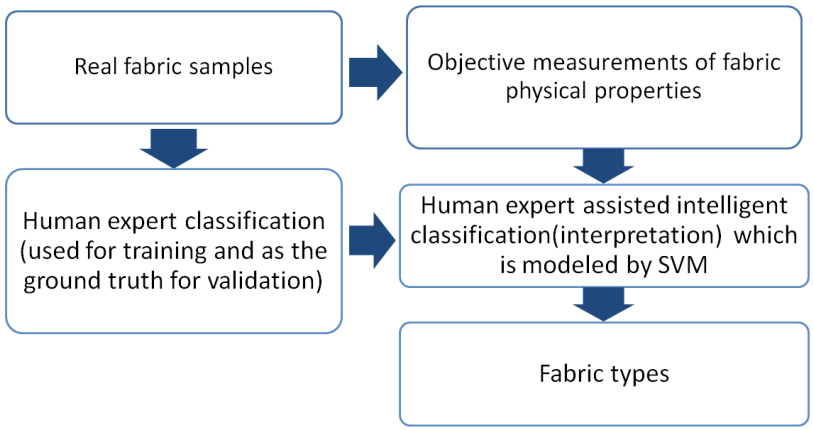

Figure 5.1: The general model of intelligent interpretation of fabric properties

ical properties of the same fabric which indirectly describe the target information. The overlook of the methods is illustrated in Figure 5.1. The physical properties of fabric are measured instrumentally. The samples are divided into two groups: the training group and the testing group for the validation purpose. Human expert helps to identify which sample in training group is belonging to the target class. This information is used to train and choose the proper kernel function of the SVM model. Human expert also need to distinguish the samples in testing group which are belong to the target class. This information is taken as the ground truth during the validation test. The outputs of the SVM model are the fabric samples labeled with target class names.

5.2.2 The construction of fabric physical features

The groups of the physical features considered for our approaches are: (1) tensile property; (2) shearing property; (3) bending property; (4) compression property; (5) surface property; (6) dimension property. Tensile and shear properties can be measured by KES-F tensile and shear tester. Bending property can be obtained by KES-F bending tester. Compression and surface properties can be made by the KES-F compression and surface testers respectively. Dimension property includes thickness and weight which can

be measured objectively as well.

The characteristic values calculated from the instrumental measurements are listed in Table 2.1. Characteristic features of surface properties include coefficient of friction (MIU), mean deviation of MIU (MMD), and geometrical roughness (SMD). All of these features are sensitive to fiber directions (weft, warp direction) and varied on different sides of fabric (face side and back side). Therefore, 12 feature values (3 characteristic features $\times$ 2 fiber directions $\times$ 2 fabric sides) are considered for describing surface property.

There are four tensile feature values: linearity of load-extension curve (LT), tensile energy (WT), tensile resilience (RT), and elongation at maximum load (EMT). All of these features are measured and calculated at both weft and warp directions. Eight feature values represent the tensile property. Three features for shearing property, which are shearing rigidity (G), hysteresis of shear force at 0.5° shear angle (2HG), and hysteresis of shear force at 5° shear angle (2HG5), are obtained from weft and warp directions as well. Consequently, six feature values describe the shearing property. Bending rigidity (B) and hysteresis of bending moment (2HB) are gathered from weft and warp directions respectively. Four resulting feature values represent the bending property.

The pressure-thickness curve and compression property are not sensitive to fiber direction or fabric side. Therefore, T_0, T_m (thickness at $0.5gf/cm^2$ and $50gf/cm^2$), linearity of pressure-thickness curve (LC), compression energy (WC) and compression resilience (RC) are measured only once for each fabric sample. In summary, 37 feature values for every fabric sample in total include 12 surface features, 8 tensile features, 6 shearing features, 4 bending features, 5 pressure-thickness and compression features, fabric weight and thickness.

5.2.3 Support vector machine (SVM) model

SVMs are the new trends in machine learning algorithm which is powerful solution to the pattern recognition problems, especially to the classification problems. SVM is a supervised, non-parametric learning system that is developed from statistical learning

theory [118, 119]. SVM is initially linear classifier designed for solving two-categories classification tasks [120] by determining the hyper-plane to separate two classes. This is done by maximizing the margin from the hyper-plane to the bounds of two classes. With the introducing of the kernel functions, it can map the input data to a higher dimensional space that extends the ability of SVM for non-linear problems. Multi-class classification is also applicable, the multi-class SVM is built up by many two-class SVM networks either by using one-against-all or one-against-one method. The winning class is identified by the highest output function value or the maximum votes respectively [121].

The unique features or advantages of SVM and kernel method are as follows: (1)they are explicitly based on a theoretical model of learning and therefore, has theoretical guarantees about the performance; (2) they have very good generalization ability that allows the user to separately implement and design their components; (3) they are not affected by local minima unlike Neural Network approaches and deliver a unique solution by applying optimization techniques; (4) they are remarkably insensitive to the dimension of training data and do not suffer from the " curse of dimensionality " [122].

In this chapter, SVM has been used for interpreting the measured fabric features and classifying the fabric samples into target classes. In the case of a linear SVM, the measured features of a fabric sample i, which has to be classified to a target fabric type A or not A, is denoted by a vector $\mathbf{x}_i$. The separating hyper-plane is expressed as:

$$\mathbf{x}_i^T \mathbf{w} + b = 0 \tag{5.1}$$

where is $\mathbf{w}$ a vector which contains the weights of the feature values and b is a constant. The corresponding decision function is:

$$f(\mathbf{x}) = sign(\mathbf{x}_i^T \mathbf{w} + b) \tag{5.2}$$

The optimal hyper-plane is shown to be the one with the maximal margin of separation between two group of feature vectors and lowest capacity as well [123]. Two

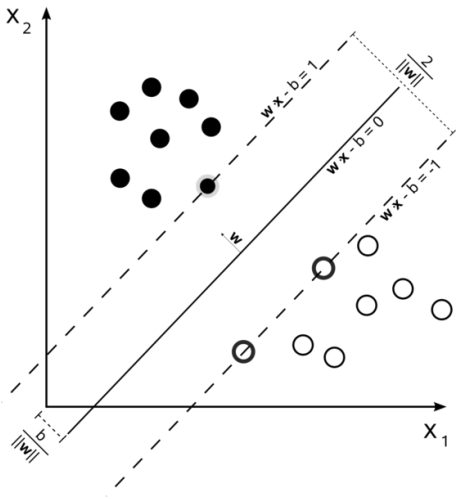

Figure 5.2: Maximal margin hyperplane and margins for an SVM trained with samples from two classes

dimensional case is illustrated in Figure 5.2. The margin is $2/\|\mathbf{w}\|$, where $\|\mathbf{w}\|$ is the norm of vector $\mathbf{w}$. The two margin boundaries are represented as $\mathbf{x}_i^T\mathbf{w} + b = 1$ and $\mathbf{x}_i^T\mathbf{w} + b = -1$. For a non-perfectly separable case, the margin can be "soft". A non-negative slack variable ξ is introduced as well as a non-negative constant C which is denoted the regularization coefficient. The optimization problem for finding $\mathbf{w}$ and b can be expressed by:

$$min\ \frac{1}{2}\|\mathbf{w}\|^2 + C\sum_{i=1}^{n}\xi_i \tag{5.3}$$

subject to

$$f_i(\mathbf{x}_i^T\mathbf{w} + b) \geq 1 - \xi_i \tag{5.4}$$

$$\xi_i \geq 0 \tag{5.5}$$

where i represent the i-th sample, $f_i = f(\mathbf{x}_i)$ and n is the size of training set.

The above constrained optimization problem can be solved by establishing the Lagrange function:

$$L(\mathbf{w}, b, \xi, \alpha, \nu) = \frac{1}{2}\mathbf{w}^T\mathbf{w} + C\sum_{i=1}^{n}\xi_i - \sum_{i=1}^{n}\alpha_i\{f_i(\mathbf{x}_i^T\mathbf{w} + b) - 1 + \xi_i\} - \sum_{i=1}^{n}\nu_i\xi_i \quad (5.6)$$

where $\alpha_i \geq 0$ are the Lagrange multipliers for the inequality constraint 5.4 and $\nu_i \geq 0$ are the Lagrange multipliers for the constraint 5.5. By using the classic Kuhn-Tucker Sufficiency Theorem, the entire task can be reduced to the quadratic programming with respect to the Lagrange multipliers α_i. The optimal weight vector is determine by:

$$\mathbf{w}_O = \sum_{i=1}^{n}\alpha_i f_i \mathbf{x}_i \quad (5.7)$$

The output $f(\mathbf{x}_i)$ of SVM after learning is described in the form:

$$f(\mathbf{x}_j) = \sum_{i=1}^{n}\alpha_i f_i \langle \mathbf{x}_i, \mathbf{x}_j \rangle + b \quad (5.8)$$

where $\langle \mathbf{x}_i, \mathbf{x}_j \rangle$ denotes the inner product. In the case of a non-linear SVM, the vector $\mathbf{x}$ is substituted by a function $\varphi(\mathbf{x})$. The kernel is a scalar function defined as the inner product of vector functions $\varphi(\mathbf{x}_i)$ and $\varphi(\mathbf{x}_j)$, i.e.

$$K(\mathbf{x}_i, \mathbf{x}_j) = \langle \varphi(\mathbf{x}_i), \varphi(\mathbf{x}_j) \rangle \quad (5.9)$$

The non-linear problem is thus solved by transforming the feature space into a higher dimensional space in which the linear threshold can be used. Using a kernel is equivalent to solve a linear SVM in a new higher dimensional feature space. Typical kernel functions include polynomial kernel with order d, Gaussian radial basis kernel with hyper-parameter σ, and sigmoid kernel which makes the SVM be equivalent to a two-layer neural network.

5.3 Experiment and Results

5.3.1 Database

The database of fabric sample physical properties used in the experiment are collected from HAPTEX project [124, 125, 126]. There are three sets of fabric samples which were chosen initially for evaluating the HAPTEX system. The aim of the fabric sample selection process was to present a wide range of very different fabric in terms of raw material, structure and dimensions. The first set of samples [124] contains 32 fabric samples which are made by natural fibers, or man-made fibers, or mix materials. In terms of structure woven textile, knitted textile and non-woven textile are all shown in these group of samples. The second set [125] has ten samples (six of them are thin and the rest are thick). They have different constructions, raw materials, and yarn densities and very different surface appearance. The third set [126] was chosen to complete the sample selection of the second set of fabrics with a group of very similar type and deformative fabrics for the automotive industry. The third set comprises foam laminated and non-laminated warp knitted fabrics. All feature values mentioned in section 5.2.2 are measured by KES-F instruments and calculated from the recorded data.

The entire database contains 54 fabric samples and for each sample a physical feature vector of 37 components is constructed. The 37 components describe the tensile, shearing, bending, surface, compression, and dimension properties of a fabric sample respectively. Among these fabric samples, samples 43 to 51, 54 are textiles for making car seats, samples 35 to 38 are fabrics for making man suit or overcoat, and samples 47 to 51, 54 are laminated materials. The rest of the materials are blended unclassified fabrics. The feature data of fifty four fabric samples are listed in Appendix A.

5.3.2 Subjective measurement assessment

In addition to the objective measurements, the subjective measurements of these fabric samples were also performed by one volunteer from a textile manufacturing in-

dustry [126]. The subjective tests were on evaluating roughness, friction, and bending properties. Four trials were made for each property evaluation. The rating scale is in the range from 1.0 to 5.0.

We computed the variance of the inter-trial subjective scores. We found that for roughness subjective tests the largest variance of the inter-trials was greater than 0.5 and the variances of 50% testing samples were larger than 0.3. The largest variance for friction subjective test was 0.6225 and the variances of 30% testing samples were greater than 0.54. The largest variance of inter-trial for bending subjective test was 0.917 and the variances of close to 30% testing samples were greater than 0.56.

Based on the variances computed from subjective test results, we draw the conclusion that the subjective evaluation scores are not suitable for training a computer learning algorithm. The subjective results of a same fabric sample given by a same human judge are varied significantly between different trials. The variation shown in subjective tests also proves the unreliability of the subjective nature.

5.3.3 The performance experiments

5.3.3.1 Leave-one-out validations

For implementation of SVM model, we use Matlab as software tool. Three SVM models are established for finding target classes: car seat fabrics, man suit fabrics and laminated fabrics respectively. The performance of the model is evaluated by cross-validation techniques. We notice that only 10 samples from 54 samples are known as car seat material, 4 samples are suitable for man suit, 6 samples are foam laminated. Since there is a relative small number of the samples which belong to target classes (positive class) and a large portion of the samples are belong to the negative class (control class). The k-fold cross-validation methods are not practical for the experiments. Instead of using k-fold techniques, we randomly pick one sample from each category for the purpose of testing and the rest samples are used for training SVM model. This testing method

is called leave-one-out validation. The validation has to be performed a number of times in order to gain a meaningful results. It is because that the leave-out sample is picked randomly each time and the disjointed evaluation sets between two tests are not guaranteed.

For the first experiment, the target class is the fabrics for making car seat textile. The samples 43-51 and 54 are identified for car seat fabric, and rest samples by default are participated into the control class. This information is taken as the ground truth, i.e. the true class label for each fabric sample. Leave-one-out validation method is used. One sample of target class and one sample of control class are selected for validation. Linear SVM and non-linear SVMs using 2nd and 3rd order polynomial kernel functions are trained respectively by the feature data of rest 52 samples. The validation is repeated 1,000 times in order to compute meaningful error rate. The performance properties which are calculated for validation are listed in the following:

Error Distribution: a numeric vector indicating how many times each sample was misclassified.

Sample Distribution: a numeric vector how many times each sample was considered in the validation.

Error Rate = Incorrectly Classified Samples / Classified Samples

Sensitivity = Correctly Classified Positive Samples / True Positive Samples

Specificity = Correctly Classified Negative Samples / True Negative Samples

In the second experiment and third experiment, the target class is changed to man suit fabric and laminated fabric respectively. The sample 33-36 is labeled as man-suit fabric in the second experiment. The samples 47-51 and 54 are labeled as laminated materials in the third experiment. Linear, 2nd order, and 3rd order polynomial SVMs are also used for testing. 1,000 times of the leave-one-out validations are performed for evaluating the model performance.

Table 5.1: The accumulated error rates for leave-one-out tests

Kernal functions	**Fabric type**		
	Car seat	**Man suit**	**Laminated**
Linear	0.269	0.427	0.011
2nd order polynomial	0.325	0.547	0.087
3rd order polynomial	0.221	0.454	0.104

Table 5.2: The sensitivity for leave-one-out tests

Kernal functions	**Fabric type**		
	Car seat	**Man suit**	**Laminated**
Linear	0.612	0.235	1.000
2nd order polynomial	0.511	0.000	0.843
3rd order polynomial	0.675	0.251	0.827

The results are shown in Table 5.1, 5.2 and 5.3. The SVM models for recognizing laminated fabrics get the best performance. The linear SVM model for classifying laminated fabric has the smallest error rate. The physical properties change a lot because of the treatment of laminate. Therefore, the laminated fabric samples can be easily separated. The linear SVM achieve the best performance among three types of SVMs. The classifier for recognizing car seat material is quite good as well. Both linear SVM and SVM using 3rd order polynomial kernel gain low error rates. The sensitivities and the specificities of these two types of SVMs are not bad. However, SVM of 2nd order kernel shows not suitable for this problem. The classifier for identifying man suit material is failed with high error rates and terrible sensitivities. The reasons may be the low number of samples (four samples) and the samples which have similar physical features in control class confuse the training of the SVM model.

Table 5.3: The specificity for leave-one-out tests

Kernal functions	**Fabric type**		
	Car seat	**Man suit**	**Laminated**
Linear	0.851	0.912	0.978
2nd order polynomial	0.840	0.907	0.973
3rd order polynomial	0.884	0.841	0.952

5.3.3.2 Modified validation tests

In order to analyze the source of errors, we compute the error rate for each sample and each validation test respectively. The error rate with respect to each sample is obtained by dividing the Sample Distribution Vector from the Error Distribution vector. The results are shown in Figures 5.3, 5.4, 5.5, 5.6, 5.7, 5.8, 5.9, 5.10, and 5.11. The results show that the errors of each validation test are focus on a specific set of samples. Once the sample of this set is picked out for testing, the error occurs. We assume that these samples are the critical samples whose feature vectors are close to the separating hyper-plane of two classes. Removing these critical samples causes the training failures. Therefore, we modified the training method a little bit by keeping the critical samples as the training data.

Table 5.4: The results for modified leave-one-out tests using linear SVM)

Performance	**Fabric type**	
	Car seat	**Man suit**
Error rate	0.0418	0.0771
Sensitivity	0.984	0.966
Specificity	0.954	0.919

The samples, whose error rates are greater than 0.5, are selected as critical samples and hold for training. The leave-one-out validations are performed again in revised version. The testing sample is randomly selected from the sample space with the absence of critical samples. Each validation test is performed on linear SVM model for classifying car seat fabric and man suit. The tests are repeated 100 times. The performance of the modified validations is shown in Table 5.4. The results are improved significantly as expectation. The accumulated error rates drop dramatically, and sensitivity and specificity increase and approach to one. Since the most confusing samples are hold for finding the boundary between target class and control class, the performance of the SVM model is enhanced as consequence. The results of experiment show that if the training samples are chosen properly SVM can be used as a model for intelligently interpreting the physical features of fabric. By establishing a new training on the same set of input data with different target classes, for example, the goal is changed from finding fabrics which can be applied for certain end-use such as car seat fabric to looking for the fabrics which have been treated by laminating, SVM can be fitted into a new model for classifying/recongnizing new target features. It demonstrates the generalization ability of SVM method.

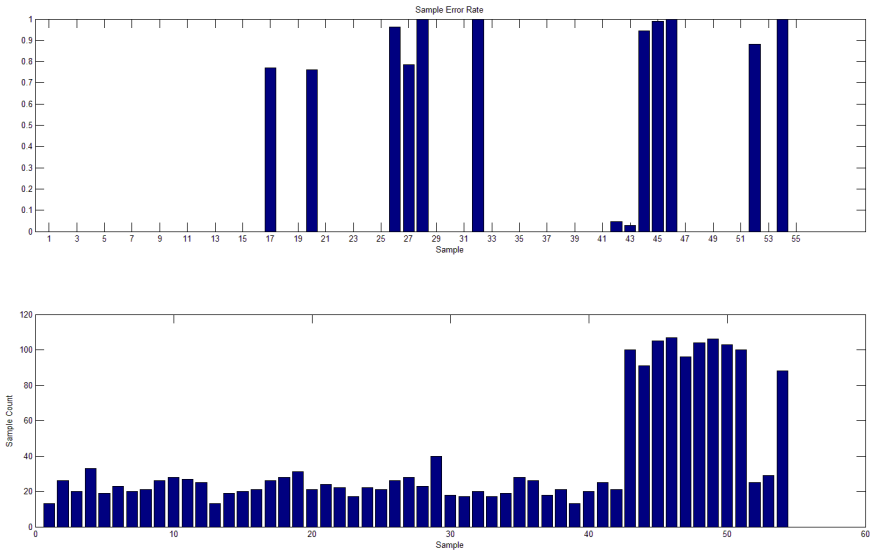

Figure 5.3: The error rates w.r.t. samples and sample distribution (linear SVM to classify car seat fabric)

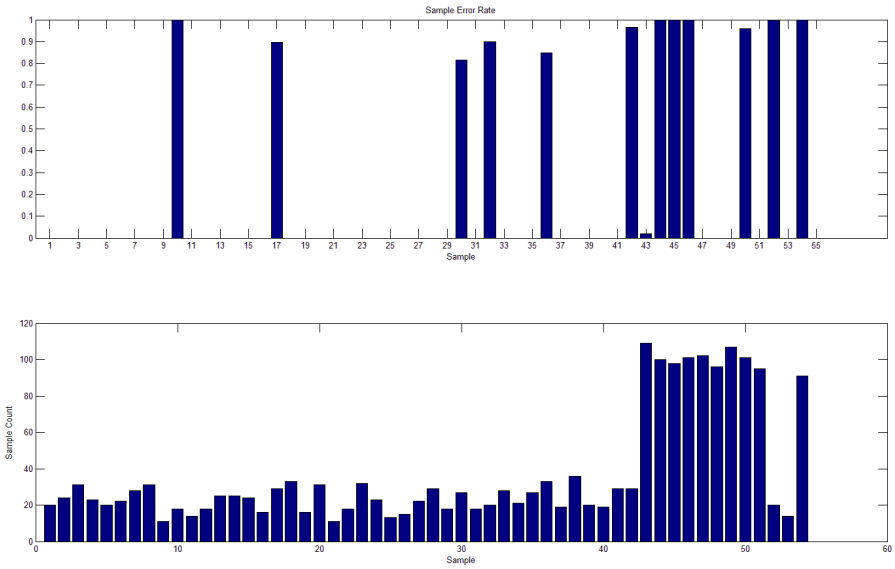

Figure 5.4: The error rates w.r.t. samples and sample distribution (2nd order polynomial SVM to classify car seat fabric)

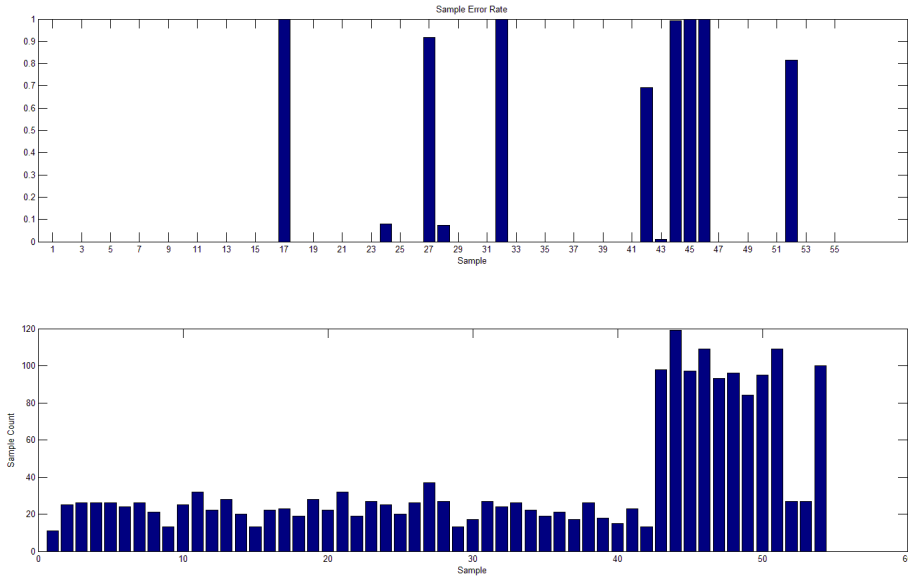

Figure 5.5: The error rates w.r.t. samples and sample distribution (3rd order polynomial SVM to classify car seat fabric)

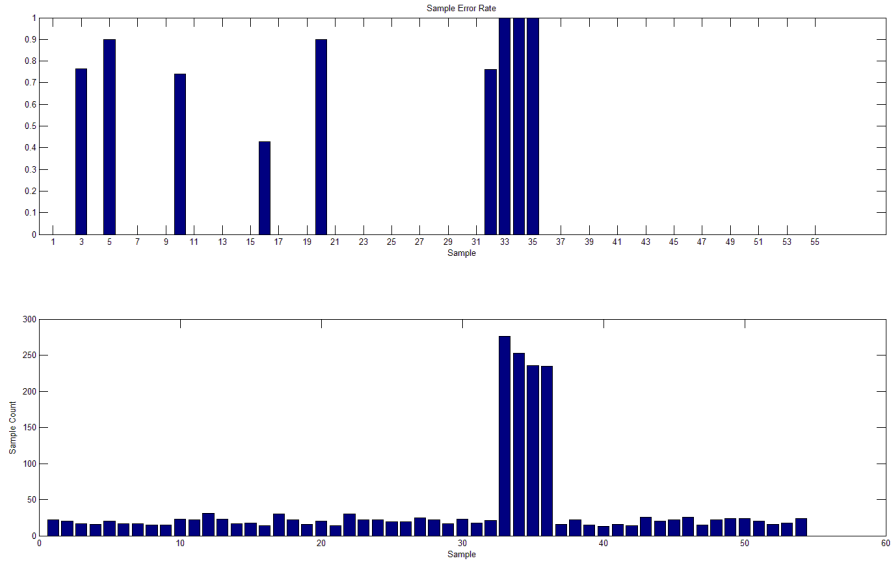

Figure 5.6: The error rates w.r.t. samples and sample distribution (linear SVM to classify man suit fabric)

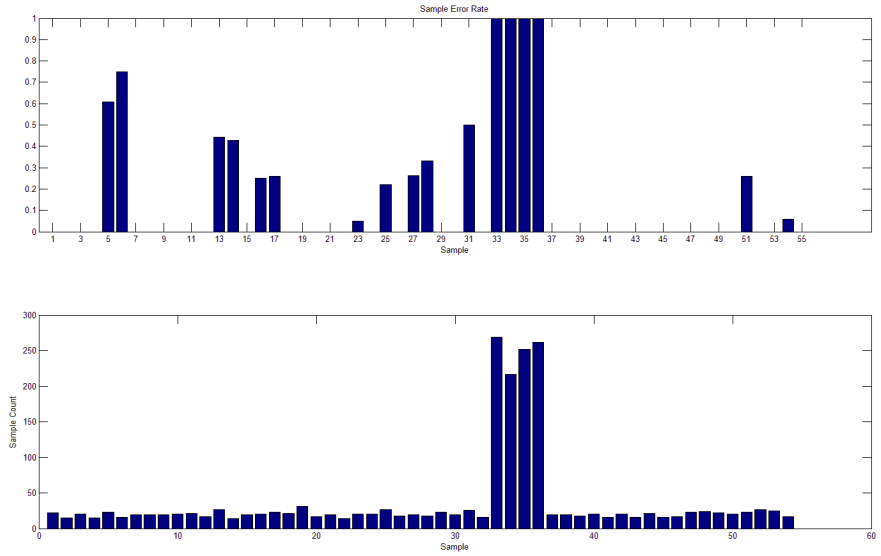

Figure 5.7: The error rates w.r.t. samples and sample distribution (2nd order polynomial SVM to classify man suit fabric)

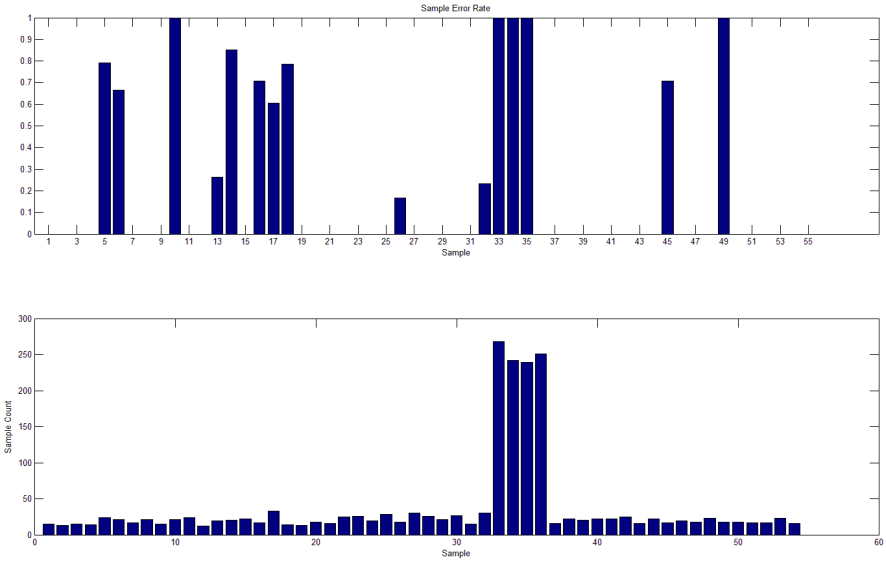

Figure 5.8: The error rates w.r.t. samples and sample distribution (3rd order polynomial SVM to classify man suit fabric)

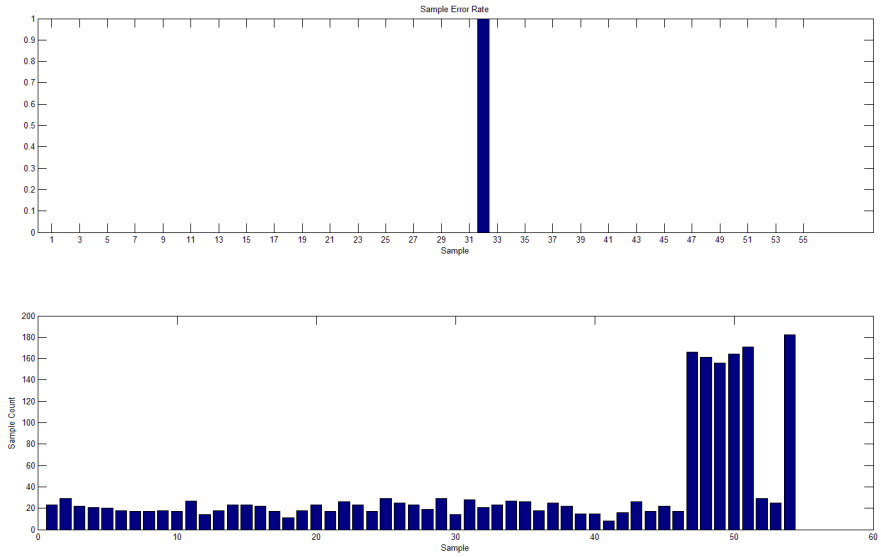

Figure 5.9: The error rates w.r.t. samples and sample distribution (linear SVM to classify laminated fabric)

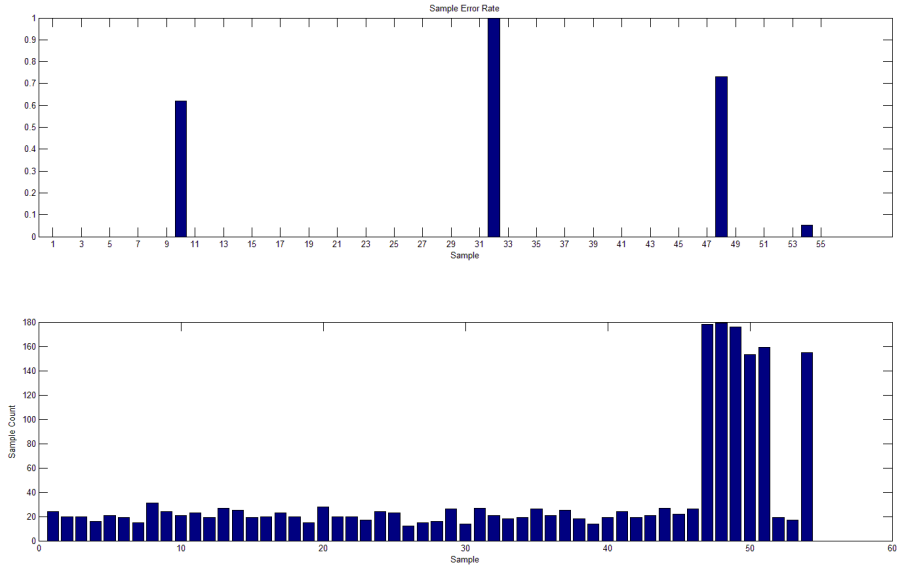

Figure 5.10: The error rates w.r.t. samples and sample distribution (2nd order polynomial SVM to classify laminated fabric)

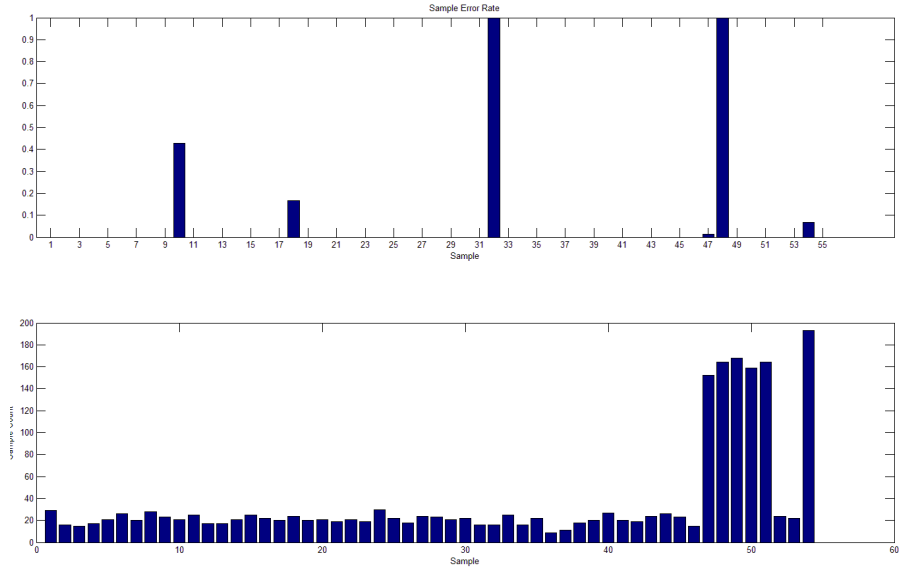

Figure 5.11: The error rates w.r.t. samples and sample distribution (3rd order polynomial SVM to classify laminated fabric)

Chapter 6

Conclusion

This thesis investigated the solutions for applying computerized methods to evaluate and intelligently interpret the texture and material properties of fabric in an inexpensive and efficient way.

In chapter 2, a comprehensive review on textile materials, the textile property measurement, and researches for fabric texture analysis, tactile sensing and haptic rendering is presented for the purpose of understanding the scope of this thesis. The complexity of fabric property and traditional evaluation methods of fabric property are discussed. The techniques that may help to develop computerized solutions for fabric property evaluation are also investigated in this chapter. The applications, for example, the fabric haptic simulations, that may benefit from the automatic fabric property evaluation are presented as well.

In chapter 3, a method which allows automatic recognition of basic weave pattern and precisely measuring the yarn count is proposed. The yarn crossed-areas are segmented by a spatial domain integral projection approach. Combining FCM and PCA on GLCM feature vectors extracted from the segments enables to classify detected segments into two clusters. Based on the analysis on texture orientation features, the yarn crossed-area states are automatically determined. An autocorrelation method is used to find weave repeats and correct detection errors. The method was validated by using computer

simulated woven samples and real woven fabric images. The test samples have various yarn counts, appearance, and weave types. All weave patterns of tested fabric samples are successfully recognized and computed yarn counts are consistent to the manual counts.

Chapter 4 shows a methodology for using the high resolution 3D surface data of fabric samples to measure surface roughness in a nondestructive and accurate way. Firstly, a parameter FD_{FFT} , which is the fractal dimension estimated from 2DFFT of 3D surface scan, is proposed as the indicator of surface roughness. The robustness of FD_{FFT} , which consists of the rotation-invariance and scale-invariance, is validated on a number of computer simulated fractal Brownian images. Secondly, in order to evaluate the usefulness of FD_{FFT} , a novel method of calculating standard roughness parameters from 3D surface scan is introduced. According to the test results, FD_{FFT} has been demonstrated as a fast and reliable parameter for measuring the fabric roughness from 3D surface data. Finally, we attempt a neural network model using back propagation algorithm and FD_{FFT} for predicting the standard roughness parameters. The proposed neural network model shows good performance experimentally.

In chapter 5, an intelligent approach for the interpretation of fabric objective measurements is proposed using supported vector machine techniques. The human expert assessments of fabric samples are used during the training phase in order to adjust the general system into an applicable model. Since the target output of the system is clear, the uncertainty which lies in current subjective fabric evaluation does not affect the performance of proposed model. The support vector machine is one of the best solutions for handling high dimensional data classification. The complexity problem of the fabric property has been optimally dealt with. The generalization ability shown in SVM allows the user to separately implement and design the components. Sufficient cross-validations are performed and demonstrate the performance test of the system.

For the future work, there are many possible improvements that can extend this work. For the method of automatic recognizing woven pattern, it requires to manually regulate the fabric images in order to ensure the weft and warp yarns are along x and

y directions. Therefore, a computerized method, which can adjust the fabric image to a right position, would be a complementary improvement of the algorithm. The system is applied on grey images currently. The further investigation on color space which contains more information of the fabric sample would also be helpful to the enhancement of the algorithm.

There are many improvements can be done in terms of the computerized measurement of surface roughness. For example, the optimization of neural network prediction model would shorten the training time and gain more accuracy; the investigation on how to apply the roughness measurement to the haptic simulation of surface texture could be an interest topic in the future.

For the intelligent interpretation algorithm, an potential improvement can be achieved from a deeper understanding of fabric features. If more human expert assessments be fused into the model, more capabilities would be shown. As the consequences, new data mining algorithms may be required. For example, the optimization of the feature space before the SVM training can increase the classification rate. It is obvious that a profound knowledge of the relationship between the input features and target output is useful for finding the optimal feature construction. A scientific study of the feature space may also be useful to improve the performance of the system.

The system developed in this dissertation can be extended to many other research topics in the field of computer intelligence and textile research. For example, the fabric structure recognition can be used for a virtual fabric simulation. Roughness measurements can be applied to a haptic fabric rendering. We also can imagine that in the near future there will be a robot agent assist a customer to find out the right fabric product from numerous products. We hope this research could trigger more investigations to make computers see, touch and think for more practical applications.

Appendix A

Feature data of Fabric Samples

A.1 Weight, thickness, and description

Sample	Description End-use	Description Laminated	Weight g/m^2	Thickness mm
1	other	other	380	1.6
2	other	other	120	0.61
3	other	other	330	1.76
4	other	other	250	1.09
5	other	other	175	0.55
6	other	other	145	0.93
7	other	other	15	0.1
8	other	other	150	0.8
9	other	other	80	0.44
10	other	other	300	1.44
11	other	other	290	1.53
12	other	other	275	1.13
13	other	other	270	1.14

14	other	other	270	3.9
15	other	other	300	1.88
16	other	other	215	2.94
17	other	other	135	0.73
18	other	other	90	0.39
19	other	other	80	0.57
20	other	other	235	1.56
21	other	other	172	1.21
22	other	other	125	0.33
23	other	other	82	0.25
24	other	other	125	0.3
25	other	other	155	1.25
26	other	other	25	0.16
27	other	other	250	3.99
28	other	other	600	2.38
29	other	other	90	0.2
30	other	other	10	0.3
31	other	other	100	0.4
32	other	other	815	1.68
33	man suit	other	195	0.57
34	man suit	other	232	0.83
35	man suit	other	324	2.64
36	man suit	other	460	3.23
37	other	other	98	0.26
38	other	other	208	1.09
39	other	other	288	1.69

40	other	other	154	0.51
41	other	other	128	0.51
42	other	other	215	0.98
43	car seat	other	278	1.22
44	car seat	other	168	1.1
45	car seat	other	147	1.6
46	car seat	other	98	1.55
47	car seat	laminated	386	4.09
48	car seat	laminated	438	4.19
49	car seat	laminated	335	4.11
50	car seat	laminated	332	3.54
51	car seat	laminated	170	4.03
52	other	other	53	0.42
53	other	other	121	0.81
54	car seat	laminated	287	3.35

A.2 Surface property

Surface property of face side

Sample	**MIU** warp	**MIU** weft	**MMD** warp	**MMD** weft	**SMD** warp	**SMD** weft
1	0.217	0.234	0.015	0.029	4.138	9.735
2	0.149	0.179	0.019	0.02	5.938	4.57
3	0.284	0.274	0.009	0.02	4.083	24.815
4	0.166	0.177	0.022	0.027	11.04	9.055
5	0.146	0.128	0.02	0.011	5.325	2.86

6	0.181	0.225	0.022	0.042	9.438	9.553
7	0.137	0.14	0.015	0.013	2.815	1.855
8	0.168	0.169	0.027	0.034	16.53	13.45
9	0.14	0.146	0.045	0.02	8.528	4.675
10	0.171	0.163	0.034	0.032	16.05	10.6
11	0.159	0.165	0.011	0.012	3	3.115
12	0.187	0.207	0.013	0.02	3.315	8.243
13	0.159	0.158	0.013	0.012	4.705	4.658
14	0.321	0.341	0.015	0.02	3.89	6.358
15	0.3	0.293	0.013	0.011	7.455	4.963
16	0.277	0.419	0.013	0.019	4.038	10.448
17	0.19	0.304	0.019	0.02	4.555	13.425
18	0.103	0.115	0.036	0.051	12.19	5.605
19	0.143	0.153	0.01	0.048	1.818	4.293
20	0.283	0.23	0.012	0.009	4.705	2.698
21	0.22	0.231	0.014	0.01	6.293	4.313
22	0.145	0.157	0.036	0.021	10.663	2.605
23	0.187	0.234	0.018	0.017	4.253	2.838
24	0.188	0.265	0.005	0.015	0.421	2.233
25	0.217	0.213	0.012	0.013	4.273	3.318
26	0.178	0.17	0.035	0.034	4.08	6.63
27	0.408	0.364	0.01	0.009	1.765	1.78
28	0.305	0.3	0.024	0.018	16.96	7.763
29	0.145	0.142	0.043	0.015	3.858	1.335
30	0.132	0.262	0.021	0.038	7.125	18.848
31	0.2	0.143	0.022	0.011	9.218	10.123

32	0.182	0.187	0.009	0.009	1.785	1.473
33	0.148	0.167	0.026	0.022	7.92	6.69
34	0.143	0.144	0.011	0.013	5.12	6.52
35	0.24	0.238	0.016	0.014	6.31	5.91
36	0.299	0.32	0.026	0.029	14.51	12.13
37	0.148	0.161	0.038	0.017	3.23	1.26
38	0.22	0.229	0.013	0.012	6.05	2.82
39	0.376	0.321	0.025	0.026	10.57	11.47
40	0.153	0.219	0.013	0.029	5.72	8.98
41	0.139	0.217	0.015	0.025	4.54	9.21
42	0.265	0.256	0.009	0.016	3.08	7.443
43	0.355	0.289	0.016	0.014	4.688	3.8
44	0.283	0.229	0.01	0.011	3.01	5.25
45	0.302	0.298	0.018	0.017	9.69	9.668
46	0.215	0.241	0.02	0.013	6.655	4.418
47	0.413	0.361	0.012	0.018	2.253	6.373
48	0.419	0.403	0.019	0.014	8.419	2.175
49	0.417	0.341	0.012	0.024	2.76	4.073
50	0.416	0.413	0.019	0.024	7.23	7.24
51	0.365	0.39	0.019	0.018	2.523	2.62
52	0.203	0.247	0.035	0.018	0	0
53	0.247	0.29	0.009	0.018	2.368	6.678
54	0.574	0.512	0.017	0.014	6.625	2.588

Surface property of back side

Sample	MIU warp	MIU weft	MMD warp	MMD weft	SMD warp	SMD weft
1	0.217	0.234	0.015	0.029	4.138	9.735
2	0.149	0.179	0.019	0.02	5.938	4.57
3	0.284	0.274	0.009	0.02	4.083	24.815
4	0.166	0.177	0.022	0.027	11.04	9.055
5	0.146	0.128	0.02	0.011	5.325	2.86
6	0.181	0.225	0.022	0.042	9.438	9.553
7	0.137	0.14	0.015	0.013	2.815	1.855
8	0.168	0.169	0.027	0.034	16.53	13.45
9	0.14	0.146	0.045	0.02	8.528	4.675
10	0.171	0.163	0.034	0.032	16.05	10.6
11	0.159	0.165	0.011	0.012	3	3.115
12	0.187	0.207	0.013	0.02	3.315	8.243
13	0.159	0.158	0.013	0.012	4.705	4.658
14	0.321	0.341	0.015	0.02	3.89	6.358
15	0.3	0.293	0.013	0.011	7.455	4.963
16	0.277	0.419	0.013	0.019	4.038	10.448
17	0.19	0.304	0.019	0.02	4.555	13.425
18	0.103	0.115	0.036	0.051	12.19	5.605
19	0.143	0.153	0.01	0.048	1.818	4.293
20	0.283	0.23	0.012	0.009	4.705	2.698
21	0.22	0.231	0.014	0.01	6.293	4.313
22	0.145	0.157	0.036	0.021	10.663	2.605
23	0.187	0.234	0.018	0.017	4.253	2.838
24	0.188	0.265	0.005	0.015	0.421	2.233

25	0.217	0.213	0.012	0.013	4.273	3.318
26	0.178	0.17	0.035	0.034	4.08	6.63
27	0.408	0.364	0.01	0.009	1.765	1.78
28	0.26	0.292	0.016	0.031	6.67	12.683
29	0.145	0.142	0.043	0.015	3.858	1.335
30	0.132	0.262	0.021	0.038	7.125	18.848
31	0.2	0.143	0.022	0.011	9.218	10.123
32	0.182	0.187	0.009	0.009	1.785	1.473
33	0.147	0.174	0.025	0.022	8.03	6.78
34	0.146	0.147	0.014	0.015	5.92	6.13
35	0.246	0.25	0.016	0.016	5.83	5.45
36	0.345	0.301	0.043	0.034	17.17	14.15
37	0.162	0.166	0.031	0.011	3.27	1.15
38	0.231	0.209	0.016	0.012	5.66	6.31
39	0.256	0.305	0.016	0.027	6.18	10.8
40	0.204	0.172	0.045	0.021	18.61	3.56
41	0.226	0.162	0.043	0.02	10.84	5.21
42	0.181	0.216	0.01	0.025	3.103	12.443
43	0.165	0.234	0.012	0.043	2.378	1.605
44	0.163	0.202	0.012	0.018	2.345	5.225
45	0.229	0.273	0.018	0.04	8.313	34.307
46	0.215	0.301	0.026	0.02	2.668	3.93
47	0.275	0.39	0.068	0.052	9.858	9.785
48	0.355	0.434	0.011	0.036	1.58	2.303
49	0.334	0.442	0.037	0.089	8.573	10.245
50	0.343	0.302	0.054	0.034	7.41	5.76

51	2.62	2.531	0.04	0.049	3.713	4.19
52	0.269	0.239	0.056	0.035	0	0
53	0.234	0.302	0.009	0.016	2.235	11.72
54	0.574	0.512	0.017	0.014	6.625	2.588

A.3 Tensile property

Sample	**LT warp**	**LT weft**	**WT warp**	**WT weft**	**RT warp**	**RT weft**	**EMT warp**	**EMT weft**
1	0.771	0.762	22.6	11.33	35.07	40.84	11.727	5.949
2	0.629	0.644	9.23	9.03	52.03	48.48	5.874	5.608
3	0.684	0.684	7.45	10.9	50.36	49.8	4.416	6.382
4	0.606	0.633	6.63	15.25	48.68	37.23	4.376	9.634
5	0.739	0.727	8.53	10.43	70.68	67.16	4.614	5.741
6	0.548	0.458	15.75	23.4	57.94	51.28	11.485	20.447
7	0.854	0.749	3	6.25	74.33	64.47	1.404	3.339
8	0.686	0.601	5.78	10.38	54.55	48.67	3.372	6.913
9	0.825	0.981	10.45	1.7	55.53	58.87	5.071	0.7
10	0.905	0.971	2.63	2.88	61.1	60.3	1.439	0.963
11	0.654	0.62	13.6	14.63	48.17	47.18	8.313	9.442
12	0.759	0.62	5.53	33.95	46.61	59.58	2.917	21.916
13	0.71	0.575	8.45	14.25	52.36	47.54	4.76	9.931
14	0.591	0.55	7.95	16.88	52.83	38.51	5.385	12.296
15	0.833	0.623	3.9	7.23	54.49	53.29	1.878	4.64
16	0.471	0.447	34.8	56.75	34.92	28.1	29.538	50.778
17	2.185	1.922	6.6	38.3	65.15	48.52	12.083	79.714

18	0.992	1.023	2.75	2.78	70.93	71.27	1.112	1.085
19	0.859	0.86	2.6	12.45	60.58	52.81	1.219	5.79
20	0.553	0.525	118.8	104	50.33	36.5	85.877	79.182
21	0.417	0.434	48.75	81.65	36.82	32.21	46.733	75.229
22	0.981	0.935	4.53	2.28	58.57	71.42	1.846	0.974
23	0.563	0.561	9.45	5.55	66.93	56.35	6.713	3.967
24	0.822	0.952	2.85	2.48	59.67	59.09	1.389	1.051
25	0.97	1.002	21.75	29.28	18.63	13.59	8.967	11.683
26	0.978	1.013	7.2	4.75	73.08	79.64	2.948	1.874
27	0.605	0.744	11	55.68	46.37	27.62	7.274	29.932
28	0.783	0.786	5.65	2.88	44.69	60.16	2.899	1.557
29	0.784	0.866	3.88	4.075	59.99	63.83	1.977	1.882
30	0.961	1.096	1.65	37.55	66.73	40.15	1.381	27.459
31	0.753	0.65	32.45	14.15	46.31	49.3	17.248	8.709
32	0.844	0.903	7.28	18.28	48.43	39.99	3.461	8.066
33	0.545	0.617	22.58	16.7	64.22	61.95	16.562	10.835
34	0.7	0.541	8.28	15.08	61.63	52.91	4.731	11.153
35	0.714	0.554	10.25	24	52.92	43.23	5.741	17.333
36	0.503	0.527	12.23	17.35	44.38	41.94	9.71	13.312
37	0.759	0.936	6.43	3.05	62.25	63.15	3.388	1.303
38	0.639	0.654	79.55	119.7	28.75	25.11	49.803	73.195
39	0.688	0.737	82.55	116.8	24.78	22.44	48.0185	63.394
40	0.665	0.674	9.7	6.58	46.39	47.56	5.835	3.909
41	0.798	0.783	11.15	10.65	52.47	46.01	5.593	5.458
42	0.782	0.862	27.03	9	47.27	41.67	13.838	4.174
43	0.878	0.932	16.5	10.63	50.77	50.72	7.5735	4.5585

44	0.878	0.932	16.5	10.63	50.77	50.72	7.5735	4.5585
45	0.827	0.895	38	10.28	38.1	45.29	18.3735	4.5955
46	0.628	0.763	23.18	17.95	47.58	49.3	14.82	9.4055
47	0.787	0.805	15.03	8	50.59	46.56	7.673	3.977
48	0.741	0.813	27.03	88.55	56.61	45.85	14.591	43.548
49	0.641	0.617	13.58	9.9	56.36	54.06	8.483	6.433
50	0.504	0.714	7.7	11.23	56.82	45.47	6.1115	6.2895
51	0.645	0.809	28.55	19.95	52.55	52.41	17.724	9.8735
52	0.543	0.567	45.68	29.88	32.62	33.81	33.5975	21.0635
53	0.514	0.584	45.65	119.15	31	21.52	35.5695	81.3595
54	0.82	0.906	21.75	64	54.7	41.74	21.2085	56.473

A.4 Shearing property

Sample	**G warp**	**G weft**	**2HG warp**	**2HG weft**	**2HG5 warp**	**2HG5 weft**
1	1.822	1.75	2.456	1.94	6.058	5.712
2	0.367	0.321	0.258	0.196	0.665	0.538
3	1.525	1.365	2.537	2.2	4.565	4.307
4	0.403	0.333	0.07	0.02	0.699	0.559
5	0.588	0.545	0.197	0.129	0.993	0.827
6	0.26	0.241	0.141	0.194	0.34	0.307
7	0.179	0.179	-0.171	-0.156	-0.026	-0.053
8	0.733	0.597	0.647	0.654	2.197	1.862
9	1.383	1.429	9.594	9.366	11.828	12.223
10	2.516	2.203	2.995	2.584	12.127	10.918
11	2.127	1.996	4.527	4.341	7.025	6.984

12	1.438	1.043	2.017	0.818	4.093	2.981
13	0.66	0.586	0.785	0.806	1.79	1.79
14	0.409	0.38	0.861	0.976	1.099	1.002
15	1.013	1.015	1.199	1.57	3.409	3.68
16	0.36	0.306	0.771	1.025	0.812	0.996
17	0.449	0.28	0.592	0.703	0.673	0.65
18	27.195	28.266	24.297	22.119	36.674	34.527
19	2.095	1.938	1.427	1.409	6.547	6.705
20	0.715	0.803	0.639	0.875	0.568	0.856
21	0.356	0.464	0.359	0.479	0.491	0.637
22	2.292	2.478	10.225	9.466	14.645	15.499
23	0.211	0.197	0.002	-0.134	0.19	0.029
24	0.522	0.412	0.343	0.121	1.927	1.297
25	3.576	3.053	4.468	5.14	11.057	8
26	0.184	0.176	-0.131	-0.148	-0.023	-0.057
27	0.973	0.92	2.923	3.058	3.234	3.631
28	3.107	2.809	6.665	5.051	14.064	12.93
29	2.315	2.328	1.832	1.27	7.451	7.837
30	2.24	5.421	2.147	9.574	1.622	9.672
31	1.296	0.907	2.881	1.233	3.748	2.01
32	30.998	31.582	54.661	55.478	57.774	56.374
33	0.718	0.764	0.23	0.287	1.411	1.405
34	0.65	0.499	0.701	0.552	1.595	1.223
35	0.613	0.667	0.835	1.427	1.374	1.917
36	0.536	0.514	0.58	0.838	0.821	1.052
37	2.357	2.285	3.515	2.583	8.732	8.659

38	0.838	0.968	1.362	1.555	1.818	1.627
39	0.488	0.459	1.169	0.784	1.271	0.999
40	2.057	1.593	5.906	3.692	7.341	5.607
41	2.567	2.538	4.047	3.785	6.174	5.311
42	2.41	2.121	5.975	3.184	7.864	5.265
43	1.076	0.948	1.228	1.473	1.034	1.401
44	2.996	3.398	12.655	9.197	6.863	5.309
45	3.608	2.625	13.078	7.415	6.849	4.105
46	1.747	1.3	6.973	4.839	6.321	3.203
47	5.474	4.987	8.866	10.392	16.115	15.353
48	3.724	3.48	5.642	6.166	6.23	6.355
49	7	6.255	8.276	8.216	22.433	21.259
50	9.891	8.635	13.378	16.201	28.927	29.885
51	3.316	3.442	4.458	6.257	7.254	6.757
52	0.639	0.614	2.382	3.228	2.231	3.052
53	0.39	0.31	0.938	1.174	0.9	1.047
54	1.961	1.862	3.239	3.612	3.714	3.85

A.5 Bending property

Sample	**B warp**	**B weft**	**2HB warp**	**2HB weft**
1	0.395	0.171	0.283	0.159
2	0.057	0.033	0.041	0.029
3	0.18	0.125	0.181	0.12
4	0.279	0.181	0.127	0.096
5	0.073	0.063	0.018	0.017

6	0.065	0.049	0.025	0.02
7	0.014	0.007	0.006	0.004
8	0.04	0.04	0.032	0.031
9	0.015	0.183	0.069	0.416
10	2.725	6.479	1.715	6.249
11	0.288	0.19	0.257	0.176
12	0.255	0.107	0.23	0.052
13	0.128	0.089	0.081	0.055
14	0	0	0	0
15	0.225	0.112	0.215	0.119
16	0.081	0.061	0.093	0.057
17	0.012	0.002	0.027	0.005
18	1.197	1.222	0.424	0.405
19	0.219	0.09	0.179	0.068
20	0.021	0.029	0.022	0.031
21	0.007	0.01	0.01	0.01
22	0.085	0.059	0.127	0.348
23	0.016	0.007	0.004	0.003
24	0.134	0.215	0.062	0.097
25	0.159	0.363	0.096	0.244
26	0.048	0.055	0.008	0.009
27	0	0	0	0
28	0.643	0.699	0.571	0.608
29	0.027	0.046	0.015	0.032
30	0.276	0.019	0.093	0.009
31	0.004	0.003	0.005	0.005

32	3.964	2.154	3.245	1.839
33	0.054	0.054	0.0176	0.0193
34	0.143	0.096	0.071	0.04
35	0.268	0.129	0.228	0.118
36	0.843	0.622	0.632	0.423
37	0.026	0.105	0.022	0.063
38	0.028	0.025	0.03	0.033
39	0.015	0.014	0.015	0.014
40	0.022	0.049	0.017	0.036
41	0.02	0.027	0.012	0.019
42	0.017	0.061	0.015	0.041
43	0.04	0.02	0.039	0.025
44	0.014	0.039	0.014	0.031
45	0.016	0.053	0.019	0.045
46	0.006	0.014	0.013	0.019
47	0	0	0	0
48	0	0	0	0
49	0	0	0	0
50	0	0	0	0
51	0	0	0	0
52	0.008	0.006	0.028	0.054
53	0.018	0.008	0.05	0.018
54	0.998	0.781	1.11	0.679

A.6 Compression and pressure-thickness property

Sample	LC	WC	RC	T_0	T_m
1	0.355	0.457	39.73	1.6	1.09
2	0.322	0.217	42.64	0.61	0.34
3	0.418	0.728	44.23	1.76	1.07
4	0.359	0.448	36.42	1.09	0.57
5	0.291	0.116	64.07	0.55	0.39
6	0.413	0.288	61.92	0.93	0.59
7	0.421	0.024	93.75	0.1	0.09
8	0.35	0.196	51.05	0.8	0.54
9	0.232	0.138	51.15	0.44	0.21
10	0.459	0.338	53.91	1.44	1.12
11	0.375	0.453	61.23	1.53	1.04
12	0.345	0.341	41.02	1.13	0.72
13	0.36	0.296	59.61	1.14	0.8
14	0.509	1.056	51.89	3.9	1.83
15	0.433	0.264	42.23	1.88	1.62
16	0.467	1.679	52.56	2.94	1.49
17	0.501	0.177	51.58	0.73	0.58
18	0.243	0.028	90.87	0.39	0.35
19	0.261	0.136	45.98	0.57	0.35
20	0.404	0.619	48.09	1.56	0.94
21	0.35	0.539	40.78	1.21	0.58
22	0.564	0.04	64.41	0.33	0.28
23	0.478	0.042	59.03	0.25	0.21
24	0.434	0.043	67.32	0.3	0.26

25	0.496	0.401	62.56	1.25	0.9
26	0.251	0.033	0	0.16	0.12
27	0.635	1.256	49.85	3.99	2.38
28	0.58	1.006	37.43	2.38	1.62
29	0.289	0.04	85	0.2	0.15
30	0.453	0.046	87.03	0.3	0.26
31	0.407	0.073	52.05	0.4	0.33
32	2.395	0.232	47.42	1.68	1.59
33	0.418	0.097	57.61	0.57	0.47
34	0.402	0.209	58.85	0.83	0.62
35	0.419	1.212	51.09	2.64	1.49
36	0.54	1.307	44.34	3.23	2.26
37	0.294	0.059	73.79	0.26	0.18
38	0.357	0.422	37.56	1.09	0.62
39	0.474	0.64	45.36	1.69	1.15
40	0.543	0.098	53.08	0.51	0.44
41	0.453	0.114	44.3	0.51	0.4
42	0.56	0.359	48.32	0.98	0.69
43	0.702	0.211	41.59	1.22	0.98
44	0.538	0.275	50.27	1.1	0.69
45	0.536	0.325	48.95	1.6	1.12
46	0.727	0.533	39.92	1.55	0.96
47	0.554	0.326	54.83	4.09	3.58
48	1.127	0.435	44.82	4.19	3.86
49	0.859	0.442	55.81	4.11	3.68
50	0.777	0.314	54.47	3.54	3.2

51	0.86	0.772	46.62	4.03	3.29
52	0.661	0.057	45.54	0.42	0.35
53	0.713	0.112	40.25	0.81	0.68
54	0.717	0.286	55.49	3.35	3.03

Bibliography

[1] G. Huang, D. Metaxas, and M. Govindaraj, "Feel the fabric: an audio-haptic interface," in *Proceedings of the 2003 ACM SIGGRAPH/Eurographics symposium on Computer animation*, pp. 52–61, Eurographics Association, 2003.

[2] A. Horrocks, S. Anand, and S. Anand, *Handbook of Technical Textiles*. CRC, 2000.

[3] L. V. Fausett, *Applied Numerical Analysis using Matlab*. NJ: Prentice Hall, 1999.

[4] J. McIntyre and P. Daniels, *Textile Terms and Definitions*. The Textile Institute, 1995.

[5] *AATCC Evaluation Procedure 5—Fabric Hand: Guidelines for the Subjective Evaluation of*. AATCC Technical Manual, AATCC, 2007.

[6] P. Volino, P. Davy, U. Bonanni, C. Luible, N. Magnenat-Thalmann, M. Mäkinen, and H. Meinander, "From measured physical parameters to the haptic feeling of fabric," *The Visual Computer*, vol. 23, no. 2, pp. 133–142, 2007.

[7] F. Peirce, "The handle of cloth as a measurable quantity," *Journal of the Textile Institute*, vol. 21, pp. 377–416, 1930.

[8] C. Luible, M. Varheenmaa, N. Magnenat-Thalmann, and H. Meinander, "Subjective fabric evaluation," in *Proc. HAVE 2009 - IEEE Int. Workshop on Haptic, Audio and Visual Environments and Games*, (Hannover), pp. 285–291, Oct. 2007.

[9] D. Bishop, "Fabrics: sensory and mechanical properties," *Textile Progress*, vol. 26, 1996.

[10] G. Winakor, C. Kim, and L. Wolins, "Fabric hand: Tactile sensory assessment," *Textile Research Journal*, vol. 50, no. 10, p. 601, 1980.

[11] D. Grinevičiūtė and M. Gutauskas, "The comparison of methods for the evaluation of woven fabric hand," *Materials Science (Medžiagotyra) ISSN 1392*, vol. 1320, no. 10, p. 1, 2004.

[12] V. SÜLAR and A. OKUR, "Sensory evaluation methods for tactile properties of fabrics," *Journal of Sensory Studies*, vol. 22, no. 1, pp. 1–16, 2007.

[13] D. Alimaa, T. Matsuo, M. Nakajima, and M. Takahashi, "Sensory measurements of the main mechanical parameters of knitted fabrics," *Textile Research Journal*, vol. 70, no. 11, p. 985, 2000.

[14] S. Kawabata, "The standardization and analysis of hand evaluation," 1980.

[15] S. Kawabata, *The Standardization and Analysis of Hand EvaluationThe Standardization and Analysis of Hand Evaluation*. Osaka: The Hand Evaluation and Standardization Committee, The Textile Machinery Society of Japan, 2nd ed., 1980.

[16] S. Kawabata and M. Niwa, "Fabric performance in clothing and clothing manufacture," *Journal of the Textile Institute*, vol. 80, no. 1, pp. 19–50, 1989.

[17] P. Minazio, "Fast–fabric assurance by simple testing," *International Journal of Clothing Science and Technology*, vol. 7, no. 2/3, pp. 43–48, 1995.

[18] L. Siew, R. Hodgson, and E. Wood, "Texture measures for carpet wear assessment," *IEEE Transactions on Pattern Analysis and Machine Intelligence*, pp. 92–105, 1988.

[19] N. Ponomarenko, V. Lukin, A. Zelensky, K. Egiazarian, M. Carli, and F. Battisti, "Tid2008-a database for evaluation of full-reference visual quality assessment metrics," *Advances of Modern Radioelectronics*, vol. 10, no. 4, pp. 30–45, 2009.

[20] D. Chetverikov, "Detecting defects in texture," in *Pattern Recognition, 1988., 9th International Conference on*, pp. 61–63, IEEE.

[21] J. Chen and A. Jain, "A structural approach to identify defects in textured images," in *Systems, Man, and Cybernetics, 1988. Proceedings of the 1988 IEEE International Conference on*, vol. 1, pp. 29–32, IEEE.

[22] X. Xie, "A review of recent advances in surface defect detection using texture analysis techniques," *Electronic Letters on Computer Vision and Image Analysis*, vol. 7, no. 3, pp. 1–22, 2008.

[23] I. Bankman, *Handbook of Medical Image Processing and Analysis*. Academic Press, 2008.

[24] N. Journet, J. Ramel, R. Mullot, and V. Eglin, "Document image characterization using a multiresolution analysis of the texture: application to old documents," *International Journal on Document Analysis and Recognition*, vol. 11, no. 1, pp. 9–18, 2008.

[25] J. Richards and X. Jia, *Remote Sensing Digital Image Analysis: An Introduction*. Springer Verlag, 2006.

[26] M. Nixon and A. Aguado, *Feature Extraction And Image Processing*. Academic Press, 2008.

[27] R. M. Haralick, K. Shanmugam, and I. Dinstein, "Textural features for image classification," *IEEE Trans. Syst. Man and Cyber.*, vol. 3, pp. 610–21, 1973.

[28] S. Arivazhagan, L. Ganesan, and T. Kumar, "Texture classification using curvelet statistical and co-occurrence features," *Pattern Recognition*, vol. 2, pp. 938–941, 2006.

[29] H. Kekre and S. Gharge, "Sar image segmentation using co-occurrence matrix and slope magnitude," in *Proceedings of the International Conference on Advances in Computing, Communication and Control*, pp. 368–372, ACM, 2009.

[30] A. Alvarenga, W. Pereira, A. Infantosi, and C. Azevedo, "Complexity curve and grey level co-occurrence matrix in the texture evaluation of breast tumor on ultrasound images," *Medical Physics*, vol. 34, p. 379, 2007.

[31] M. Petrou, P. Sevilla, and J. Wiley, *Image processing: dealing with texture*. John Wiley & Sons Inc., 2006.

[32] Z. Wang and J. Yong, "Texture analysis and classification with linear regression model based on wavelet transform," *Image Processing, IEEE Transactions on*, vol. 17, no. 8, pp. 1421–1430, 2008.

[33] F. Campbell and J. Robson, "Application of fourier analysis to the visibility of gratings," *The Journal of Physiology*, vol. 197, no. 3, p. 551, 1968.

[34] M. Varma and R. Garg, "Locally invariant fractal features for statistical texture classification," in *Computer Vision, 2007. ICCV 2007. IEEE 11th International Conference on*, pp. 1–8, IEEE, 2007.

[35] R. Paget and I. Longstaff, "Texture synthesis via a noncausal nonparametric multiscale markov random field," *Image Processing, IEEE Transactions on*, vol. 7, no. 6, pp. 925–931, 1998.

[36] D. Lu and Q. Weng, "A survey of image classification methods and techniques for improving classification performance," *International Journal of Remote Sensing*, vol. 28, no. 5, pp. 823–870, 2007.

[37] E. Avci, "An expert system based on wavelet neural network-adaptive norm entropy for scale invariant texture classification," *Expert Systems with Applications*, vol. 32, no. 3, pp. 919–926, 2007.

[38] W. Wong, C. Yuen, D. Fan, L. Chan, and E. Fung, "Stitching defect detection and classification using wavelet transform and bp neural network," *Expert Systems with Applications*, vol. 36, no. 2, pp. 3845–3856, 2009.

[39] S. Choy and C. Tong, "Statistical properties of bit-plane probability model and its application in supervised texture classification," *Image Processing, IEEE Transactions on*, vol. 17, no. 8, pp. 1399–1405, 2008.

[40] D. Wu, H. Yang, X. Chen, Y. He, and X. Li, "Application of image texture for the sorting of tea categories using multi-spectral imaging technique and support vector machine," *Journal of Food Engineering*, vol. 88, no. 4, pp. 474–483, 2008.

[41] W. Spangler, "A method for adapting a k-means text clustering to emerging data," Apr. 28 2010. EP Patent 1,191,463.

[42] Y. Gong, "Simplified method of kernel fuzzy c-means clustering for image texture classification [j]," *Journal of Beijing University of Aeronautics and Astronautics*, vol. 3, 2008.

[43] B. S. Jeon, J. H. Bae, and M. W. Suh, "Automatic recognition of woven fabric patterns by an artificial neural network," *Textile Research Journal*, vol. 73, pp. 645–650, Jul. 2003.

[44] C. F. J. Kuo, C. Y. Shih, and J. Y. Lee, "Automatic recognition of fabric weave patterns by a fuzzy c-means clustering method," *Textile Research Journal*, vol. 74, pp. 107–111, Feb. 2004.

[45] B. G. Xu, "Identifying fabric structures with fast fourier transform techniques," *Textile Research Journal*, vol. 66, pp. 496–506, Aug. 1996.

[46] M. Kinoshita, Y. Hashimoto, R. Akiyama, and S. Uchiyama, "Determination of weave type in woven fabric by digital image processing," *J. Textile. Mach. Soc. Jpn.*, vol. 35, pp. 1–4, 1989.

[47] A. Lachkar, T. Gadi, R. Benslimane, and L. D'Orazio, "Textile woven fabric recognition using fourier image analysis techniques : Part i : A fully automatic approach for crossed-points detection," *J. Text. Inst.*, vol. 94, pp. 194–201, 2003.

[48] A. Lachkar, R. Benslimane, L. D'Orazio, and E. Martuscelli, "Textile woven fabric recognition using fourier image analysis techniques : Part ii - texture analysis for crossed-states detection," *J. Text. Inst.*, vol. 96, pp. 179–183, 2005.

[49] C. F. J. Kuo, C. Y. Shih, and J. Y. Lee, "Repeat pattern segmentation of printed fabrics by hough transform method," *Textile Research Journal*, vol. 75, pp. 779–783, Nov. 2005.

[50] T. J. Kang, C. H. Kim, and K. W. Oh, "Automatic recognition of fabric weave patterns by digital image analysis," *Textile Research Journal*, vol. 69, pp. 77–83, Feb. 1999.

[51] C. F. J. Kuo and C. C. Tsai, "Automatic recognition of fabric nature by using the approach of texture analysis," *Textile Research Journal*, vol. 76, pp. 375–382, May 2006.

[52] J. Escofet, M. S. Millán, and M. Ralló, "Modeling of woven fabric structures based on fourier image analysis," *Applied Optics*, vol. 40, pp. 6170–6176, Dec 2001.

[53] M. Ralló, J. Escofet, and M. S. Millán, "Weave-repeat identification by structural analysis of fabric images," *Applied Optics*, vol. 42, pp. 3361–3372, Jun 2003.

[54] E. M. Petriu, S. K. S. Yeung, S. R. Das, A.-M. Cretu, and H. J. W. Spoelder, "Robotic tactile recognition of pseudorandom encoded objects," *IEEE Transactions in Instrumentation and Measurement*, vol. 53, no. 5, pp. 1425–1432, 2004.

[55] M. Eltaib and J. Hewit, "Tactile sensing technology for minimal access surgery–a review," *Mechatronics*, vol. 13, pp. 1163–1177, 2003.

[56] D. Darioand and D. D. Rossi, "Tactile sensors and the gripping challenge," *IEEE Spectr*, vol. 5, pp. 46–52, 1985.

[57] K. E. Pennywitt, "Robotic tactile sensing," *BYTE*, vol. 11, no. 1, pp. 177–200, 1986.

[58] H. R. Nicholls and M. H. Lee, "A survey of robot tactile sensing technology," *International Journal of Robotics Research*, vol. 8, no. 3, pp. 3–30, 1989.

[59] B. V. Jayawant, "Tactile sensing in robotics," *Journal of Physics E: Scientific Instruments*, vol. 22, pp. 684–692, 1989.

[60] M. H. Lee and H. R. Nicholls, "Tactile sensing for mechatronics–a state of the art survey," *Mechatronics*, vol. 9, no. 9, pp. 1–31, 1999.

[61] W. W. Mayol-Cuevas, J. Juarez-Guerrero, and S. Munoz-Gutierrez, "A first approach to tactile texture recognition," in *Systems, Man, and Cybernetics, 1998. 1998 IEEE International Conference on*, vol. 5, pp. 4246–4250, 1998.

[62] N. Jamali and C. Sammut, "Material classification by tactile sensing using surface textures," in *2010 IEEE International Conference on Robotics and Automation*, pp. 2336–2341, 2010.

[63] T. L. McDaniel and S. Panchanathan, "Peceptual surface roughness calssification of 3d textures using support vector machines," in *HAVE 2007 - IEEE International Workshop on Haptic Audio Visual Environments and their Applications*, pp. 154–159, 2007.

[64] S. H. Kim, J. Engel, C. Liu, and D. L. Jones, "Texture calassification using a polymer-based mems tactile sensor," *Journal of Micromechanics and Microengineering*, vol. 15, pp. 912–920, 2005.

[65] "Haptic." available at `http://www.merriam-webster.com/dictionary/haptic`.

[66] S. J. Lederman and R. L. Klatzky, "Human haptics," *Encyclopedia of Neuroscience*, vol. 5, pp. 11–18, 2009.

[67] M. A. Srinivasan, *In Virtual Reality: Scientific and Technical Challenges*, ch. Haptic Interfaces, pp. 161–187. National Academy Press, 1995.

[68] J. K. Salisbury, D. Brock, T. Massie, N. Swarup, and C. Zilles, "Haptic rendering: Programming touch interaction with virtual objects," *Proc. of ACM Symposium on Interactive 3D Graphics*, pp. 123–130, 1995.

[69] P. Payeur, C. Pasca, A.-M. Cretu, and E. M. Petriu, "Intelligent haptic sensor system for robotic manipulation," *IEEE Transactions in Instrumentation and Measurement*, vol. 54, no. 4, pp. 1583–1592, 2005.

[70] E. A. Bier and K. R. Sloan, "Two-part texture mapping," *IEEE Computer Graphics and Applications*, pp. 40–53, 1986.

[71] A. Watt and M. Watt, *Advanced Animation and Rendering Techniques*. Addison-Wesley, NY., 1992.

[72] M. Minsky, *Computational Haptics: The Sandpaper System for Synthesizing Texture for a Force-Feedback Display*. PhD thesis, Program in Media Arts and Sciences, MIT, Cambridge, MA, 1995. Thesis work done at UNC-CH Computer Science.

[73] C. H. Ho, C. Basdogan, and M. A. Srinivasan, "Efficient point-based rendering techniques for haptic display of virtual objects," *Presence*, vol. 8, no. 5, pp. 477–491, 1999.

[74] J. F. Blinn, "Simulation of wrinkled surfaces," *Computer Graphics (SIGGRAPH '78 Proceedings)*, pp. 286–292, 1978.

[75] J. Siira and D. K. Pai, "Haptic texturing - a stochastic approach," in *Proceedings of the IEEE International Conference on Robotics and Automation*, (Minneapolis, Minnesota), pp. 557–562, 1996.

[76] Fritz and Barner, "Haptic scientific visualization," in *Proceedings of the First PHANToM Users Group Workshop* (J. K. Salisbury and M. A. Srinivasan, eds.), 1996.

[77] R. L. Klatzky and S. J. Lederman, *Experimental Psychology*, vol. 4, ch. Touch, pp. 147–176. Wiley, 2003.

[78] M. Otaduy, N. Jain, A. Sud, and M. Lin, "Haptic display of interaction between textured models," in *Proceeding of IEEE Visualization Conference*, pp. 297–304, 2004.

[79] V. Theoktisto, M. Fairen, I. Navazo, and E. Monclus, "Rendering detailed haptic textures," in *Workshop on Virtual Reality Interaction and Physical Simulation*, 2005.

[80] N. Magnenat-Thalmann, P. Volino, U. Bonanni, I. Summers, M. Bergamasco, F. Salsedo, and F. Wolter, "From physics-based simulation to the touching of textiles: The haptex project," *The International Journal of Virtual Reality*, vol. 6, no. 3, pp. 35–44, 2007.

[81] M. Bergamasco, F. Salsedo, M. Fontana, F. Tarri, C. Avizzano, A. Frisoli, E. Ruffaldi, and S. Marcheschi, "High performance haptic device for force rendering in textile exploration," *The Visual Computer*, vol. 23, no. 4, pp. 247–256, 2007.

[82] G. Böttcher, D. Allerkamp, D. Glöckner, and F. Wolter, "Haptic two-finger contact with textiles," *The Visual Computer*, vol. 24, no. 10, pp. 911–922, 2008.

[83] D. Allerkamp, G. Böttcher, F. Wolter, A. Brady, J. Qu, and I. Summers, "A vibrotactile approach to tactile rendering," *The Visual Computer*, vol. 23, no. 2, pp. 97–108, 2007.

[84] "Textile." available at `http://en.wikipedia.org/wiki/Textile`.

[85] H. K. Kaynak and M. Topalbekiroğlu, "Influence of fabric pattern on the abrasion resistance property of woven fabrics," *Fibers and Textiles in Eastern Europe*, vol. 16, no. 1(66), pp. 54–56, 2008.

[86] S. Srisuwan and P. Chumsamrong, "Effects of weave type and fiber content on physical properties of sisal fiber/epoxy composites," *Advanced Materials Research*, vol. 123, pp. 1139–1142, 2010.

[87] M. Mori and M. Matsudaira, "The effect of weave density on fabric handle and appearance of men's suit fabrics," *Research Journal of Textile and Apparel*, vol. 11, no. 3, pp. 71–78, 2007.

[88] D. A. Clausi, "An analysis of co-occurrence texture statistics as a function of grey-level quantization," *Canadian Journal of Remote Sensing*, vol. 28, no. 1, pp. 45–62, 2002.

[89] I. T. Jolliffe, *Principal Component Analysis Second Edition*. New York: Springer-Verlag, 2002.

[90] E. Anderson, Z. Bai, C. Bischof, S. Blackford, J. Demmel, J. Dongarra, J. D. Croz, A. Greenbaum, S. Hammarling, A. McKenney, and D. Sorensen, *LAPACK User's Guide Third Edition*. Philadelphia: SIAM, 1999.

[91] W. Chumsamrong, P. Thitimajshima, and Y. Rangsanseri, "Synthetic aperture radar (sar) image segmentation using a new modified fuzzy c-means algorithm," *Proceedings of Geoscience and Remote Sensing Symposium*, vol. 2, pp. 624–626, 2000.

[92] P. Palisson, N. Zegadi, F. Peyrin, and R. Unterreiner, "Unsupervised multiresolution texture segmentation using wavelet decomposition," in *Proc. of the First IEEE International Conference on Image Processing*, (Austin TX), pp. 625–629, 1994.

[93] H. Sari-Sarraf and J. J. S. Goddard, "Online optical measurement and monitoring of yarn density in woven fabrics," *Proc. SPIE*, vol. 2899, pp. 444–452, Oct. 1996.

[94] G. P. P. Gunarathne and K. Christidis, "Measurements of surface texture using ultrasound," *IEEE Transactions on Instrumentation and Measurement*, vol. 50, no. 5, pp. 1144–1148, 2001.

[95] A. W. Domanski and T. R. Wolinski, "Surface roughness measurement with optical fibers," *IEEE Transactions on Instrumentation and Measurement*, vol. 41, no. 6, pp. 1057–1061, 1992.

[96] K. Zhang, C. Butler, Q. Yang, and Y. Lu, "A fiber optic sensor for the measurement of surface roughness and displacement using artificial neural networks," *Instrumentation and Measurement, IEEE Transactions on*, vol. 46, no. 4, pp. 899–902, 1997.

[97] S. Moslehpour, C. Campana, D. Shetty, and B. Deryniosky, "Stand-alone surface roughness analyzer," *IEEE Transactions on Instrumentation and Measurement*, vol. 58, no. 3, pp. 698–706, 2009.

[98] T. J. Kang, S. C. Kim, J. R. Y. I. H. Sul, and K. Chung, "Fabric surface roughness evaluation using wavelet-fractal method: Part i: Wrinkle, smoothness and seam pucker," *Textile Research Journal*, vol. 75, pp. 751–760, 2005.

[99] X. Wang and N. D. Georganas, "GLCM texture based fractal method for evaluating fabric surface roughness," *Proc. IEEE CCECE'9 - Canadian Conference on Electrical and Computer Engineering*, pp. 104–107, May 2009.

[100] X. Wang, N. D. Georganas, and E. M. Petriu, "Fabric texture analysis using computer vision techniques," *IEEE Transactions on Instrumentation and Measurement*, vol. PP, no. 99, pp. 1–13, 2010.

[101] M. Bergmann, I. Herbst, R. Von-Wieding, and F. E. Wolter, "Haptical rendering of rough surfaces using their fractal dimension," in *Proc. of the First PHANToM Users Research Symposium*, (German Cancer Research Center, Heidelberg, Germany,), pp. 9–12, 1999.

[102] R. Zwiggelaar and C. Bull, "Optical determination of fractal dimensions using Fourier transforms (Journal Paper)," *Optical Engineering*, vol. 34, no. 05, pp. 1325–1332, 1995.

[103] A. K. Jain and J. Mao, "Artificial neural networks: a tutorial," *Comupter*, vol. 26, no. 3, pp. 31–44, 1996.

[104] M. H. Hassoun, *Fundamentals of artificial neural networks*. Cambridge,MA: MIT press, 1995.

[105] F. Chen, "Back-propagation neural networks for nonlinear self-tunning adaptive control," *IEEE Contr. Syst. Mag.*, vol. 10, pp. 44–48, 1990.

[106] J. Freeman and D. Skapura, *Neural Networks: Algorithms, Applications, and Programming Techniques*. Addison-Wesley, 1991.

[107] L. Saini and M. Soni, "Artificial neural network based peak load forecasting using Levenberg-Marquardt and quasi-Newton methods," in *Generation, Transmission and Distribution, IEE Proceedings-*, vol. 149, pp. 578–584, IET, 2002.

[108] U. of Illinois at Urbana-Champaign. Center for Supercomputing Research, Development, and G. Cybenko, *Continuous Valued Neural Networks With Two Hidden Layers Are Sufficient*. 1988.

[109] E. Dreby, "Physical methods for evaluating the hand of fabrics and for determinig the effects of certain textile finishing process," *Am. Dyestuff Reporter*, vol. 497, p. 31, 1942.

[110] B. Ellis and R. Garnsworthy, "A review of techniques for the assessment of hand," *Textile Research Journal*, vol. 50, no. 4, p. 231, 1980.

[111] V. Dawes and J. Owen, "The assessment of fabric handle part i: stiffness and liveliness," *Journal of the Textile Institute*, vol. 62, no. 5, pp. 233–244, 1971.

[112] O. Tokmak, O. Berkalp, and J. Gersak, "Investigation of the Mechanics and Performance of Woven Fabrics Using Objective Evaluation Techniques. Part I: The Relationship Between Fast, Kes-F and Cusicks Drape-Meter Parameters," *FIBRES & TEXTILES in Eastern Europe*, vol. 18, no. 2, p. 79, 2010.

[113] M. Jacobsen, A. Fritz, R. Dhingra, and R. Postle, "Psychophysical evaluation of the tactile qualities of hand knitting yarns.," *Textile Research Journal*, vol. 62, no. 10, pp. 557–566, 1992.

[114] J. Hu, W. Chen, and A. Newton, "A psychophysical model for objective fabric hand evaluation: An application of stevens's law," *Journal of the Textile Institute*, vol. 84, no. 3, pp. 354–363, 1993.

[115] G. Mazzuchetti, R. Demichelis, M. Songia, and F. Rombaldoni, "Objective measurement of tactile sensitivity related to a feeling of softness and warmth," *Fibres & Textiles in Eastern Europe*, vol. 16, no. 4, p. 69, 2008.

[116] X. Zeng, L. Koehl, M. Sanoun, M. Bueno, and M. Renner, "Integration of human knowledge and measured data for optimization of fabric hand," *International Journal of General Systems*, vol. 33, no. 2, pp. 243–258, 2004.

[117] C. Hui, T. Lau, S. Ng, and K. Chan, "Neural network prediction of human psychological perceptions of fabric hand," *Textile Research Journal*, vol. 74, no. 5, p. 375, 2004.

[118] C. Burges, "A tutorial on support vector machines for pattern recognition," *Data Mining and Knowledge Discovery*, vol. 2, no. 2, pp. 121–167, 1998.

[119] N. Cristianini and J. Shawe-Taylor, *An introduction to support Vector Machines: and other kernel-based learning methods*. Cambridge university press, 2006.

[120] V. Vapnik, *The Nature of Statistical Learning Theory*. Springer Verlag, 2000.

[121] G. Fung and O. Mangasarian, "Multicategory proximal support vector machine classifiers," *Machine Learning*, vol. 59, no. 1, pp. 77–97, 2005.

[122] J. Shawe-Taylor and N. Cristianini, *Kernel Methods for Pattern Analysis*. Cambridge Univ Pr, 2004.

[123] M. Hearst, S. Dumais, E. Osman, J. Platt, and B. Scholkopf, "Support vector machines," *Intelligent Systems and Their Applications, IEEE*, vol. 13, no. 4, pp. 18–28, 1998.

[124] M. Mäkinen and C. Luible, "First set of measurements." available at `http://haptex.miralab.unige.ch/public/deliverables/HAPTEX-D3.1.pdf`.

[125] M. Mäkinen and C. Luible, "Second set of measurements." available at `http://haptex.miralab.unige.ch/public/deliverables/HAPTEX-D3.2-p1.pdf`.

[126] M. Mäkinen and C. Luible, "Database of properties for various kinds of fabrics." available at `http://haptex.miralab.unige.ch/public/deliverables/HAPTEX-D3.2-p2.pdf`.